University of Thessaly

School of Health Sciences

Department of Biochemistry & Biotechnology

Doctoral Thesis

«Development of nanodispersions as carriers for bioactive compounds and their biological applications»

Theochari Ioanna

Chemist

Larissa, 2020

Development of nanodispersions as carriers for bioactive compounds and their biological applications

Examination committee

- **Papadimitriou Vassiliki (supervisor)**
  Researcher B' – Group of Biomimetics & Nanobiotechnology
  Institute of Chemical Biology, National Hellenic Research Foundation (NHRF).

- **Pletsa Vasiliki**
  Researcher B' – Group of Chemical Carcinogenesis and Genetic Toxicology
  Institute of Chemical Biology, National Hellenic Research Foundation (NHRF).

- **Leonidas D. Demetres**
  Professor – Biochemistry
  Department of Biochemistry & Biotechnology, University of Thessaly (UTH).

- **Leal – Calderon Fernando**
  Professor – Group of Colloids and Lipids for Industry and Nutrition
  Institute of Chemistry & Biology of Membranes & Nano-objects (CBMN),
  University of Bordeaux, Pessac, France.

- **Psarra Anna-Maria**
  Assistant Professor – Biochemistry
  Department of Biochemistry & Biotechnology, University of Thessaly (UTH).

- **Skamnaki Vasiliki**
  Assistant Professor – Biochemistry, Metabolism
  Department of Biochemistry & Biotechnology, University of Thessaly (UTH).

- **Xenakis Aristotelis**
  Research Director – Group of Biomimetics & Nanobiotechnology
  Institute of Chemical Biology, National Hellenic Research Foundation (NHRF).

Theochari Ioanna

Development of nanodispersions as carriers for bioactive compounds and their biological applications

Abstract

The aim of this thesis was initially the formulation of nanodispersions, as carriers of bioactive compounds and also their biological evaluation as potent delivery systems. Two types of nanodispersions, namely micro- and nanoemulsions were formulated and structurally characterized, performing different methods. The nanodispersions were used as matrices for the nanoencapsulation of bioactive compounds with pharmacological interest including chemotherapeutic and anti-inflammatory agents.

The study of structural characteristics was performed by viscosity measurements, Dynamic Light Scattering (DLS), Electron Paramagnetic Resonance Spectrometry (EPR) and Cryogenic Transmission Electron Microscopy (cryo-TEM). The measurements were conducted in both empty nanodispersions and loaded nanodispersions with bioactive compounds. The structural study revealed both differences and similarities, induced both by the different composition of the formulated delivery systems and by the encapsulation of the bioactive compounds. In order to evaluate the efficacy of nanodispersions in biological applications, both *in vitro* and *ex vivo* assays were performed. The cytotoxic effect of both drug free and loaded nanodispersions, was examined through cell viability assays. For this purpose, selected colorectal and skin cancer cell lines, namely WM 164, Caco-2, HT-29 and Colon 205 were used. The mechanism of the cell death caused by the bioactive compounds was investigated through different techniques, among them Fluorescence-activated cell sorting (FACS) analysis, Comet assay and Western Blotting of specific cell death and apoptosis markers. Overall, it was found that oil-in-water (o/w) nanodispersions are appropriate delivery systems of the bioactive compounds in all cell lines tested.

The *ex vivo* experiments included different assays, namely *ex vivo* permeation study through Franz cell device and differential tape stripping. Through the *ex vivo* approach, it was found that the encapsulated compounds were promptly distributed within full-thickness of stratum corneum (SC). Moreover, the quantity of the bioactive compounds that may enter the blood circulation was determined. Subsequently, the proposed o/w nanodispersions are proper carriers to deliver bioactive compounds through skin and improve the dermal/transdermal administration of the encapsulated compounds.

Περίληψη

Ο κύριος στόχος αυτής της μελέτης ήταν αρχικά η ανάπτυξη νανοδιασπορών ως φορέων των βιοδραστικών ενώσεων καθώς και η αποτίμηση της βιολογικής τους δρασης ως πιθανά συστήματα χορήγησης των βιοδραστικών ενώσεων. Αναπτύχθηκαν δύο τύποι νανοδιασπορών, τα μικρο- και νανογαλακτώματα, τα οποία χαρακτηρίστηκαν δομικά, χρησιμοποιώντας διάφορες μεθόδους. Οι νανοδιασπορές χρησιμοποιήθηκαν ως μήτρες για την ενθυλάκωση βιοδραστικών ενώσεων με φαρμακολογικό ενδιαφέρον όπως χημειοθεραπευτικοί και αντιφλεγμονωδεις παράγοντες.

Η μελέτη των δομικών χαρακτηριστικών πραγματοποιήθηκε με μετρήσεις ιξώδους καθώς και με χρήση Δυναμικής Σκέδασης Φωτός (DLS), φασματοσκοπίας Ηλεκτρονικού Παραμαγνητικού Συντονισμού (EPR) και Κρυογονικής Ηλεκτρονικής Μικροσκοπίας (cryo-TEM). Οι μετρήσεις πραγματοποιήθηκαν τόσο απουσία όσο και παρουσία βιοδραστικών ενώσεων, στις νανοδιασπορές. Η δομική μελέτη αποκάλυψε τις διαφοροποιήσεις που προκαλούνται τόσο από τη διαφορετική σύσταση των νανοδιασπορών, όσο από την ενθυλάκωση των βιοδραστικών ενώσεων. Προκειμένου να αξιολογηθεί η αποτελεσματικότητα των νανοδιασπορών σε βιολογικές εφαρμογές, διεξήχθησαν πειράματα *in vitro* και *ex vivo*. Η κυτταροτοξική επίδραση τόσο των νανογαλακτωμάτων ως φορέων όσο και των ενθυλακωμένων βιοδραστικών ενώσεων εξετάστηκε μέσω μελέτης κυτταρικής βιωσιμότητας κυττάρων. Για το σκοπό αυτό, χρησιμοποιήθηκαν επιλεγμένες κυτταρικές σειρές όπως η WM 164, Caco-2, HT 29 και Colon 205. Ο μηχανισμός του επαγόμενου κυτταρικού θανάτου διερευνήθηκε μέσω κυτταρομετρίας ροής (FACS), ανάλυσης Comet και ανοσοτύπωσης κατά Western με χρήση δεικτών κυτταρικού θανάτου και απόπτωσης. Διαπιστώθηκε ότι η προτεινόμενες νανοδιασπορές είναι κατάλληλες ως φορείς βιοδραστικών ενώσεων.

Τα *ex vivo* πειράματα περιλάμβαναν τη μελέτη διαπερατότητας μέσω συσκευής Franz και την τεχνική differential tape stripping. Μέσω της *ex vivo* προσέγγισης, βρέθηκε ότι οι ενθυλακωμένες ενώσεις κατανεμήθηκαν στην κεράτινη στιβάδα. Επιπλέον, προσδιορίστηκε η ποσότητα της βιοδραστικής ένωσης που μπορεί πιθανά να εισέλθει στην κυκλοφορία του αίματος. Ως αποτέλεσμα, οι προτεινόμενες νανοδιασπορές είναι κατάλληλοι φορείς για την μεταφορά βιοδραστικών ενώσεων μέσω του δέρματος καθώς και την ενίσχυση της δερματικής/διαδερμικής απελευθέρωσης τους.

Theochari Ioanna

Larissa, 2020

«Development of nanodispersions as carriers for bioactive compounds and their biological applications»

Doctoral Thesis

University of Thessaly

School of Health Sciences

Department of Biochemistry & Biotechnology

Number of primary pages: 17

Total number of pages: 158

Total number of figures: 60

Total number of tables: 3

Total number of references: 255

Prologue

The principle aim of the thesis was the formulation of nanodispersions, as carriers of bioactive compounds and also their biological evaluation as potent delivery systems. Two types of nanodispersions, namely micro- and nanoemulsions were formulated and structurally characterized, performing different methods. The nanodispersions were used as matrices for the encapsulation of bioactive compounds with pharmacological interest, including chemotherapeutic and anti-inflammatory agents. In order to assess the efficacy of the proposed nanodispersions, in vitro and ex vivo studies were performed.

This PhD thesis was carried out during the years 2016-2019 at the Biomimetics & Nanobiotechnology Group of Institute of Chemical Biology (ICB) at National Hellenic Research Foundation (NHRF) in collaboration with the Department of Biochemistry and Biotechnology of University of Thessaly, under the supervision of Dr. Vassiliki Papadimitriou. This project was initially funded by the Greece and the European Regional Development Fund of the European Union under the Operational Program "Competitiveness, Entrepreneurship and Innovation" (NSRF 2007–2013) and the Regional Operational Program of Attica (STHENOS project within GSRT'S KRIPIS). We were also financially supported by the project "STHENOS-b: Targeted therapeutic approaches against degenerative diseases with special focus on cancer and ageing-optimisation of the targeted bioactive molecules", in the context of "Action for the Strategic Development on the Research and Technological Sector" and funded by the Operational Program "Competitiveness, Entrepreneurship and Innovation" (NSRF 2014-2020).

Acknowledgements

I would like to express my honest gratefulness to my supervisor Dr. Vassiliki Papadimitriou for her support in my PhD study and research, for her patience, inspiration, enthusiasm, and knowledge. Her assistance encouraged me in all the way of research, design of scientific work and writing of this thesis. I would like to thank Dr. Vasiliki Pletsa, for her consistent guidance, as she has always been available to provide me with her help and knowledge at all stages of this study and gave me the chance to discover the difficult pathway of biology. I would like to thank Prof. Demetres Leonidas, member of the supervising committee, who has provided his professional guidance and gave me the chance to work on this subject.

I am really grateful to Dr. Aristoteles Xenakis, who has been really supportive to all my ambitions and worked really hard to provide me with the necessary skills and knowledge to start and finally accomplish this study. His trust encouraged me to continue in good and bad times. Finally, I would like to thank all the members of the Biomimetics and Nanobiotechnology group and but especially Dr. Maria D. Chatzidaki, Dr. Eugenia Mitsou, Dr. Ilias Matis, Ms Evdokia Vassileiadi and Ms Sotiria Demisli who encouraged me on a daily basis and offered me their support and their advice, giving me the strength to continue.

I am grateful to all of those people I had the chance to work with during this and other related projects. I would also like to thank Prof. Fernando Leal-Calderon, Assistant Prof. Anna-Maria Psarra and Assistant Prof. Vassiliki Skamnaki for their contribution to this thesis. Nobody has been more supportive to me during this project than my family. I would like to thank my beloved husband, John, whose love and guidance were with me in whatever I decided to follow. He supported me and inspired me in every step and remined me every day how family should be.

Contents of Figures & Tables

DMSO at a concentration of 0.063 M, DMSO/PLX C2 refers to PLX 4720 dissolved in DMSO at a concentration of 0.12 M. Standard Deviation (S.D.) was used for error bar creation.

Figure 40. Results in cell proliferation assay using HT-29 cell line after 48h after the treatment onset. DMEM and DMSO 0.1% were used as positive control samples, μ/e empty refers to o/w microemulsions without the drug, μ/e loaded refers to o/w microemulsions loaded with PLX 4720, DMSO/PLX C1 refers to PLX 4720 dissolved in DMSO at a concentration of 0.063 M, DMSO/PLX C2 refers to PLX 4720 dissolved in DMSO at a concentration of 0.12 M. Standard Deviation (S.D.) was used for error bar creation.

Figure 41. Results in cell proliferation assay using WM 164 (a) and Caco-2 (b) cell lines 48, 72h after the treatment onset. DMEM and DMSO 0.1% v/v were used as positive control samples, μ/e empty refers to o/w microemulsions without the drug, μ/e loaded refers to o/w microemulsions loaded with at 5.6μM. DPS-2 was also solubilized in DMSO at 5.6 μM.

Figure 42. Results in cell proliferation assay using WM 164 and Caco-2 cell lines 96 h after the treatment onset. DMEM and DMSO 0.1% v/v were used as positive control samples, μ/e empty refers to o/w microemulsions without the drug, μ/e loaded refers to o/w microemulsions loaded with at 5.6μM. DPS-2 was also solubilized in DMSO at 5.6 μM.

Figure 43. Results in cell proliferation assay using A549 cell line 72 h after the treatment onset. DMEM was used as positive control samples, μ/e empty refers to o/w microemulsions without the drug, μ/e loaded refers to o/w microemulsions loaded with at 5.6μM. DPS-2 was also solubilized in DMSO at 5.6 μM.

Figure 44. Confocal Microscopy revealed that the oil-phase was co-localized with the cytoskeleton in all cell lines tested within 72h. The red refers to staining with Nile Red used to label oil phase, the green refers staining with fluorescent antibody for β-actin used to label the cytoskeleton and yellow represents the merging of the two pictures.

Figure 45a,b. Diagrams of cell cycle analysis of non-treated (DMEM) Caco-2 cells and treated Caco-2 cells with either o/w microemulsion empty 0.2% v/v or o/w microemulsion loaded with DPS-2 at 5.6μM. The nuclei were stained using propidium iodide A representative experiment out of triplicate is depicted.

Contents

Chapter 1

Introduction

Chapter 1 – Introduction

1.1 Nanocarriers: Terminology and recent state

Nanotechnology is a multidisciplinary field related to the science and technology of nanosized and nanostructured materials. Nanotechnology finds application in many fields, including foods, cosmetics, coatings, materials and medicine (nanomedicine). Nanomedicine, as a term, was launched in the late 1960's, but only in the early 2000's, a significant step towards this direction was made by emerging technologies in combination with increase of funding, from international academic and industrial sources, and thus by increase of number of publications [1]. Nanomaterials are defined as materials with size range in nanoscale that possess unique physico-chemical and biological properties. As a result, nanomaterials find many applications in medicinal field, especially in diagnosis and therapy. In this context, nanomedicine enables the development, monitoring and control of nanocarriers as vesicles of bioactive compounds such as drugs, peptides, protein, nutrients, antioxidants etc., possessing significant encapsulation capacity. Recent advances report effective delivery of promising bioactive compounds to target tissues, by overcoming biological barriers. The routes of administration of delivery systems include oral, parenteral, topical, transdermal, nasal and ocular route [2,3].

Many studies have been performed considering the use of nanocarriers as drug delivery systems. Towards this approach, various types of delivery systems in nanoscale have been developed in order to overcome difficulties related to poor solubility and bioavailability of active compounds [4]. As nanocarriers are considered the materials in nanoscale (1-300nm) and are composed of biocompatible and/or biodegradable ingredients. Liposomes, nanodispersions such as nano- and micro-emulsions, Pickering emulsions, solid lipid nanoparticles (SLNs), dendrimers, biopolymer-based and organic or inorganic nanoparticles are few of recently developed delivery systems that provide promising perspectives in drug delivery and thus are currently being investigated [5,6]. Nanocarriers have been extensively studied for the transport and effective release of a variety of drugs and/or bioactive compounds with different polarity, including hydrophilic and lipophilic ones. The main target in all cases was to achieve effective

delivery, enhanced permeation in biological membranes and increased bioavailability of the encapsulated compound. Researchers in nanomedicine are more focused in the delivery of lipophilic compounds, as most of the commercially available drugs, but also the novel synthesised lead-compounds, are poorly soluble or insoluble in water. Towards this approach, nanocarriers encounter a plethora of biological barriers within the route to their target, such as blood brain barrier, gastrointestinal track and skin barrier, enhancing the transportation and permeation of the insoluble cargo [7]. In order to specify the challenges of release, especially in tumours by means of nanotechnology, it is mandatory requirement to relate the experimental design of these delivery systems with the understanding of the biological background.

In general, nanocarriers are divided into two categories, "soft" or "hard", and this classification is strongly related to their composition, physicochemical characteristics and entrapment process of bioactive compounds. In most of the cases, the incorporation of the drug is achieved through different processes such as nanoencapsulation, surface conjugation or entrapping [8]. In "soft" nanocarriers, the inner cavity operates as a "host" for bioactive molecule ("guest") and "guest" is protected and surrounded by an interface layer. This category includes microemulsions, nanoemulsions, Pickering emulsions, liposomes, dendrimers, polymer-based nanoparticles, solid-lipid nanoparticles (SLN) and nanostructured lipid carriers (NLC) (Figure 1). Soft nanomaterials are extensively used to deliver both water soluble and insoluble compounds [9]. On the other hand, "hard" nanomaterials are considered to be materials which either adsorb the bioactive compound or form a covalent bond with the bioactive compound, in their external surface. Hard nanocarriers include quantum dots, carbon nanotubes, inorganic nanoparticles and metal oxides. [10].

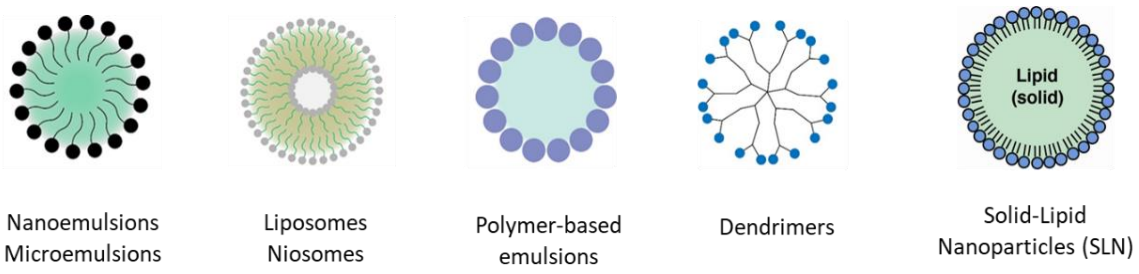

Figure 1. Types of "soft" nanocarriers [11].

Nanocarriers have been in the center of interest for many research groups in terms of the delivary and effective release of a variety of drugs and/or lead compounds against inflammation, pathogenic microbia and cancer [12,13]. Delivery systems have attracted researchers' interest by affecting pharmacokinetics and biodistribution of drugs, providing perspectives for future applications. The principle aim, in the majority of studies, is the development of biocompatible and/or biodegradable delivery systems that could enhance the penetration of drugs within biological barriers and, at the same time, increase drug's bioavailability and nanocarriers' lifetime in blood circulation [14]. Recently, nanocarriers emerge as a promising approach towards cancer treatment. Although strategies for chemotherapy have been improved, there are still cases of patients that despite their treatment, presented low chemosensitivity [15]. In particular, most of the commercially available chemotherapeutic drugs, are slightly soluble or insoluble in water. This problem of solubility of the drugs, led to administrating high dosages and consequently leadind to toxic side effects. As a result, there is an urgent need to improve drugs' bioavailability through the rational design of nanoformulations and by investigating permeation and release mechanisms.

The foremost target of this thesis was the formulation of nanodispersions (micro- and nano-emulsions) as effective vesicles of transport of bioactive substances with pharmacological interest and investigate their effectiveness in selected biological systems. Microemulsions and nanoemulsions are considered as colloidal nanodispersions that can be formulated by mixing water, oil and surfactants. In this context, through *in vitro* and *ex vivo* experimental approaches, the mechanism of transport and their effect on the selected biological target was clarified, with an emphasis on the treatment of melanoma.

1.2 Nanodispersions: Theory and physico-chemical properties

1.2.1 Microemulsions

The term microemulsion refers to thermodynamically stable, optical isotropic colloidal systems which are formed spontaneously by mixing oils, surfactants and aqueous phase, as defined by Danielsson et al [16]. Mixtures of these three

components can be formed by varying their composition and environmental conditions (temperature, pressure). The microemulsions were first reported in 1943, when T. P. Hoar et al. combined a milky solution and hexanol to produce a homogeneous, monophasic formulation [17,18]. Up to 1960, microemulsion research had been broaden, by studying the mechanism of formation of microemulsions but also understanding the physicochemical background [19,20].

Microemulsions consist of aqueous phase, oil phase and surfactants. The term "oil" describes any liquid which is insoluble in water. As "oils" different compounds and mixtures can be used, depending on the type of application that microemulsion is proposed for. In food, cosmetic and pharmaceutical industry, the oils that are used for the formulation of microemulsions are safe and biocompatible oils such as olive oil (extra virgin and refined), sunflower oil, soybean oil, medium chain triglycerides, isopropyl myristate, isopropyl palmitate, but also essential oils (limonene, thyme, oregano etc.) [21].

As surfactants or emulsifiers, are defined the amphiphiles that contribute in the formation of nanodispersions in general, as they exhibit two regions of different polarity. Surfactant molecule is composed of a polar head, which is oriented towards the aqueous phase and a non-polar tail, which is oriented towards the oil phase. Due to the existence of surfactants, the interface between the two miscible liquids is increased and thus, the aqueous and oil phase are dispersed within each other as the the surface tension between these two phases decreases. However, the presence of surfactants is not always capable of reducing sufficiently the surface tension, which is the reason why co-surfactants are often used. Co-surfactants are amphiphiles, that are widely used in a variety of applications such as food, cosmetics, pharmaceutical application etc. The cosurfactants that are commonly used are medium chain alcohols, as it has been reported that they reduce the interfacial tension and increase the flexibility of the oil-water interface, so the entropy of the system is also increased [22].

Based on their structure, microemulsions are divided into three main categories: water-in-oil (w/o), oil-in-water (o/w) and bi-continuous structures (Figure 2) [23]. In the first case, water droplets are dispersed in the oil phase and surfactant molecules are leaned with their polar head towards the aqueous phase and their non-polar tail towards oil phase (reverse micelles). On the contrary, in oil-in-water microemulsions, oil droplets are dispersed in the aqueous phase and surfactant

molecules are leaned with their polar head towards the continuous aqueous phase and their non-polar tail towards the dispersed oil phase. Bicontinuous microemulsions contain comparable quantity of water and oil and the surfactant molecules are less tightly packed than those in reversed or swollen micelles. As a result, this type of microemulsion can be described by extended structure of continuous water and oil regions, separated by surfactant monolayers [24–26].

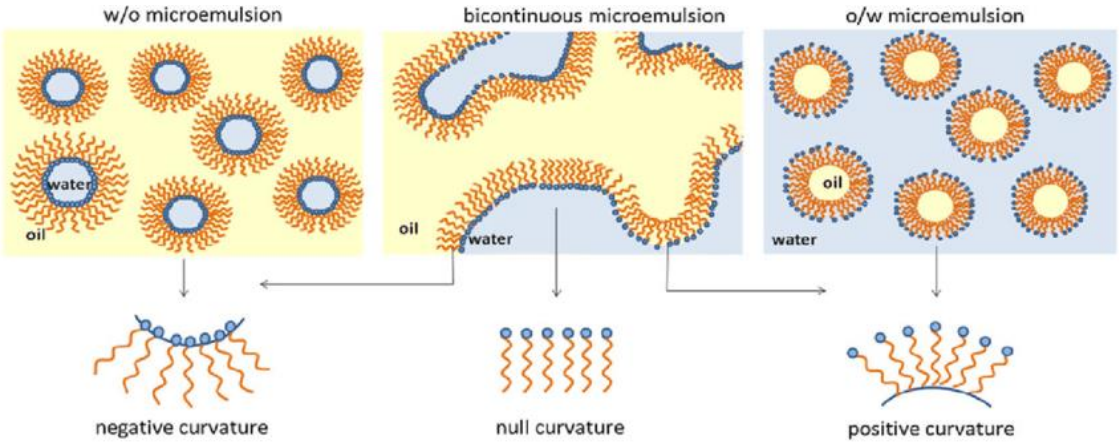

Figure 2. Classification of microemulsions including w/o microemulsions, bicontinuous and o/w microemulsions [27].

The interfacial tension between the aqueous and oil phases is significant low and provides many advantages to such formulations. Microemulsions can be spontaneously formed, and thus they present thermodynamic stability. As external energy is not necessary for producing such formulations, simplicity of production contributes to the potential application of microemulsions in many industrial processes and consumer products. Microemulsions are capable of encapsulating lipophilic, amphiphilic or hydrophilic compounds, depending on their type (o/w microemulsions, w/o microemulsions, bicontinuous microemulsions). Moreover, microemulsions provide increased solubilization and bioavailability of insoluble or slightly soluble drugs and they are proposed for potential permeation enhancement, in many biological barriers [28]. Microemulsions can find application in various fields, including drug delivery, food, cosmetics, nutraceuticals etc. [2].

1.2.2 Nanoemulsions

The last decades, various research groups have been interested in the formation of nanoemulsions. Nanoemulsions are colloidal dispersions consisting of two immiscible liquids (water and oil) and surfactants. One of two liquids is dispersed in the form of nanodroplets (dispersed phase) in the mass of the other liquid (continuous phase). The dispersed droplets are spherical, in terms of shape, with a diameter usually ranging from 50 to 200 nm and thus, nanoemulsions can appear clear or slightly turbid. They are kinetically stable in contrast to microemulsions, which exhibit thermodynamic stability [29]. Nanoemulsions, are described in literature as "*non-equilibrium*" systems, that cannot be formed spontaneously. Thus, energy contribution is necessary to obtain a formulation stable against various destabilization processes. The commonest methods that are performed for the formulation of nanoemulsion are either high energy methods (high pressure homogenization, ultrasonication) or low energy methods (PIT; phase inversion temperature, self-emulsification, EIP; emulsion inversion point) [30]. The different approaches used to formulate nanoemulsions, are described in paragraph 1.2.4.

Nanoemulsions are characterized by small droplet size, in comparison to the wavelength of light and this property allow them to be either clear and transparent (such as microemulsions) or turbid. In addition, as their size is ranged in nanoscale, nanoemulsions resist in separation or nanodroplets aggregation compared to macro-emulsions. The size distribution of nanodroplets is affected by various factors; In high energy methods the size distribution is influenced mainly by the duration of emulsification and the amount of external energy that is provided. In low energy methods the size distribution is influenced mainly by the selected composition, the surfactant type, the relative amount of each component and the conditions of the experiment [31].

The scientific community had adopted the term "microemulsion" several years ago, generally for emulsions whose droplets are on a sub-micrometer scale. For historical reasons and since microemulsions have been studied earlier than nanoemulsions, these definitions have prevailed, although in nanoemulsions the average diameter of nano-droplets is higher than the average diameter of microemulsions. The first scientific article that used the term ''microemulsion'' was

released in 1961 while the first scientific article that used the term ''nanoemulsion'' was released in 1996 [19,32]. Nanoemulsions, similarly to microemulsions, find applications in many fields including food, pharmaceutical, cosmetics and agrochemical industry [33,34]. Their lower content of surfactants, compared to microemulsions, gives to nanoemulsions many advantages, especially in cases where the concentration of surfactants is subject to legislative restriction.

1.2.3 Surfactants

Surfactants are amphiphilic compounds that are composed of two regions in their molecule, possessing different polarity; a polar head and a non-polar tail (Figure 3). Surfactants are divided into two categories, depending on the existence and type of charge, on the polar head of the molecule. The classification of surfactants is listed as follows: (a) when the polar head possess no charge surfactant is described as non-ionic; (b) when the polar head possess charge surfactant is described as ionic. The second class consists of three distinct subcategories, namely; anionic surfactants when the polar head has a negative charge; cationic surfactants when the polar head has a positive charge; zwitterionic surfactants when the polar head contains both positive and negative charges [35].

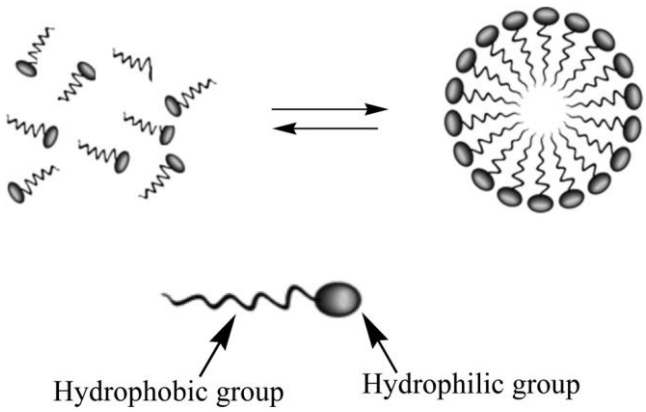

Figure 3. Schematic structure of a surfactant molecule when forming micelles, presenting two regions of different polarity [36].

In general, the use of surfactants for pharmaceutical and drug delivery purposes is limited due to toxicity issues. Non-ionic surfactants are more favorable in medical and food applications, as they are proven to be more biocompatible compared to ionic ones [37]. Even when dealing with non-ionic surfactants, the toxicity aspect is a parameter that needs to be clarified, especially when formulation contains high surfactant concentrations. In this context, toxicity levels may significantly vary, when comparing different non-ionic surfactants [38,39]. In this context, the formulations that are proposed for pharmaceutical and drug delivery applications, are consisted of surfactants characterized as non-toxic and safe ("GRAS"). Furthermore, selection of the appropriate surfactant is very important, since the use of high surfactants concentration may result in non-biocompatible systems.

Surfactant-based delivery systems have been in the center of interest, reporting the role of surfactants especially in the structure and phase behavior of micro- and nano-emulsions [40]. Surfactants adsorb at the oil-water interface, depending on their solubility, since their molecular structures possess polar and non-polar regions. The interfacial tension, between aqueous and oil phase, is reduced by the addition of surfactants and thus, this parameter plays a major role to the increase of the interfacial area between the two phases [41].

The "*packing*" of the chosen surfactants at the oil-water interface verifies the inclination of the surfactants' monolayer to curve either towards water or towards oil phase. Thus, for hydrophilic surfactants, the interfacial area covered by polar heads is considerably larger compared to the non-polar tails and the monolayers' curvature is around oil resulting in oil-in-water micro- and nanoemulsions. For more lipophilic surfactants, the interfacial area covered by non-polar tail is considerably larger compared to the polar heads and the monolayers' curvature is around water resulting in water-in-oil micro- and nanoemulsions [42].

Hydrophilic-Lipophilic Balance (HLB) is a parameter used to evaluate the emulsification properties of a surfactant or of a blend of surfactants. HLB scale is generally used to determine the relative degree of hydrophilic and lipophilic character between the polar and the non-polar groups of a nonionic surfactant molecule. HLB values range between 0 to 20, where values below 10 describe surfactants which tend to be more lipophilic and values above 10 describe surfactants which tend to be more hydrophilic. Thus, HLB value may help to foresee the type of

microemulsions/nanoemulsions that surfactant will promote. More specifically, a lipophilic surfactant promotes the development of water-in-oil microemulsions/nanoemulsions and a hydrophilic surfactant promotes the formulation of oil-in-water microemulsions/nanoemulsions [43].

The presence of surfactant enables the formation of molecular assemblies, namely micelles. Macroscopically, nanodispersions appear homogenous but due to the formation of micelles they are considered as micro-heterogeneous. The minimum concentration in which micelles are formed, is defined as the *critical micelle concentration* (CMC). Above this concentration, surfactant molecules and micelles co-exist in a dynamic equilibrium [44]. Hydrophobic effect is the main driving force for the formation of micelles, as the interface between water and oil is predisposed to reduce due to the amphiphilic nature of surfactant molecules; their non-polar tails are leaned towards the oily core, whereas their polar heads are leaned towards the aqueous phase [45]. The determination of CMC may give useful information about the interactions of surfactants, as the CMC value depends on mixture composition but also on buffer pH, temperature, ionic strength of electrolyte etc.

1.2.4 Emulsification Methods

As described above, microemulsions and nanoemulsions are colloidal dispersions, possessing different properties. Microemulsions are formulated spontaneously by mixing aqueous phase, oil phase and surfactant at specific ratios and thus, are thermodynamically stable and remain transparent and monophasic in specific conditions. Nanoemulsions can be formulated using different approaches, but generally the methods can be classified either as high-energy or as low-energy methods, depending on the providing amount of external energy. In general, external energy is required to increase the interface, $\Delta A*\gamma$, where ΔA represents the expanding in interfacial area and γ refers to the interfacial tension. Interfacial tension γ is positive, and as a result the energy that is needed to increase the interface is also positive. The term $\Delta A*\gamma$ does not balance the entropy factor $T\Delta S$ (which is also positive) and the total free energy of formation of a nanoemulsion, ΔG results positive:

$$\Delta G = \Delta A * \gamma - T * \Delta S$$

Thus, to formulate a nanoemulsion is not a spontaneous process and consequently, either the input of external energy is necessary or a substantial amount of surfactant, to produce the nanodroplets. Surfactants have a significant role in the formulation of nanoemulsions, as they decrease the interfacial tension γ, and consequently decrease the Laplace pressure (the difference in pressure between the core and the external environment of the droplet). As a result, the energy which is needed to reduce the size of a droplet is also decreased as the surfactant content increases [29,46]. The formation of droplets in microscale, for example in the case of macro-emulsions, is much easier and can be achieved by mechanical stirring in case of nanoemulsions though, higher amount of energy or higher quantity of surfactants is needed to obtain droplets in nanoscale.

The formulation of nanoemulsions by performing high energy emulsification procedures can be achieved, using different techniques such as; high shear stirrer, high pressure homogenizer or ultrasonic devices (Figure 4). In literature, many studies have been performed to relate the size of nanodroplets with the type of surfactant, the power of applied pressure/stirring or ultrasound, the number of cycles (in case of high pressure homogenization) or emulsification time [47–49]. In general, the size of nanodroplets depends on the time of emulsification procedure; the longer lasts the emulsification, the smaller nanodroplets can be obtained. Moreover, it has been stated that the size of nanodroplets also depends on the power applied by the device [30,48].

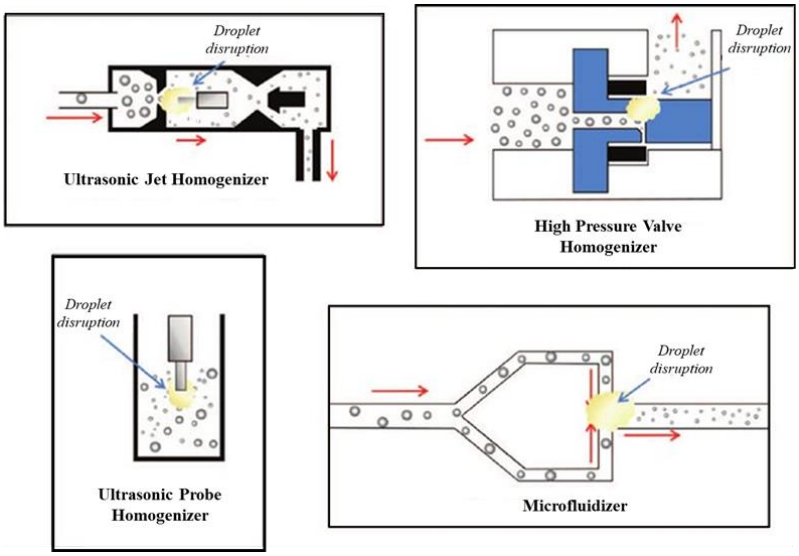

Figure 4. Devices that can be used for the formulation of nanoemulsions by applying high energy methods [50].

The principles of high pressure homogenization are based on the high pressure that is exerted on a dispersion system of two immiscible liquids, as it is pumped through a valve, reducing the diameter of the dispersed droplets. The strong shear stress facilitates the formulation of very small nanodroplets in a range of 50-200nm. Initially, the components are mixed while stirring to form a macro-emulsion. The mix enters the valve at a low speed and the pressure is then generated by the pump that causes the sample to flow through the stream. Then, the formulation flows in high speed and due to the droplets' break up, which is promoted by the high pressure, the procedure results in the reduction of the droplets' size [51]. Similarly, micro-fluidizer provides an equivalent magnitude of pressure generated by a pump. The droplet size is reduced due to high agitation caused by the collision of two impacting jets. The micro-fluidizer technique is based on the flow of a macro-emulsion into two streams, and then the two streams are redirecting in a chamber. In this chamber, the two streams of emulsion collide upon each other, resulting in droplets' size reduction due to high agitation and shear caused by this collision [52].

Ultrasonic emulsification is a technique that produces high shear forces which are generated by high-power ultrasound. Initially, ingredients are mixed while gentle stirring to formulate a macro-emulsion. Then, an interfacial acoustic wave enables the droplets of one phase to disperse into continuous phase. Droplets furtherly break up through cavitation, due to the effect of acoustic waves and the produced formulation is characterized by droplets sized in nanoscale [53].

Low energy methods can also provide stable nanoemulsions by phase inversion technique (PIT), self-emulsification, emulsification by applying low shearing, emulsion inversion point (EIP) method [54,55]. The alterations in parameters such as temperature, pH value and salinity while stirring, may lead to the conversion of an oil-in-water emulsion to a water-in-oil emulsion and vice versa, as these parameters alter the spontaneous curvature of the surfactant's layer [56]. Self-emulsification is an alternative method, as through the dilution of a microemulsion with continuous phase at constant temperature, a nanoemulsion is formulated without any phase transitions (Figure 5) [57]. By applying low shearing, nanoemulsions can be formulated in low

energy conditions, using a Couette cell, an emulsion is submitted in a shear rate and subsequently, by this technique, polydisperse emulsion droplets are fragmented and fine nanodroplets are formed [55,58]. Emulsion inversion point (EIP) method describes the formation of nanoemulsions, based on the impulsive formation of nanodroplets as a result of changing the composition in a mixture of oil, water and surfactant [59]. Low energy methods possess advantages when compared to high-energy techniques as they have lower cost in terms of equipment and energy input. In contrast, their use presents restrictions and limitations, such as choosing the suitable combination of oils and surfactants to form stable nanoemulsions.

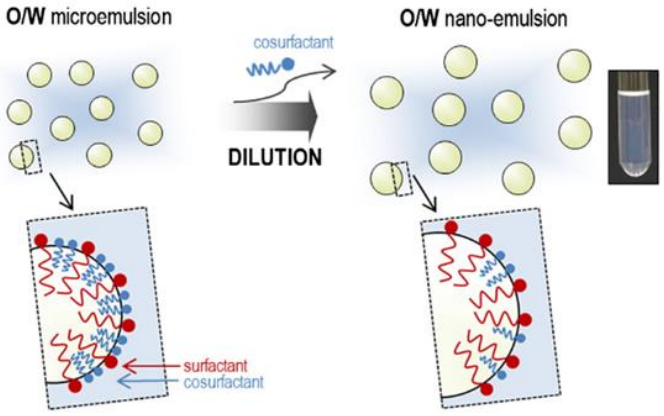

Figure 5. The mechanism of self-emulsification by dilution of an o/w microemulsion [54].

1.2.5 Destabilization phenomena

Nanoemulsions, as kinetically stable formulations, separate in two phases during storage time. There are various destabilization mechanisms occurring, namely flocculation, coalescence, Ostwald ripening and creaming/sedimentation (Figure 6). As nanoemulsions are not thermodynamically stable, their free energy is reduced when the droplet size increases, due to the decrease of the interfacial area. The sufficient time needed to phase separation is affected by various factors such as ingredients combination, surfactants concentration, temperature, ionic strength or pH value, but still nanoemulsions present greater stability compared to conventional macro-emulsions.

Although both flocculation and coalescence refer to nanodroplet aggregation, there are significant differences between these two destabilization mechanisms. When flocculation occurs, the nanodroplets collide to each other, creating aggregations. In this state, nanodroplets are not combining but stick together and move as an entity. Flocculation is more likely to happen when intermolecular repulsive forces between the droplets are strong enough to keep the two droplets separated, so aggregates are formed. On the other hand, when coalescence occurs, the nanodroplets fuse to each other and merge to create bigger droplets. In this case, interfacial film collapses and the two droplets are combined. These two phenomena are based on colloidal interactions between droplets including Van der Waals interactions, electrostatic forces and hydrophobic interactions [31,60].

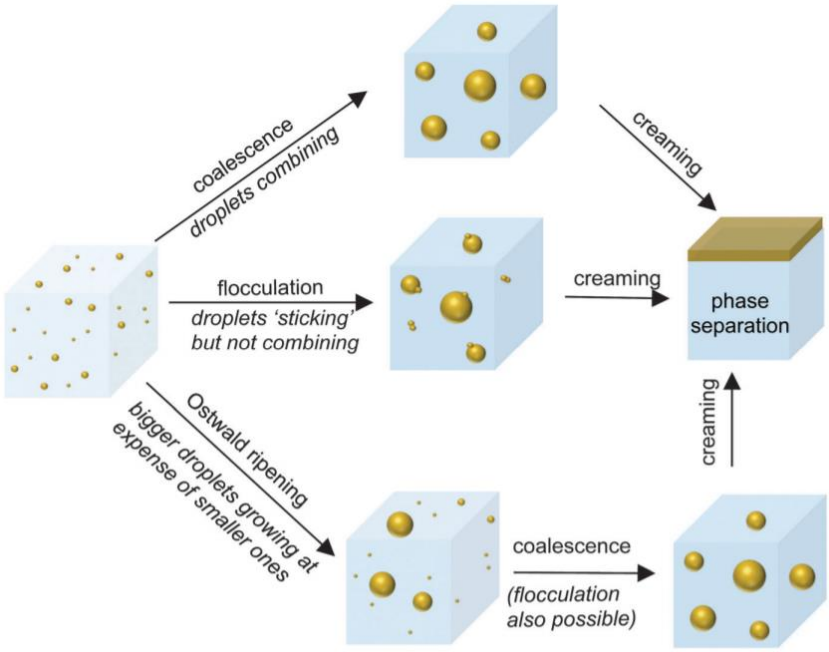

Figure 6. Schematic representation of nanoemulsions' destabilization mechanisms [61].

Ostwald ripening is a destabilization mechanism that describes the increase in size of a nanodroplet to the detriment of the smaller ones. Although it is an irreversible incident, Vincent et al. suggested a criterion to predict and evaluate the deterioration of a nanoemulsion through this mechanism [62]. This phenomenon occurs due to the difference in the Laplace pressure between nanodroplets that have different diameter. As a result, the dispersed phase transports from smaller to larger nanodroplets [62,63].

Destabilization due to Ostwald ripening, is an irreversible state and thus, many studies have been performed to predict the rate or the possibility for this phenomenon to occur. Lifshitz, Slyozov and Wagner proposed the leading order theory (LSW theory) which proposes a linear function between the cube of the radius, r and time, t. As a result, Oswald ripening rate can be predicted through the gradient of the diagram [64]. In general, the main parameter that affects the stability of a nanoemulsion against Ostwald ripening is the degree of solubility of the oil phase in water; The more soluble is the oil phase in water, the more likely for Oswald ripening to occur [65,66]. Overall the average radius of the emulsion droplets increases over time, until nanoemulsion collapses. Therefore, Ostwald ripening is a phenomenon that affects the long-term stability of nanoemulsions.

Creaming or sedimentation describes a destabilization mechanism, where the dispersed droplets collapse across the continuous phase due to the gravity force. As a result, nanodroplets precipitate at the bottom and this phenomenon leads progressively to phase separation. This process is strongly connected to coalescence as it can occur either at the same time or after coalescence. In this aspect there are various factors that affect this phenomenon such as droplet size, ratio of dispersed phase, viscosity, and type of surfactants [67].

1.2.6 Microemulsions versus Nanoemulsions

Microemulsions and nanoemulsions are colloidal dispersions that present similarities and differences, in terms of formulation, physicochemical properties and structure. In literature, there is often a misunderstanding to distinguish these two different delivery systems, as both micro- and nanoemulsions' droplets are described by sizes that range in nanoscale and find application is similar fields.

Microemulsions are colloidal nanodispersions, consisting of water, oil, and amphiphile molecules and their nanodroplets size ranges between 5-50nm, according to literature. In this respect, microemulsions are formulated spontaneously by simple blending of the ingredients and formulations remain stable under specific conditions (temperature, pressure, pH value, salinity etc.). Thus, microemulsions are affected and propably destabilize by condition changes or upon dilution. Formulation and stability issues against condition alterations, play an important role especially when potent

application of microemulsion is designed. For example, in oral administration the formulation passes through gastrointestinal track, where pH value is altered in stomach or intestinal epithelium. The passage through this route may affect the stability of the formulation, which in some cases may lead to collapse. Moreover, in parenteral administration, the formulation is diluted in blood and it is substantial to monitor if this dilution affects microemulsions stability [68].

As described above, microemulsions are formed spontaneously and are thermodynamically stable formulations, as the free energy of the monophasic system is lower than the free energy of the bi-phasic system (Figure 7). In some cases, due to the existence of energetic barriers (e.g. activation energy), it is necessary to agitate gently or even heat the mixture of the ingredients to obtain a monophasic, transparent formulation [29]. Nanoemulsions are colloidal nanodispersions, consisting of water, oil, and amphiphile molecules and their nanodroplets size ranges between 50-200nm. In the literature, there is misunderstanding about the droplets size range proposed to differentiate a nanoemulsion from a macro-emulsion [69]. A nanoemulsion is a thermodynamically non-stable formulation so it is expected to collapse during storage. As a result, the formulation of nanoemulsion requires the imput of external energy, as in terms of energy the monophasic system in this case is not favorable (Figure 7). Nanoemulsions can be formulated by performing either high energy methods or low energy methods, as described in section 1.2.4 in comparison to microemulsions that are formed without providing external energy.

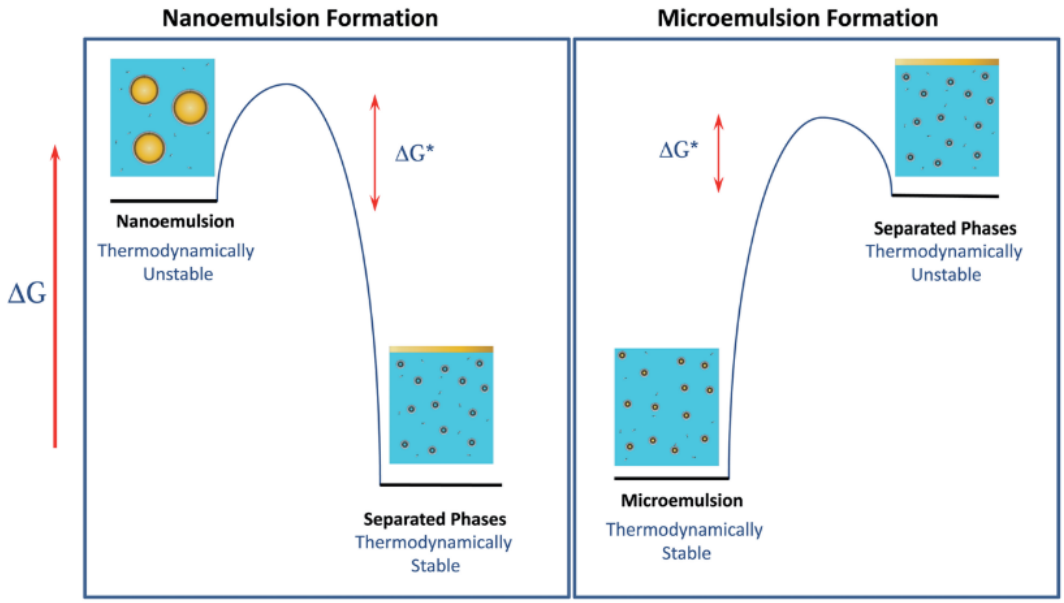

Figure 7. The free energy of microemulsions and nanoemulsions in comparison to the separate phases state. [29].

Ingredients that are chosen to formulate a nanoemulsion are quite similar to ones that are chosen for microemulsions, although used in different ratios. However, it has been reported that small surfactant molecules are frequently used for the formulation of both micro- and nanoemulsions, whereas larger ones (including polysaccharides, proteins etc.) are more likely to formulate nanoemulsions rather than microemulsions. Another important distinction between micro- and nanoemulsions is the quantity of surfactant, which is present in each nanodispersion. More specifically, the contain of surfactant in microemulsions is higher compared to the contain of surfactant in nanoemulsions. Subsequently, nanoemulsions find application in fields where the surfactant content is subject to limitations [29].

1.3 Nanoencapsulation of bioactive compounds

Nanoencapsulation as a term, refers to the technology that involves the incorporation of an active compound within a specific carrier, sized on the nanoscale. Nanoencapsulation is applied in both pharmaceutical and food industry, to control the interactions between the active ingredients but also their release in the body. In addition, nanoencapsulation ensures availability of the active compound for a specific period of time within the body, protecting it against chemical and biological degradation during formulation, use and storage. Nanoencapsulation as a process, allows bioactive compounds to be dispersed in environments of different polarity [70].

In general, a plethora of physicochemical characteristics including size of nanoparticle, size distribution, shape and morphology, compound's solubility, encapsulation efficiency and mechanisms of compound's release have been reported to be altered by different techniques of encapsulation and types of delivery systems. Subsequently, it is really important to choose the suitable encapsulation technique based on the physicochemical characteristics of both bioactive compound and delivery system. In literature, various nanoencapsulation techniques have been reported such as emulsification, coacervation, nanoprecipitation, inclusion complexation,

emulsification–solvent evaporation, and supercritical fluid. Techniques used to stabilize formulations, such as spray drying and freeze drying, have also been studied. Nanoencapsulation, as a method to entrap bioactives, offers many advantages in the field of colloids, namely; (a) increase of bioactive's solubility, (b) increase of bioactive's bioavailability, (c) protection of bioactive from chemical or enzymatic alterations [71]. For the nanoencapsulation of both water soluble and insoluble bioactive compounds, techniques such as emulsification, coacervation, and supercritical fluid technique are generally proposed. In contrast, emulsification–solvent evaporation, inclusion complexation and nanoprecipitation are techniques that are regularly applied for the nanoencapsulation of lipophilic compounds [72,73].

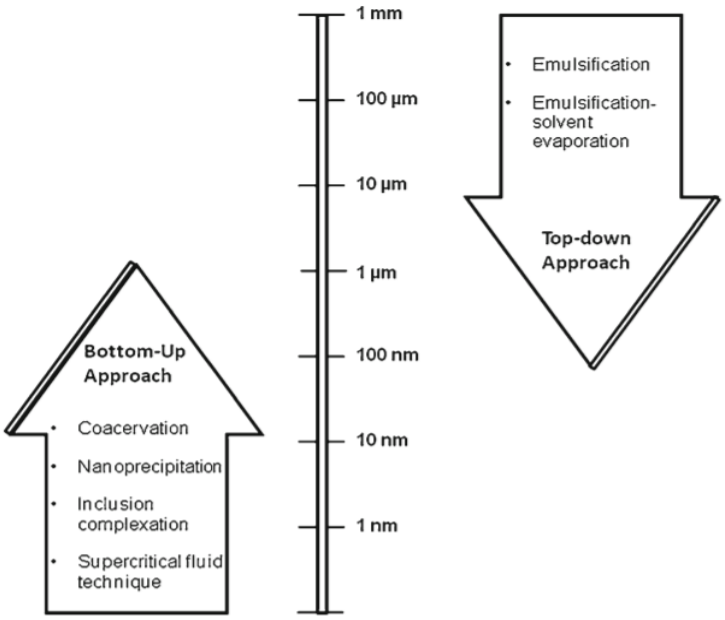

Figure 8. Classification of nanoencapsulation techniques, concerning the size of the nanocarrier [70].

Emulsification is one of the techniques performed for the encapsulation of the bioactive compounds in nanodispersions, such as micro- and nanoemulsions. High pressure homogenization, ultrasonic emulsification, phase inversion technique (PIT), self-emulsification, and emulsion inversion point (EIP) method include the emulsification methods and have been described in detail in paragraph 1.2.4. Solvent evaporation technique involves the emulsification of an organic solution of polymers

into the aqueous phase. Subsequently, the organic solvent evaporates and the polymer complex precipitates, forming structures called "nanospheres". As a technique, solvent evaporation technique is performed in mild conditions, commonly at constant temperature while stirring. Thus, this technique does not affect the bioactivity of the incorporated bioactive compound, especially in cases where the compound is sensitive in changes of temperature [74].

Nanoprecipitation technique was firstly studied and reported in 1989 by Fessi et al. In this method organic and aqueous phases, containing the bioactive compound and a natural or synthetic polymer respectively, were mixed under mild magnetic stirring. Afterwards, organic solvent evaporated at room temperature and then nanoparticles (NPs) were obtained, as a suspension in the aqueous phase. To remove the aqueous phase, either ultra-centrifugation or freeze drying was performed [75,76]. Under specific conditions, nanoparticles' aggregation may be observed, so the addition of surfactants may improve the formulation. However, this addition is likely to affect physicochemical characteristics of NPs [77].

The coacervation is a technique that refers to the phase separation of a polyelectrolyte from a solution, followed by the deposition of the aggregated hydrocolloids around the bioactive compound. The hydrocolloid's shell can be conjugated with a chemical or enzymatic agent to increase its rigidity. Through coacervation technique, nanocapsules in a range between 100 – 600 nm can be formulated. However, the size and morphology of nanocapsules, depend on the drying technique which follows the coacervation process, such as vacuum drying or freeze-drying. Freeze-drying and spray-drying techniques are performed to dry the nanosuspensions and contributes in the stabilization of nanocapsules. Natural polymers including gelatin, different gums and chitosan are frequently used as the core shell material in coacervation [78].

Inclusion complexation describes the encapsulation of a bioactive compound inside a cavity that behaves as a substrate. This binding can be achieved through hydrogen bonding, hydrophobic effect or van der Waals interactions. This technique is used to cover undesired flavors and preserve aromas and thus, is particularly proposed for the encapsulation of volatile compounds. Although inclusion complexation presents high encapsulation efficiency, only a few compounds, like cyclodextrins and

ß-lactoglobulin are commonly proposed for encapsulation through inclusion complexation method [70].

Supercritical fluids are widely used for the nanoencapsulation of bioactive compounds that present sensitivity in relatively high temperatures. As a process, supercritical fluid technique presents many similarities to spray drying. Both the bioactive compound and a polymer are solubilized in a supercritical fluid and the solution passes through an orifice. The supercritical fluid is then evaporated using spray drying process and then, nanoparticles subsequently precipitate. This technique has been extensively performed in experiments of low critical temperatures and to minimize the quantity of organic solvents [72].

1.4 Skin as a biological barrier

1.4.1 Skin structure

Skin is the biggest organ of the body and acts as a barrier that covers the whole body (approximately at a surface of 1.8 m^2). Its function is to protect the body against various pathogenic factors (chemical, biological or physical). Skin surface is one of well-studied routes for drug delivery as it allows both transdermal (systemic delivery through skin) and dermal (topical) drug delivery depending on the proposed formulation. It has been reported that nanocarriers within a size range over 10 nm are not likely to penetrate the initial skin barrier (stratum corneum-SC) so easily compared to smaller ones. Thus, the majority of nanocarriers that are suggested for treatment through skin, are relatively small. However, hair follicles are distributed in the total skin surface and they provide a significant contribution to enhance drug penetration. Even though hair follicles cover almost 0.1% of the skin surface, it has been reported that drug delivery may be accomplished via follicular route as the drug can reach sebum layer more easily than passing through stratum corneum [79].

Skin barrier is divided in two layers: (a) epidermis and (b) dermis, each providing a significant impact, in terms of skin functionality (Figure 8). Epidermis divides into four separate layers, namely: stratum corneum (SC), stratum basale (SB), stratum spinosum (SS) and stratum granulosum (SG). Thus, stratum corneum is the outer skin layer of epidermis and its thickness is 10-20μm (up to 18-21 cell layers). Despite its small

thickness, it is reported as the major barrier in skin structure and it is widely used to evaluate topical application of drug delivery systems [80]. Stratum corneum consists mainly of unviable cells, in most of the cases keratinocytes, that contain keratin and lipids. Below stratum corneum, epidermis consists of viable cells (Langerhans cells, keratinocytes, stem cells and melanocytes) with total thickness of 100μm. Unlike dermis, epidermis is not covered by blood vessels or nerve endings. In this case, topical delivery is proposed for pain-free and non-systemic drug delivery [81].

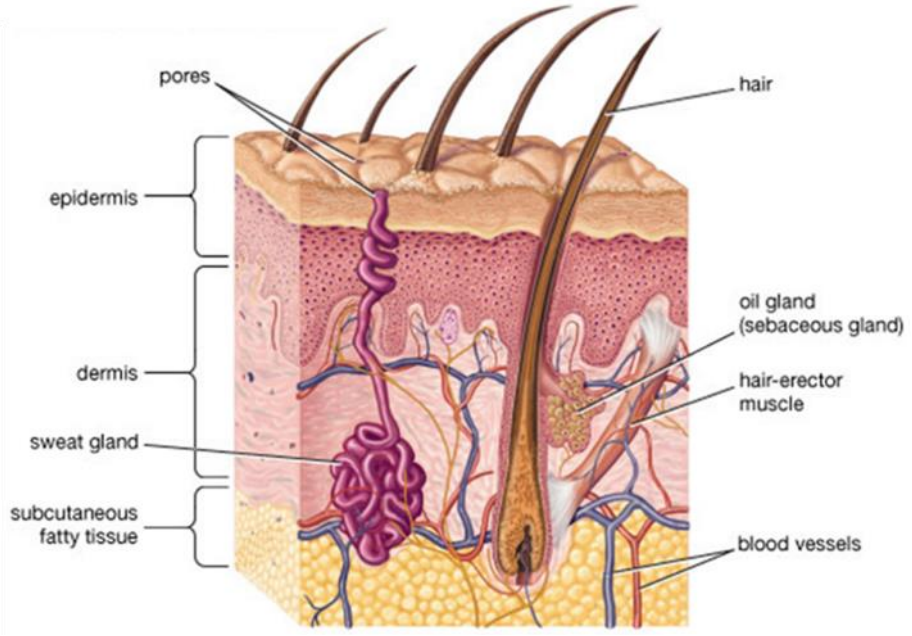

Figure 9. Anatomy of skin structure (source: www.britanica.com).

Dermis layer supports structurally epidermis layer, but also provide nutrients, and it is activated in cases of immune response. Its thickness ranges between 500-1000μm and among others, includes proteins (elastin, collagen), polysaccharides, glycosaminoglycans, blood vessels and nerve connections [82]. The diffusion rate of a lipophilic drug through dermis is approximately 1000 times higher than through stratum corneum, as it is considered more dense and low-hydrated compared to dermis. Moreover, the presence of keratin, that creates a cross-linked network of fibres, delays transport of the lipophilic drug [83]. As a result, a drug which is distributed in dermis it is likely to be delivered through systemic circulation, but this is not possible when it is distributed in epidermis.

The hair comprises a section outside the skin called the trunk and a section underneath the skin, defined as root. The trunk of the hair comes out from the surface of the skin, while root is located inside the hair follicle. In a daily basis, hair follicles produce approximately a million new keratinocytes. The main role of these cells is to synthesize keratin, a fibrous structural protein that is an essential hair component which makes them extremely resistant. At its inner base, the hair follicle has a bulb, namely dermal nipple, where several small blood vessels pass and are filled with nutrients and oxygen. Each hair follicle is coupled with at least one sebaceous gland and produce sebum to lubricate the hair (Figure 10) [84].

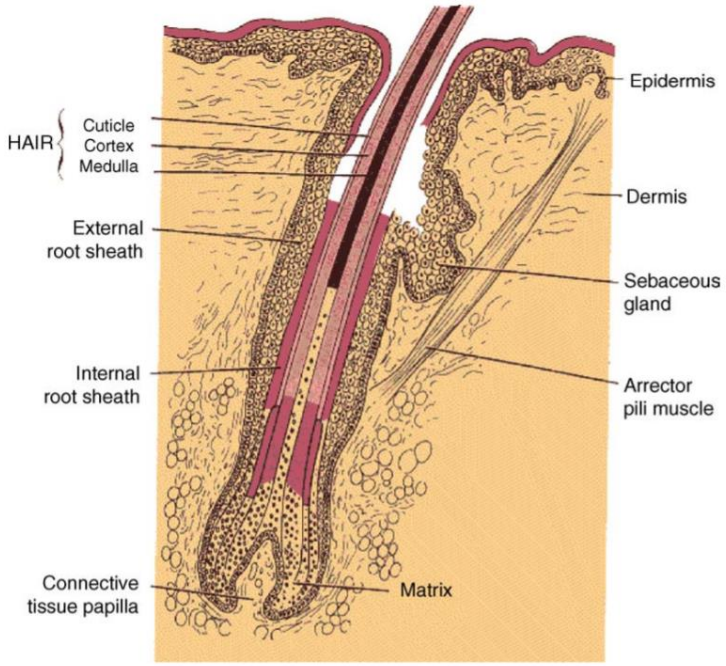

Figure 10. Anatomy of a human hair follicle [84].

1.4.2 Skin as barrier: the case of stratum corneum

Dermal penetration through stratum corneum still remains a great challenge, as it is considered the main barrier in skin structure and acts as a restricting factor for dermal delivery. Physicochemical characteristics of the loaded drug such as partition coefficient (logP), molecular mass, water solubility, and dissociation constant (pK_a) are also factors that affect drug's penetration through skin. Nanodispersions are widely studied and proposed for topical delivery as they are easy to apply as a treatment, but

they also improve patient compliance, as their application is pain-free. As long as drug is considered, the encapsulation in nanodispersions provide enhanced stability and bioavailability and decreased side effects [85].

Depending on their compositions and their cargo, nanodispersions can transport the drug to different layers of skin through different mechanisms. As shown in Figure 11, nanocarriers in general interact with biological membranes in different ways: (1) they can integrate with lipids, (2) they can pass through the spaces between the skin cells, (3) they penetrate due to osmotic phenomena, caused by the high water content beneath stratum corneum, (4) they can penetrate transcellularly (through the keratinocytes), (5) they get adsorbed to the stratum corneum and release their cargo through diffusion and (6) they pass through hair follicles and sebaceous glands [86].

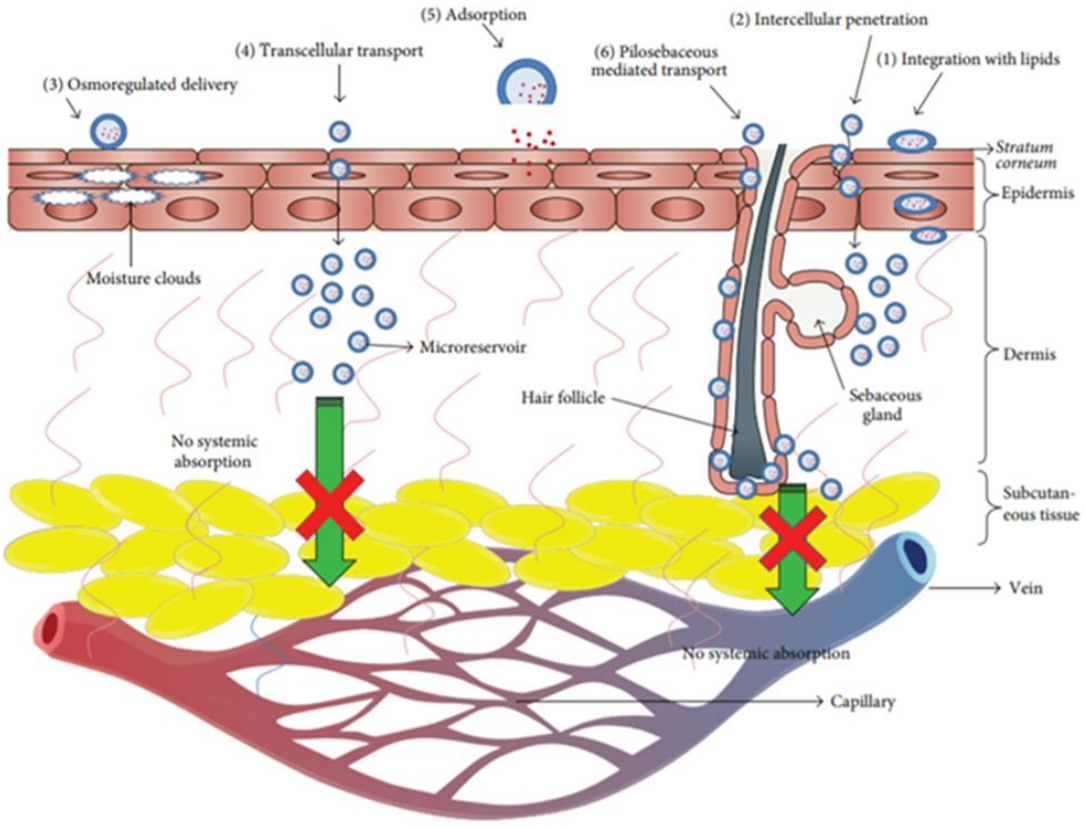

Figure 11. Different penetration mechanisms of drug-loaded drug delivery systems through skin [86].

There are three different routes that can be reached, concerning application of drugs through human skin. When the desired drug/bioactive remains at skin surface

and not penetrate into deeper skin layers, then epidermal administration is applied. This is the case for cosmetics, nutraceuticals, repellents and sun-protection creams. Topical administration is proposed when the desired effect of the drug/bioactive is observed into deeper regions of the skin (epidermis, dermis), without being distributed into blood circulation. Transdermal administration is achieved when the drug/bioactive penetrates through epidermis and dermis, but it can also be absorbed systemically and thus, can be distributed through blood circulation in other tissues. Epidermal, topical and transdermal administration are related to different factors such as skin type drug properties and physicochemical properties of nanodispersions. In terms of monitoring the type of administration, it is significant to control the described features [87].

The use of nanodispersions (micro- and nano-emulsions) but also the use of other types of nanocarriers, has opened a promising path in drug delivery through skin. In literature there are various penetration enhancers that facilitate the delivery of the desired drug/bioactive through skin layers. Various surfactants and co-surfactants (as propylene glycol), have been proposed as penetration enhancers, as they interact both with the lipids of stratum corneum and with keratin. In general, cationic surfactants are considered to be more effective as compared to anionic or non-ionic ones. However, skin irritation has been related with the effect of cationic surfactants and as a result in case of dermal route, non-ionic surfactants proven more favorable, regarded as safe.

Except from surfactants, propylene glycol, various esters and fatty acids, terpenes and terpenoids are some of the commonest compounds that are frequently used in nanodispersions proposed for skin penetration in an effort to replace common organic solvents as dimethyl sulfoxide (DMSO) [87–89]. The problem that arises by using chemicals such as DMSO, is the skin irritancy. This may occur when these chemicals are used in relatively high concentrations that are required to achieve skin penetration. Studies have reported various symptoms such as erythema, scaling, feel of burning and systemic symptoms, after application of DMSO [90].

1.5 Nanodispersions in dermal delivery

Nanodispersions (micro- and nanoemulsions) have attracted researchers' interest as potential drug carriers, because they are able to affect the pharmacokinetics and the distribution of drugs. These delivery systems present many advantages,

including enhanced penetration of biological barriers, increased blood circulation lifetime, increased solubility and bioavailability of highly lipophilic drugs [14]. Generally, nanodispersions are used to improve solubility of compounds while increasing their stability against chemical or enzymatic alterations upon storage or administration. Recent advances in nanotechnology enable delivery of promising bioactive compounds to human tissues beyond biological barriers. The routes of administration of bioactive compounds by such delivery systems to specific tissue or cell targets include oral, parenteral, topical, nasal and ocular route [2,3]. Topical delivery refers either to dermal or to transdermal drug delivery. In the case of dermal delivery, the bioactive compound is delivered through the layer of epidermis and dermis, but it does not reach blood circulation. In the case of transdermal delivery, the bioactive compound is delivered through all layers of skin and finally reaches blood capillaries through which enters the blood circulation.

1.5.1 Microemulsions in dermal and transdermal drug delivery

Transdermal and dermal delivery provide an easy and convenient self-treatment for patients. Many research groups report the enhancement of skin penetration and the increase in bioavailability of poorly soluble drugs when administrated through transdermal route. Both microemulsions and microemulsion-based gels are frequently used in dermal and transdermal administration. Shinde et al. suggested the formulation of a microemulsion-based gel, consisted of Capryol-90, Cremophor EL, Transcutol P, water and xanthan gum to improve the effect of repaglinide, a drug against diabetes, compared to its oral administration [91]. *Ex vivo* studies have also indicated skin retention of sertaconazole, an antifungal drug, when administrated through microemulsion-based hydrogel [92]. Rastogi et al. formulated and assessed a microemulsion as carrier of the transdermal delivery of E. Coli specific T4 bacteriophages against bacterial infections, by performing *ex vivo* and *in vivo* assays [93]. Savic et al. formulated microemulsion, rich in lecithin, for the effective skin administration of tacrolimus, an immunosuppressive drug, and performed *in vitro* and *in vivo* permeability studies [94]. Biopolymers such as chitosan and hyaluronic acid have been extensively used as coating agents in microemulsion formulations to enhance skin penetration [95]. Kumari et al. studied the effect of a microemulsion, that

has been coated with chitosan, for efficient dermal delivery of clotrimazole against fungi infections [96]. Similar results were obtained by Zhang and coworkers [97]. Sood et al. designed and evaluated microemulsions in ex vivo studies. The proposed microemulsions enhanced the transport of valsartan and nifedipine against blood pressure-decreasing effects, when delivery systems evaluated for *ex vivo* permeation studies [98].

Moreover, cancer treatment remains a major issue in transdermal applications. A variety of anticancer drugs and lead compounds, with potent anticancer activity, are examined for their efficacy when administrated by microemulsions. Yehia et al. performed *in vivo* studies to investigate the efficacy of a phytochemical anticancer agent, namely methyl dihydrojasmonate, when administrated via microemulsion [99]. In another study microemulsion was also prepared using triacetin, and Tween 80 with the addition of Transcutol-P as co-surfactant to encapsulate celecoxib, a non-steroid anti-inflammatory drug (NSAID). To enhance celecoxib's viscosity and retention in the skin, gel that contained microemulsion was prepared by adding carbopol 934. *Ex vivo* penetration and *in vivo* studies were performed and results indicated enhanced bioavailability of drug [100].

1.5.2 Nanoemulsions in dermal and transdermal drug delivery

Drug delivery via dermal/transdermal route helps in the reduction of dosages and ensures topical constant drug concentration for a long period of time [101]. This drug delivery route has been proposed for different diseases and pathologies including cardiovascular disease, inflammations, bacterial and fungi infections, skin cancer and others, especially in cases of lipophilic drugs. Sakeena et al. developed a palm oil ester containing nanoemulsion to entrap ketoprofen in order to overcome gastrointestinal side effects of the already existed orally administered market product [102]. Khurana et al. showed the suitability of nanoemulsion-based gels (NE gels) containing caprylic acid, for transdermal application of meloxicam (MLX). This gel exhibited enhanced skin penetration and anti-inflammatory effects when compared to MLX solution [103]. Nanoemulsion consisted of isopropyl myristate, surfactant blending of Span 20 and Tween 80 and water promoted the skin permeation of dapsone for the treatment of leprosy [104]. Alves et al., focused on the skin penetration of nimesulide from

hydrophobic gels containing nanoemulsions or other types of nanocarriers. They showed that, in case of the gel that contained loaded nanoemulsion, the drug had permeated to the dermis [105]. Nanoemulsions were also used as skin enhancers for minoxidil, a drug which is used to treat hair loss [106].

Fontana et al., aimed to develop dermatological hydrogels containing clobetasole propionate-loaded nanoemulsions in order to monitor the release of drug from hydrogels and also to evaluate the potential use of the system against dermatitis [107]. Penetration through rat abdominal skin was compared between conventional gel and nanoemulsion-gel, both loaded with aceclofenac [108]. Shakeel et al., encapsulated 5-fluorouracil in nanoemulsions and performed toxicity studies on SK-MEL-5 skin cancer cells. The results indicated that encapsulated 5-fluorouracil has an improved effect compared to solubilized 5-fluorouracil [109]. Kim et al. measured and compared the permeability of the capsaicin-loaded nanoemulsion to capsaicin ethanol solution. Skin penetration experiments were performed *in vitro* experiments using an artificial membrane as a model to human skin and *ex vivo* experiments using pig skin layers [110]. Nanoemulsion consisted of Labrafac lipophile, propylene glycol, Labrasol and Plurol oleique was formulated as carrier of nystatin. Pharmacokinetic and permeability studies showed that nystatin did not pass into systemic circulation and remained into skin layers acting as antifungal agent [111].

The *in vivo* efficacy of a nanoemulsion as carrier for paclitaxel was evaluated in rats and revealed enhanced penetration of the drug into deeper skin layer. Results also indicated an increase in bioavailability of paclitaxel in dermis up to 70% [112]. Moreover, *in vivo* study was performed for anti-inflammatory efficacy of clobetasol propionate encapsulated in nanoemulsion, suggested for psoriasis and atopic dermatitis [113]. Kuo et al., formulated nanoemulsions composed of γ-, α- or δ-tocopherol and indicated enhanced anti-inflammatory properties in CD-1 mice and increased bioavailability compared to tocopherol suspensions [114]. There are also other *in vivo* studies that reported administration of dacarbazine, encapsulated in nanoemulsions, in xenograft mouse melanoma and epidermoid adenocarcinoma models. In all cases, encapsulated dacarbazine caused significant reduction of tumor sizes compared to suspensions effect [115,116]. Hussain et al. developed nanoemulsions for topical delivery of Amphotericin B. The system was assessed, among all, for *in vitro* release of the bioactive compound, *ex vivo* skin permeation in rat's skin

and interaction with the skin through scanning electron microscopy [117]. Primo et al., studied the encapsulation of Foscan®, a chlorine derivate, currently applied in photodynamic therapy, in a novel magnetic nanoemulsion for cancer treatment. The results revealed that magnetic nanoemulsion improved the skin penetration of drug, when administered *in vivo* [118].

Some groups have worked on encapsulation of hydrophilic drugs for dermal/transdermal applications and evaluation of their permeability in skin. However, the study of transportation of hydrophilic drugs is not as extensive as the study of transportation of lipophilic drugs. *In vitro* permeability studies of w/o nanoemulsion and lecithin organogels loaded with caffeine using Franz cell, indicated improved skin penetration in case of nanoemulsion when compared to aqueous solution of caffeine [119,120]. Different w/o nanoemulsions were formulated using various mixtures of Span 80, tween 80, olive oil and water. The nanoemulsions were assessed *in vitro* for their ability to deliver inulin, through either hairless or hairy mouse skin and hairy rat skin followed by topical administration [121].

1.6 Skin cancer as a target for dermal drug delivery

1.6.1 Skin cancer types

Skin protects humans against a variety of environmental attacks, as it is constantly affected by them. UV radiation [UVA (320–400 nm), UVB (290–320 nm) and UVC (< 290 nm)], is a high-energy electromagnetic radiation that causes genotoxic effects on all living organisms and is one of the major threats of skin. In particular, UV-B may cause damage to the majority of biological macromolecules and intense inflammatory skin corruptions, such as erythema. Long-term exposure to UV-B radiation causes skin aging, suppression of immune response, induction of apoptosis, carcinogenesis and skin cancer [122]. Skin cancer can be categorized as melanoma skin cancer and non-melanoma skin cancer. The two types of non-melanoma skin cancer, namely the basal cell cancer and squamous cell cancer, are treatable either by administrating suitable medications or by surgery and the percentage of cure is significant, especially when cancer is diagnosed in early stages. On the other hand, skin melanoma is the most malignant skin cancer and refers to almost 5-7% of fatal skin

diseases and almost to 75% of skin tumor deaths. In an early-stage state, melanoma may be treated by surgery, but metastatic melanoma is persistent on standard treatments. The process of skin carcinogenesis is not totally clarified yet. However, several studies have been conducted to illuminate the mechanisms that lead to carcinogenesis and metastasis [123].

1.6.2 ERK/MAP-Kinase Pathway and the relation with melanoma

Melanoma originates from melanocytes, which are cells that produce pigment, and are located mainly at skin epidermis and other regions of the body (inner ear, bones heart and others). In the very early stages of life, during fetus development, melanocytes are created from the differentiation process of embryonic neural crest cells (NCCs). Mature melanosomes produce melanin in specific organelles, namely melanosomes, through melanogenesis, in which tyrosine oxidation products form melanin through polymerization. Then, melanosomes are transferred to keratinocytes and the life cycle of a melanocyte comes to an end through cell death [124]. The genesis of melanoma derives from melanocytes through a multi-step mechanism that leads to destructive genomic alterations. After the development of melanoma, tumor cells overrun epidermis and dermis, and ultimately penetrate the endothelium and enter the blood circulation, a state which leads to metastasis [125]. In the literature, Mitogen-Activated Protein Kinase (MAPK)/Extracellular Signal-Regulated Kinase (ERK) signal transduction pathway is strongly related to skin melanoma cases (Figure 12).

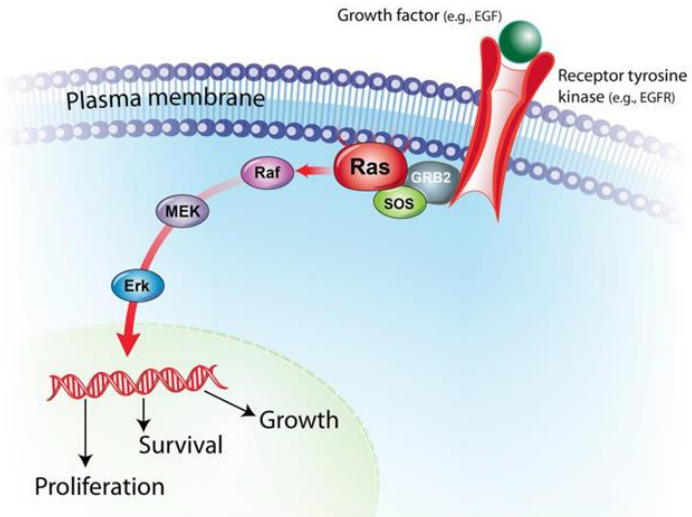

Figure 12. MAPK/ ERK signal transduction pathway [126].

This pathway regulates essential biochemical processes related to cell functions, namely cell growth, cell proliferation, cell differentiation and apoptosis. The pathway is triggered by extracellular signals including growth factors and mitogens. The activation of tyrosine kinases receptor, such as epidermal growth factor (EGF), is achieved through phosphorylation of RAS groups. RAS groups, through the signaling cascade, subsequently activate RAF proteins. The phosphorylation of RAF proteins leads to the activation of MEK, and finally various genes that get involved in different cellular processes, are induced through this signal transduction [126]. In 2002, it have been reported that various BRAF mutations have been found in more than 50% of melanomas cases. The commonest mutation occurs in codon 600 where a valine is replaced from glutamic acid ($BRAF^{V600E}$). MAPK/ERK pathway is not only related to melanomas where BRAF is mutated at residue 600, but also to other cases of melanomas that carry wild type BRAF ($BRAF^{wt}$). Interestingly, even melanomas that possess $BRAF^{wt}$, typically present different mutations that still affect upstream proteins of the MAPK/ERK pathway [127].

1.6.3 The $BRAF^{V600E}$ kinase as a target for melanoma

BRAF is an oncogene that encodes a serine/threonine protein kinase, which is activated through MAPK pathway. The commonest mutation in melanoma cases (more than 66% of malignant melanomas), as described above is $BRAF^{V600E}$ [128]. In general, $BRAF^{wt}$ kinase is physiologically activated by KRAS and then the activation of signaling cascade described in paragraph 1.6.2 follows. When $BRAF^{V600E}$ is encoded instead of $BRAF^{wt,}$ then this protein kinase possesses an uncontrolled kinase activity that leads to constant activation of MEK1/2. MEK1/2 phosphorylates and activates, through the signaling cascade, ERK1/2 and this incident causes cell-specific responses as cell proliferation, cell growth/survival and differentiation. In case of constant activation of ERK1/2, cell proliferation is constantly stimulated. Interestingly, even melanomas that possess $BRAF^{wt}$ present mutations in other genes, that encode proteins in the same signaling pathway. This fact strongly supports the suggestion that the MAPK/ERK

pathway is constantly activated in cases of melanoma pathogenesis, either by $BRAF^{V600E}$ or by other(s) mutations [129].

In recent years, different research groups have been performed studies to clarify BRAF function and role. Its regulation was affected through various types of mutations, and thus, the identification of the different mutations in BRAF and the solving of its crystal structure allowed a targeting approach (Figure 13) [130]. $BRAF^{V600E}$ kinase is a key-target for melanoma and towards this direction, various drugs or lead-compounds have been developed and been evaluated as $BRAF^{V600E}$ inhibitors (Type I, Type II and Unclassified).

The kinase conformational state is an important issue on inhibitor selectivity. In particular, in the case of BRAF kinase, the conformation of the DFG motif (Asp-Phe-Gly), is important for potential selective binding of inhibitors [90]. Inhibitors that bind to the active conformation of BRAF kinase, defined as "DGF-in", are named type I inhibitors, and interact mainly with the ATP binding site of the protein. In contrast, the type II inhibitors bind both to the ATP binding site and the hydrophobic region close to it. This conformation of BRAF kinase is described as "DFG-out" conformation [91].

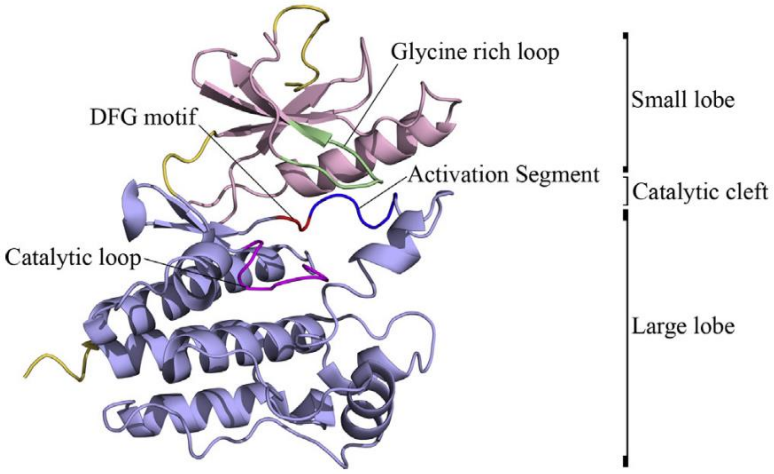

Figure 13. Structure of BRAF kinase domain. The small lobe region is depicted in light pink, the large lobe in light blue, the glycine rich loop in green, the catalytic loop in purple, the DFG motif in red and the activation segment in blue [131].

Dabrafenib and trametinib are type I ATP-competitive $BRAF^{V600E}$ inhibitors and were authorized as a treatment of metastatic melanoma by Food and Drug

Administration (FDA) in 2013. Vemurafenib (PLX 4032) is also a selective $BRAF^{V600E}$ inhibitor for metastatic melanoma. In contrast to dabrafenib, vemurafenib reached the clinical phase I trial, although dabrafenib was proved more selective to $BRAF^{V600E}$ compared to vemurafenib [132,133]. Other Type I $BRAF^{V600E}$ inhibitors that reached preclinical and clinical trials are LGX818 (Phase-I clinical trials), PLX 4720, SB-590885 and GDC-0879. In all cases, type I inhibitors were proven efficient against $BRAF^{V600E}$ but not towards $BRAF^{wt}$ [131].

Sorafenib was also evaluated as a Type II $BRAF^{V600E}$ inhibitor and through preclinical and clinical trials it was proven efficient towards various cancer types including melanoma, thyroid cancers, renal cell cancer, breast cancer, prostate cancer, hepatocellular cancer, non-small cell lung cancer. The efficacy of sorafenib is also explained as it inhibits some other kinases like VEGFR2, KIT and Flt-3, except for BRAF kinase. Regorafenib is a Type II kinase inhibitor which inhibits both $BRAF^{wt}$ and $BRAF^{V600E}$. It has been reported that it is also efficient towards other kinases such as CRAF, c-KIT and others [134]. XL281 and RAF265 are another potent BRAF inhibitors towards $BRAF^{wt}$, $BRAF^{V600E}$ and CRAF [135].

This type of chemotherapy, in many cases, is not efficient to treat metastatic melanoma due to its low chemosensitivity. Subsequently, the patient suffers from a variety of toxic symptoms due to the death of normal cells instead of cancer cells. In literature, nanotechnology contributes to the optimization of these therapeutic approaches as many delivery systems including lipid-based nanoparticles, carbon nanotubes and liposomes have been reported to be used in melanoma treatment [136]. Also, plenty of chemotherapeutic drugs against melanoma such as simvastatin, paclitaxel and piplartine have been encapsulated in nanoemulsions. However, it is the first time that $BRAF^{V600E}$ inhibitors are encapsulated and studied in micro- and nanoemulsions.

1.6.4 The role of p53 in $BRAF^{V600E}$-mutated melanoma

The p53 is the product of the tumor suppressor gene TP53, and its main role is to maintain genomic integrity . There is a plethora of genes regulated by p53 that are related or involved in the apoptotic pathways. However, the elucidation of the mechanisms through which p53-induced apoptosis is activated, still remains an issue

of intensive research. The p53 in a non-pathological state, is expressed and exists at low levels; In contrast, its expression is activated as a response to DNA damage incidents [137]. Once activated, p53 can either disrupt the cell cycle by activating p21 or lead the cells to apoptosis through various mechanisms [138]. In particular, p53 is one of the main milestones in controlling cell cycle mainly at the G1/S checkpoint but has also been reported to regulate the G2/M checkpoint. The precise mechanism of regulation remains unclear. However, it is known that both p53 and the MDM2 protein, include several post-translational modifications which facilitate the cleavage of the MDM2-p53 complex. MDM2 is an oncogene that plays a critical role in controlling p53, as MDM2-p53 complex is primarily responsible for maintaining levels of p53 [139,140]. In addition, numerous other proteins also affect p53 stability. p53 may induce the expression of specific proteins in order to regulate the passage of cells through the different phases of the cell cycle. This ability of p53 is crucial to achieve genome stability, but it also contributes to certain repair mechanisms [141].

1.6.5 Cell cycle and DNA Damage Response

As mentioned previously, the cell genome is threatened or attacked from several genotoxic agents. The cell response to these effects contributes in the inhibition or delay of the cell cycle at specific regulation checkpoints. The cell division process is divided into four distinct phases, as shown in figure 14. G_0 refers to the non-proliferating state of cells and its lastingness depend on different factors (cell age, differentiation state etc.). Thus, the cells remain in the G_0 phase for hours, days, weeks, or years. G_1 refers to the state where the cell grows in size and begins the synthesis of RNA and proteins. Moreover, in this state cells respond to extracellular signal by deciding if it will procced to division or not. Still, DNA replication has not started, before the cell enters S phase. The S phase refers to the state where DNA is replicated to produce an exact copy of the genome. As soon as replication of DNA is completed, the cell grows and produces proteins needed to ensure the successful formation of the daughter cells. Finally, the cell enters the Mitosis (M) phase where the chromosomes are organized to ensure the formation of two genetically identical cells. Thus, the cell cycle can start again, as it is potentially continuous [142].

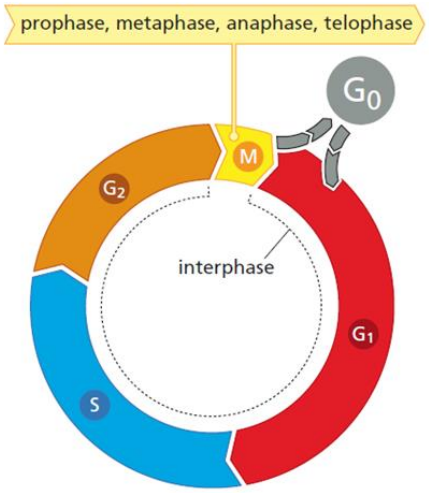

Figure 14. Mammalian cell growth and division cycle which illustrates the five distinct phases; G_0, G_1, S, G_2 and M [99].

Cell cycle inhibition is mainly caused due to an interaction of the cell with the extracellular environment and/or with neighbouring cells. The incoming messages transport through specific signal transduction paths to activate (or inactivate) certain proteins and processes. Thus, these messages are interpreted either as signals to inhibit replication or as signals to induce cell division. Through the same regulating system, DNA integrity is safeguarded. In a normal cell cycle, the passage from one phase to the next is tightly regulated by various cellular proteins.

DNA Damage Response (DDR) includes a wide network of signaling transduction pathways that are related to cell cycle regulation, DNA repair mechanisms and programmed cell death. All these factors determine the processes through which cells maintain their genomic integrity. In the case of cancer, DDR contributes to the response towards various types of genotoxic incidents caused by cytotoxic agents. The cytotoxic factors may be endogenous such as reactive oxygen species or inhibition of duplication, but they also include environmental factors such as radiation or different genotoxic substances. DDR may occur through different mechanisms such as single-strand breaks (SSBs), double- strand breaks (DSBs), or chemical modifications [143].

When DDR is activated, in an effort to repair the damage, the cell undergo through different mechanisms for repairing. This is achieved through the activation of different and distinct checkpoint pathways, either by preventing the entry into the S phase of the cell cycle (G1/S checkpoint), or by delaying S phase progression (S phase

checkpoint) or by preventing mitosis (G2/M checkpoint). Under these conditions, various repair mechanisms suitable for each checkpoint are activated, in order to slow down or even disrupt DNA replication and thus, cell proliferation. In the end, if the repair process fails, the checkpoints trigger apoptosis which can be either related or not related to p53. Therefore, the checkpoints are the primary regulators of DDR network. Unfortunately, these checkpoints are generally inactive in tumour cells, enhancing constant and uncontrollable cell growth [144].

1.6.6 Types of cell death

Programmed cell death (PCD) is a general term that refers to cell death caused through intracellular responses in any pathological state. PCD includes three different types of cell death namely apoptosis, autophagy and programmed necrosis. In particular, apoptosis and programmed necrosis regularly contribute to cell death, but in contrast, autophagy is related to pro-survival or pro-death processes, especially in cases of cellular stress, as starvation. These three types of cell death can be recognized due to different characteristics in morphology of the cells. However, in a biochemical approach, the related signaling pathways appear to combine and even connect apoptosis, autophagy and programmed necrosis (Figure 15) [145].

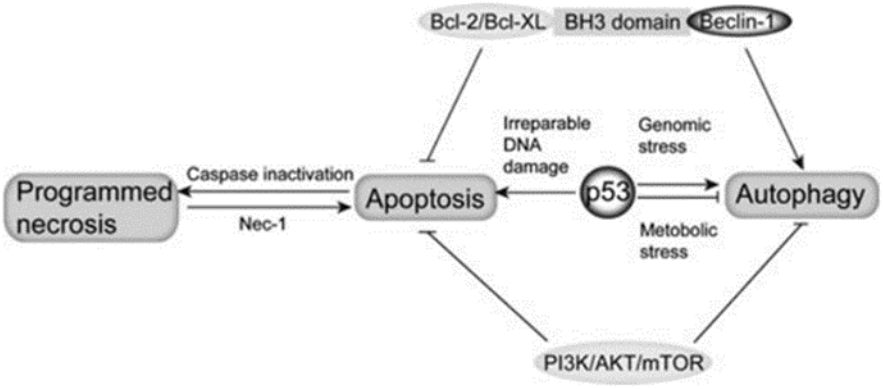

Figure 15. Relation between apoptosis, autophagy and programmed necrosis [104].

Apoptosis was studied and defined for the first time by Kerr et al. and was characterized both through characteristics in morphology and the biochemical

features. Apoptosis causes various changes in the cell including cell shrinkage, cell destruction, membrane blister and loss of adhesion to neighbouring cells [146]. Chromosomal DNA is cleaved into fragments, and also various intracellular substrates are cleaved through proteolysis. There are many signaling pathways related to apoptosis including death receptor-mediated pathways and mitochondrial-mediated pathways. The most common include regulators of apoptosis such as Bcl-2 family, tumour necrosis factor receptors, initiation of caspases (e.g. caspase 3 or caspase 9), transcriptional regulation factors such as NF-kB and p53-dependent pathways [147].

Autophagy acts as a mechanism that intent to rescue diseased or damaged cells from death, such as tumor cells. Autophagy occurs during periods of starvation or stress situations, where cells try to maintain nutrients to satisfactory levels, in order to functionalize properly. During autophagy, cells face various genetic and epigenetic defects which can be related to specific genes that activate crucial signalling pathways, such as the PI3KCI/AKT/mTOR pathway. ERK/MAP-Kinase pathway is considered to contribute in the initiation of autophagy, in combination with JNK related pathways which are activated by stress factors such as UV irradiation and oxidative stress. ERK/MAP-Kinase pathway is constantly active in most melanomas' cases due to mutations in the BRAF gene. The constant activation is mandatory for the survival of tumor by facilitating and accelerating the passage of cells into the S phase of cell cycle. ERK/MAP-Kinase pathway in combination with JNK are able to induce both apoptosis and autophagy, depending on the case. In case of autophagy, JNK pathway include activation of various target genes, such as Fox-O, ATG-genes, Bcl-2, p53-dependent and others [148].

Necrosis is described in literature as a genetically regulated cell death procedure. When necrosis occurs, it causes cellular leakage and various morphological changes such as cytoplasmic granulation and cellular swelling. Different pathways are activated during necrosis and depending on the mechanism induced, there are different kinds of necrosis namely necroptosis, parthanatos, oxytosis, ferroptosis, ETosis, NETosis, pyronecrosis and pyroptosis. Various studies have shown that these different types of necrosis are strongly related to RIPK1/RIPK3 and MLKL related pathways but also related to TNF signalling pathway, including the inactivation of caspases [149,150].

Chapter 2

Description of the Experimental Procedure

Chapter 2 – Description of the Experimental Procedure

2.1 Aim of the study

The goal of this thesis is the development of oil-in-water (o/w) nanodispersions as carriers of bioactive compounds in selected biological systems. An important part of the work concerns the formulation, the structural characterization and the biological evaluation of the developed nanodispersions. In particular, biocompatible o/w microemulsions and o/w nanoemulsions have been formulated, as carriers for drugs and lead-compounds, proposed for dermal application, especially for the treatment of skin melanoma. The encapsulation of bioactive substances, with pharmacological interest, offers them "protection" through their delivery to the target tissue and improves their bioavailability. The skin is a standard biological target system for delivery systems as it acts as the primary body's defense against a variety of environmental attacks. Efforts are focused on the development of formulations that can be administered topically to protect the skin or heal serious skin damage, including cancers. This study is divided in two categories, each of which includes the formulation of micro- or nanoemulsion, the nanoencapsulation of the bioactive compound, the structural characterization of the proposed delivery system but also the *in vitro* and *ex vivo* evaluation. The experimental part will be analyzed in detail in the next paragraph (paragraph 2.2).

2.2 Description experimental procedure

2.2.1 Formulation and structural characterization of oil-in-water (o/w) microemulsions, as delivery systems of potent $BRAF^{V600E}$ inhibitors

The target of the section was the formulation of o/w microemulsions, composed of biocompatible ingredients. These colloidal structures were proposed for the encapsulation of a commercially available $BRAF^{V600E}$ selective inhibitor, namely PLX 4720, and for the encapsulation of DPS-2, which is a lipophilic potent inhibitor of $BRAF^{V600E}$. PLX 4720 is a commercially available analogue of Vemurafenib, which is an antitumor drug against melanoma and other cancer types that are correlated with

$BRAF^{V600E}$ mutation. DPS-2 is a pharmaceutical benzothiophene derivative which was designed to inhibit the $BRAF^{V600E}$ kinase and demonstrated important cytotoxic effect towards human colon cancer cells [151]. o/w microemulsions were consisted of PBS buffer 1X as the aqueous phase, polysorbate 80 (Tween 80) as the surfactant and triacetin as the dispersed oil phase. In this context, a ternary phase diagram was conducted in order to determine the monophasic area. The microemulsion that was chosen for further study composed of 81.5% w/w PBS buffer, 10.6% w/w Tween 80 and 7.9% w/w triacetin.

The structural study was performed by Dynamic Light Scattering (DLS), Electron Paramagnetic Resonance Spectrometry (EPR) and Cryogenic Transmission Electron Microscopy (cryo-TEM). DLS technique was used to measure the mean diameter of the dispersed oil nanodroplets, but also to assess the homogeneity of the samples by measuring the polydispersity index value (PdI). The measurements were conducted in empty and loaded microemulsions with either PLX 4720 or DPS-2. Moreover, the properties of the interface of the surfactants' monolayer were studied by EPR spectroscopy using the spin-probing technique both in empty and loaded microemulsions with PLX 4720 or DPS-2. Cryo-TEM was performed to study the inner structure of the delivery systems.

2.2.2 *In vitro* & *ex vivo* evaluation of oil-in-water (o/w) microemulsions, as delivery systems of potent $BRAF^{V600E}$ inhibitors

In vitro cell proliferation assays are presented, using either sulforhodamine B (SRB) or thiazolyl blue tetrazolium bromide (MTT) test in human colon cancer cell lines (Colo-205, HT-29 and Caco-2) and in skin melanoma cell lines (WM 164). The selected cell lines possess the $BRAF^{V600E}$ mutation. The cell lines were treated with the lipophilic compounds (PLX 4720 and DPS-2) and were either diluted in DMSO or encapsulated in o/w microemulsions. The percentage of alive cells was determined photometrically, in all cases. The *in vitro* assessment was performed to determine the effect of microemulsions' compounds, and also to evaluate the efficacy of the microemulsion as a delivery system. In order to study the efficient release of a model lipophilic compound which was encapsulated in microemulsion, Confocal Microscopy was used. All the studies concerning empty and loaded with PLX 4720 microemulsions,

performed to test the efficacy of microemulsion as a potent drug carrier for topical applications. As far as microemulsion was proven suitable and efficient carrier, the mechanism of the DPS-2-induced cell death was examined through various techniques. Fluorescence-activated cell sorting (FACS) analysis, Comet assay and Western Blotting of specific biomarkers related to cell death and apoptosis, were applied to elucidate the effect of DPS-2 administrated in cell cultures, when encapsulated in microemulsion. The results showed that DPS-2 was encapsulated in microemulsion and by the time it was transported to the cells, it caused a non-apoptotic cell death. DPS-2 was not considered as an immediate genotoxic agent, however, S-phase delay was observed in both WM 164 and Caco-2 cells indicating that DPS-2 acts as a DNA replication inhibitor.

The assessment of dermal and/or transdermal absorption of bioactive compounds was examined through ex vivo approaches. In this context, an *ex vivo* permeation protocol was applied using porcine ear skin in order to assess the retention DPS-2. Permeation study was performed using modified Franz diffusion cells and porcine ear skin was used as a skin model membrane. The permeation trend of DPS-2 was obtained by calculating the percentage of drug that permeated in the receptor chamber of the cell, in relation of time. The quantity of DPS-2 was determined using LC MS/MS method. Furthermore, differential tape stripping was performed on the porcine ear skin to measure the quantity of drug that retained in the stratum corneum and in the hair follicles. Differential tape stripping also gave information about the affinity of DPS-2 to hair follicles, forming a kind of depot for prolonged delivery. Samples were analysed for DPS-2 content performing a LC MS/MS method.

2.2.3 Nanoemulsions as carriers of a model lipophilic drug: the case of Ibuprofen – Formulation, structural study and in vitro/ex vivo evaluation

The subject of the study was the formulation and structural characterization of biocompatible o/w nanoemulsions as nanocarriers, efficient for the encapsulation and transport of model lipophilic compounds with pharmacological interest. o/w nanoemulsions have been formulated, using generally recognized as safe "GRAS" ingredients, namely: distilled water as the aqueous phase, polysorbate 80 (Tween 80), Labrasol® and lecithin as the surfactant blend and medium chain triglycerides (MCT) as

the dispersed oil phase. The chosen model lipophilic drug was Ibuprofen ((RS)-2-(4-(2-methylpropyl)phenyl) propanoic acid). Ibuprofen is a non-steroid, anti-inflammatory drug (NSAID) which decreases the secretion of specific hormones that are responsible for inflammation and pain. The structural study was performed by Dynamic Light Scattering (DLS) and Electron Paramagnetic Resonance (EPR) spectroscopy. DLS technique was used to verify the mean diameter of the oil nanodroplets and to estimate system's homogeneity by measuring the polydispersity index value (PdI). Moreover, DLS provided information about nanoemulsion's stability during storage time. EPR spectroscopy was used in order to evaluate the properties of the interface of the surfactants monolayer and estimate the degree of encapsulation of Ibuprofen.

In vitro assays for cell proliferation (MTT assay), concerning empty and loaded nanoemulsions with Ibuprofen, were performed in different cancer cell lines and more specifically in MW 164 skin melanoma cell line and the Caco-2 human epithelial colorectal adenocarcinoma cell line. The percentage of alive cells was measured in order to evaluate the effect of nanoemulsions' ingredients and the effect of Ibuprofen in the selected cell cultures. Furthermore, an *ex vivo* permeation protocol was applied using porcine ear skin in order to assess the retention of Ibuprofen. Permeation study was carried out using modified Franz diffusion cells and porcine ear skin was used as a model membrane. The permeation trend of Ibuprofen was obtained by calculating the percentage of drug that permeated in the receptor chamber of the cell, in relation of time. The quantity of Ibuprofen was determined using LC MS/MS method. Furthermore, differential tape stripping was performed on the porcine ear skin to measure the quantity of drug that retained in the stratum corneum and in the hair follicles. Samples were analysed for Ibuprofen content performing a LC MS/MS method.

Chapter 3

Materials, Protocols & Methods

Chapter 3 – Materials, Protocols & Methods

3.1 Materials

Triacetin (>98%) was purchased from TCI Chemical Industry Co., Ltd. (Tokyo, Japan). Polyoxyethylene sorbitan mono-oleate (Tween 80) suitable for cell cultures 5-(1-oxyl-2,2-dimethyl-oxazolidin) stearic acid (5-DSA), is a free radical were purchased from Sigma-Aldrich (Taufkirchen, Germany). Nile Red was purchased from Sigma-Aldrich (Taufkirchen, Germany) and prepared as a stock solution of 0.2 mg/mL in triacetin. High-purity water was obtained from a Millipore Milli-Q Plus water purification system. N-(3-(5-chloro-1H- pyrrolo [2,3-b] pyridine-3-carbonyl)-2,4-difluorophenyl) propane- 1-sulfonamide (PLX 4720) 99.56% was purchased from Selleck Chemicals, USA. Dimethyl sulfoxide (DMSO) was purchased from Sigma-Aldrich, Germany. Medium chain triglycerides (MCT 65/35) were kindly donated by Stearinerie Dubois (Boulogne-Billancourt, France). Soybean lecithin 90% was purchased by Thermo Fisher Scientific (Kandel, Germany). Labrasol® ALF suitable for oral applications was kindly donated by Gattefosse (Saint-Priest, France). 16-Doxyl stearic acid [16-(1-oxyl-2,2- dimethyl-oxazolidin) stearic acid] free radical was procured from Sigma-Aldrich (Taufkirchen, Germany).

HT-29 and Colo-205 human colon adenocarcinoma cell lines were obtained from American Type Culture Collection (ATCC). All cell lines used in this study were grown in DMEM medium supplemented with 10% FBS, antibiotics and amino acids, all from Invitrogen. The human melanoma cell line WM 164 ($BRAF^{V600E}$, $p53^{Y220C}$; Wistar Institute Melanoma Research Centre) were provided by Dr. G. Skrettas (National Hellenic Research Foundation, Athens, Greece) The human colorectal adenocarcinoma cell line Caco-2 ($BRAF^{V600E}$, $p53^{null}$) and non-small cell lung carcinoma cell line A549 ($p53^{wt}$) were purchased from the American Type Culture Collection (ATCC, Manassas, VA, USA).All other chemicals used in the study were of analytical grade. High-purity water was obtained from a Millipore Milli Q Plus water purification system.

Phenol red Dulbecco's modified Eagle medium (DMEM), nonessential amino acids solution (100X), fetal bovine serum (FBS), L-glutamine (200 mM), bovine serum albumin (BSA), trypsin 0.25%, and phosphate-buffered saline (PBS) were purchased from Gibco- Life Technologies (Grand Island, NY, USA). Thiazolyl blue tetrazolium

bromide and dimethyl sulfoxide (DMSO) were obtained from Sigma-Aldrich (Taufkirchen, Germany). PI/RNase staining solution was purchased from Cell Signaling Technology (Danvers, MA, USA), radio immunoprecipitation assay (RIPA) lysis buffer from Santa Cruz Biotechnology, Inc. (Heidelberg, Germany) and the enhanced chemiluminescence (ECL) Western blotting detection reagent kit from Amersham (Amersham Life Science, Little Chalfont, UK).

Antibodies were purchased from Santa Cruz Biotechnology, Inc. (Santa Cruz Biotechnology, Dallas, TX, USA), R&D Systems (Minneapolis, MN, USA), and Cell Signaling Technology (Danvers, MA, USA). Absolute ethanol, 2-propanol, methanol and acetonitrile (HPLC grade) were obtained by Thermo Fisher Scientific (Kandel, Germany). Porcine ears were kindly donated by a local provider in Serbia, as the ex vivo experiments were performed in University of Belgrade.

3.2 Understanding the phase behavior

Phase behavior and structure are strongly related in all fields of application of microemulsions. Phase diagrams and more specifically ternary or/and pseudo-ternary phase diagrams are usually constructed to study the phase behavior of systems that consist of different components (water, oil, surfactants) at certain temperature and pressure conditions [152]. A ternary phase diagram is presented by an equilateral triangle (Figure 16). Each peak of the triangle corresponds to a 100% of one out of the three pure components or mixtures of components at constant ratio. Hence, the resulting diagram is called a ternary or pseudo-ternary phase diagram, respectively. Every point of the diagram corresponds to a certain composition of all components [153]. Microemulsions are placed in the single-phase region and their type depends on the relative quantity of water and oil. Microemulsions that contain excess of water (compared to the amount of oil) are classified as oil-in-water and ones that contain excess of oil (compared to the amount of water) are classified as water-in-oil. In literature, are found studies reporting that the use of components as ethanol and propylene glycol lead to the formation of U-type microemulsions. This type of microemulsions refer to systems that their single-phase region was extended, due to phase inversion, supported by components like ethanol and propylene glycol [154].

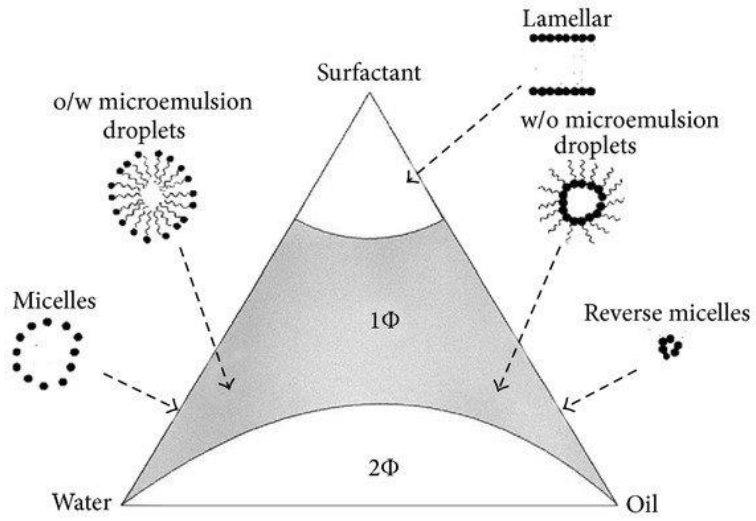

Figure 16. Ternary phase diagram that represents the phase study of a system composed of oil, water, and surfactant [152].

In the present study, in order to determine the single-phase region of systems consisting of oil, surfactant, and water, the ternary phase diagram was constructed as described below. Aqueous phase was blended with the surfactant in ratio from 9: 1 to 1: 9 wt. The mixtures were titrated stepwise with the oil phase until turbidity was observed. After each addition of oil phase, the systems were mechanically stirred and left to equilibrate from several minutes up to 24 hours in a water bath at 25° C. It is significant to mention that the quantity of oil phase that was added in each step, was determined in terms of mass and not by volume to ensure accuracy of measurements. The formulated microemulsions were stable and visually clear. Experimental data of the titration were analyzed and plotted using the ProSim Ternary Diagram software.

3.3 Structural Study of Nanodispersions

In this study, the developed micro- and nanoemulsions aim to encapsulate and deliver bioactive compounds for topical application. In any case, it is essential to study their phase behavior and physicochemical properties, as structural characteristics strongly affect biological behavior and applications. In general, determination of shape, size, size distribution, and interfacial properties of liquid drug nanocarriers are important to understand both their structure and the impact of compound's

encapsulation. For this purpose, a variety of techniques were performed, including Dynamic Light Scattering (DLS), Electron Paramagnetic Resonance Spectrometry (EPR) and Cryogenic Transmission Electron Microscopy (Cryo-TEM).

3.3.1 Dynamic Light Scattering (DLS)

Physico-chemical properties of nanoformulations micro- and nanoemulsions, play a key-contributor role especially when are proposed for biomedical applications. Dynamic light scattering (DLS) is a technique used, in principle, to evaluate the size of colloidal nanodispersions or/and suspension of particles that move by the means of Brownian motion. The Brownian motion expresses the arbitrary motion of nanoparticles within a fluid or suspension. This movement is a result of the collisions between the nanoparticles and the molecules within the fluid/solvent [155].

By performing Dynamic Light Scattering, a laser beam of He-Ne hits the nanodroplets that are moving randomly, following Brownian motion. An important finding in Brownian motion is the fact that small particles are moving faster than large particles. This finding led to Stokes-Einstein equation that relates the velocity of the nanoparticle, with its size, considering the Brownian motion. The velocity of the nanoparticle is described by a factor reported as the translational diffusion coefficient (D). The mean diameter of the dispersed nanoparticles was calculated by Stokes-Einstein's law:

$$R_H = \frac{k_B T}{6\pi\eta D}$$

where R_H refers to the hydrodynamic radius of the nanoparticle, k_B refers to the Boltzmann constant, T refers to the temperature in Kelvin, η refers to the viscosity of the sample and D refers to the translational diffusion coefficient. The translational diffusion coefficient (D) is related to size of nanodroplet, its surface structure and the concentration of the sample. This equation presents a model to determine the size of nanodroplets based on light scattering but its main restriction is that can be used only in infinitely dilute concentrations and not in highly concentrated samples [155].

When the size of nanoparticles is less (<1/10) than the wavelength of light, the scattering follows Rayleigh law and scattering is observed the same in all directions [156]. On the contrary, when nanoparticle's size is considered equal or greater compared to the wavelength of the light, then forward scattering appears more intense than backscattering. In order to detect even smaller particles, Malvern Nano ZetaSizer particle size analyzer was used, equipped by a detector that is placed at 173° angle and able to detect backscattering (NIBS technology) (Figure 17). Backscattering presents many advantages in size determination. Firstly, the light beam does not travel through the whole sample, but choses a shorter path that allows the measurement of more concentrated samples. Moreover, backscattering decreases the signal of multiple scattering in cases when particles are scattered by other particles. Finally, backscattering enhances the signal of smaller particles, as the majority of larger ones' scatter in the forward direction [157].

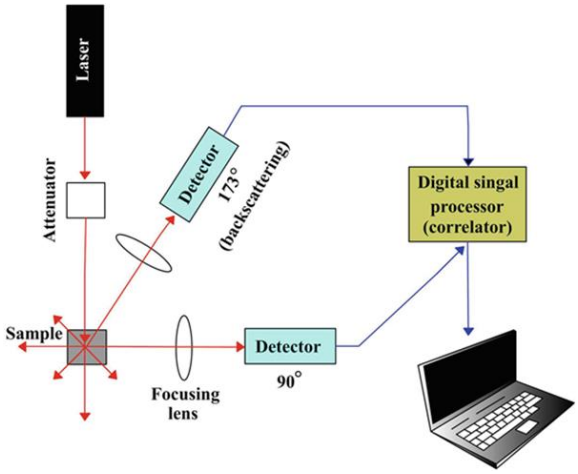

Figure 17. Schematic representation of Dynamic Light Scattering infrastructure [158].

In order to evaluate droplet size and size distribution of the nanodispersions both empty and drug loaded samples were prepared. Before measurement, nanodispersions were filtered using 0.45μm filters to obtain dust-free conditions and then were left overnight to equilibrate. Measurement data were obtained by the Malvern Zetasizer Nano software (version 6.32, Malvern Panalytical Ltd, Enigma Business Park, UK) which is equipped with a spherical model of nanoparticles. The measurements provided data about the mean diameter and the size distribution of

nanodroplets and also information about Polydispersity Index value (PdI). Polydispersity Index gives information about the degree of dispersion of nanodroplets; the lower the polydispersity index, the more monodispersed the nanosystems and vice versa. PdI values can range between 0 to 1. Regularly, PdI values below 0.3 (PdI<0.3) define a monodispersed system [159].

3.3.2 Electron Paramagnetic Resonance Spectroscopy (EPR)

Electron Paramagnetic Resonance Spectroscopy (EPR) is a spectroscopic technique based on the absorbance of microwave energy from molecules that possess unpaired electrons, in a magnetic field. EPR theory presents similarities to Nuclear Magnetic Resonance Spectroscopy (NMR) theory, as they share the same basic physico-chemical principles. Thus, since 1944, that EPR was discovered, it has been extensively used in many different fields including biology, chemistry, physics, material and food science. More specifically, EPR can be applied in many fields and applications, including the study of reactions that contain free radicals or and also structural studies on materials that possess unpaired electrons [160]. In the medical field, EPR permits the direct and non-invasive determination of micro-viscosity and micro-polarity of colloidal drug carriers such as micro- and nanoemulsions [161].

The spin quantum number that refers to spin of electrons, is equal to $m_s=\pm1/2$ and leads to a degenerative double energetic state. Inside a magnetic field, the lowest energetic state refers to the electron that is oriented in the same direction with the magnetic field ($m_s=+1/2$) and the highest energetic state refers to the electron that is oriented in the opposite direction of the magnetic field. The transition between the two states occurs when microwave energy is absorbed. The state of tuning is described by:

$$\Delta E = hv = g\beta H_0$$

where ΔE refers to difference between the two energetic states, h refers to the Planck constant, v refers to the frequency of microwave radiation, g refers to the isotropic factor g, β refers to the Bohr magneton and H_0 refers to the intensity of the magnetic field [162].

In literature, nitroxides are commonly used as compounds that possess free electrons and despite being free radicals, they present remarkable stability as their methyl groups provide chemical protection towards the nitroxide ring. In this study, 5-doxyl stearic acid (5-DSA) and 16-doxyl stearic acid (16-DSA) were used to study the interfacial properties of micro- and nanoemulsions. 5-DSA is a spin-labelled fatty acid composed of a stearic acid and a doxyl group which is bonded to the C-5 position of the hydrocarbon chain. 16-DSA is a spin-labelled fatty acid composed of a stearic acid and a doxyl group which is bonded to the C-16 position of the hydrocarbon chain (Figure 18a,b).

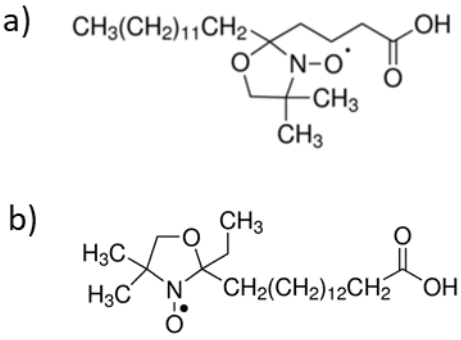

Figure 18a,b. Chemical structure of a) 5-DSA and b) 16-DSA (source: www.sigmaaldrich.com).

This molecule is brought in an alignment with the oriented surfactant molecules at the interface, subjecting the doxyl group close to the surfactant tails. The EPR spectrum of 5-DSA is affected by its microenvironment and thus any change in spectral characteristics may be associated with structural changes of the micro- and nanoemulsion before and after encapsulation. Among the parameters calculated, parameter S gives information about the rigidity of the membrane surfactants' monolayer and parameter τ_R gives information about rotational correlation time of the spin probe. Overall, spin probe's spectra can give information about the coherence of the surfactants layer, the rigidity of the membrane and the degree of compound's encapsulation [163].

Parameter S is calculated through spectra analysis and by the following equation:

$$S = \frac{(A_{max} - A_{min})}{[A_{zz} - {}^{1}/_{2}\,(A_{XX} + A_{YY})] * k}$$

where A_{XX}, A_{YY} και A_{ZZ} are single crystal values of spin probe equal to 6.3 G, 5.8 G and 33.6 G, respectively and $k = {}^{A_0}/_{A'_{0.}}$ A_{max} refers to the half distance between external lines of spectrum and A_{min} refers to the half distance between internal lines of spectrum (Figure 19). $k = {}^{A_0}/_{A'_{0.}}$ refers to the polarity correction factor, A_0 refers to isotropic hyperfine splitting constant of 5-DSA and A'_0 refers to hyperfine splitting constant for the nitroxide in the crystal state:

$$\mathrm{A_0} = \frac{1}{3}\,(\mathrm{A_{max}} + 2\mathrm{A_{min}})$$

$$\mathrm{A'_0} = \frac{1}{3}\,(\mathrm{A_{XX}} + \mathrm{A_{YY}} + \mathrm{A_{ZZ}})$$

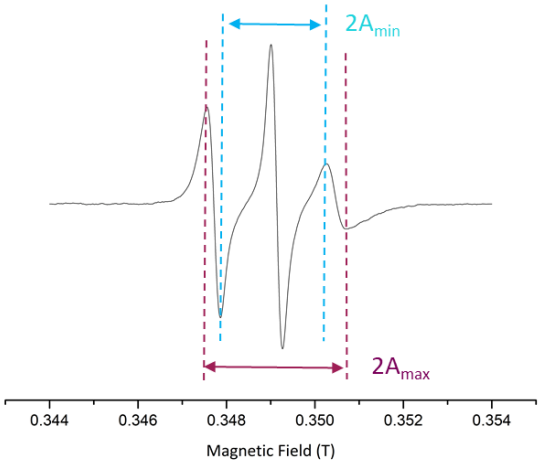

Figure 19. Spectrum of 5-DSA, presenting the parameters A_{max} and A_{min}.

Parameter τ_R is calculated through spectra analysis and by the following formula:

$$\tau_R = 6 * 10^{-10}\,[\,(\frac{h_0}{h_{+1}})^{1/2} + (\frac{h_0}{h_{-1}})^{1/2} - 2]\;\Delta H_0$$

Where h_0, h_{+1}, h_{-1} refer to the intensity of the peaks of spectrum and ΔH_0 the width of the middle peak expressed in Tesla (Figure 20) [164].

The preparation of samples for EPR measurements is described as follows. Firstly, a concentrated solution of 5-DSA in absolute ethanol was prepared at a concentration of 7.8 mM. Then the suitable quantity of the 5-DSA solution was transferred in an eppendorf and the solvent was left to evaporate. 1g of the formulation (micro- or nanoemulsion) was added and left for 24 hours at perpetual temperature (25℃) in a water bath. The samples were then introduced into a flat quartz cell and the spectra were obtained at perpetual temperature (25℃) with the Bruker EMX EPR instrument, set to: range 0.01 T, receiver gain 5.64 x 103, time constant 5.12 ms, modulation amplitude 0.4 mT, frequency 9.78 GHz. Data processing was performed using Bruker WinEPR software followed by simulation of the spectra obtained with the MATLAB program using the Easy Spin for EPR toolbar [165].

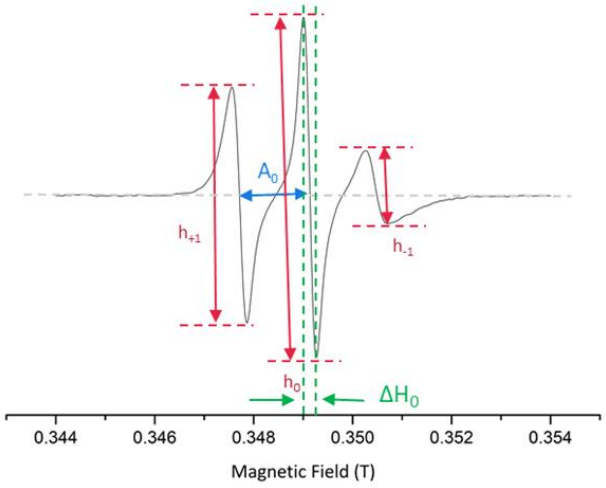

Figure 20. Spectrum of 5-DSA, presenting the parameters h_0, h_{+1}, h_{-1} and ΔH_0.

3.3.3 Cryogenic Transmission Electron Microscopy (Cryo-TEM)

Transmission electron microscopy (TEM) is one of the most well-established techniques for the evaluation of the structure of colloidal formulations (Figure 21). In Cryogenic Transmission Electron Microscopy (Cryo-TEM) the sample is freezed and the internal structure of the formulation is investigated in a frozen-hydrated state. Cryo-TEM technique may provide information about the structure of nanodroplets including morphology, size and shape. The sample is studied at temperatures like liquid-nitrogen temperatures. A beam of electrons crosses a very thin layer of sample and it

cooperates with its molecules. Then, an image of the sample is projected onto the detector. The wavelength of electrons is shorter compared to the wavelength of light and thus, a detailed micrograph of sample's structure is obtained [166]. In case of evaporation of components from the freezed formulation (e.g. water molecules), they are trapped by a decontaminator.

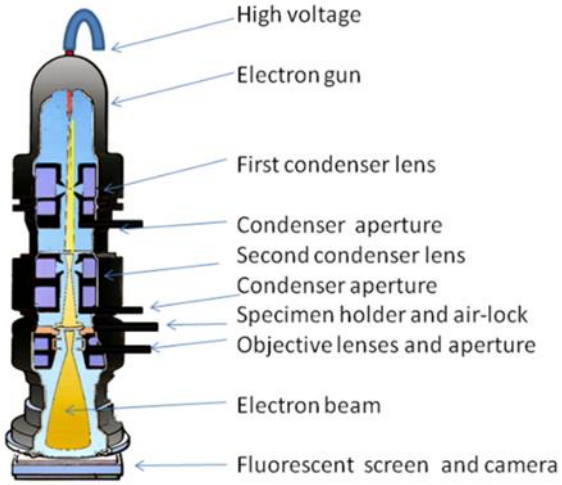

Figure 21. Transmission Electron Microscope (https://www.microscopemaster.com)

In this study, Cryo-TEM was applied to study the morphological characteristics and inner structure of the microemulsions. Samples for direct imaging with Cryo-TEM were prepared in the Vitrobot (FEI, The Netherlands) at specific temperatures and at 100% water relative humidity. 6μL of each microemulsion was positioned on a TEM copper grid covered with a punched carbon film. A filter paper was used to eliminate the excess solution and thus, a thin sample film covered the grid holes. After blotting the grids, they were extinguished in liquid ethane at its freezing temperature (−183 ◦C) and the vitrified samples were stored in liquid nitrogen (−196 ◦C). The samples were examined in a Tecnai 12 G2 TEM (FEI) at accelerating voltage of 120 kV and were recorded on a cooled high-resolution 2k × 2k Ultrascan1000 using a Gatan 626 cryo-holder cooled to below (−175 ◦C). Images were obtained on a cooled high-resolution 2 k × 2 k Ultrascan1000 camera (Gatan) with the Digital Micrograph 3.6 software (Gatan). Images were obtained under low dose conditions to minimize electron beam exposure and radiation damage. The experiments were conducted at the Faculty of

Biotechnology & Food Engineering, Technion-Israel Institute of Technology, in Haifa, Israel.

3.3.4 Viscosity

Viscosity measurements of the o/w microemulsions were obtained at a shear rate of 375 s^{-1}, using a DV-I Prime Digital Viscometer (Brookfield Engineering Laboratories, USA), equipped with core spindle (CPA-40Z). The temperature was kept stable at 25 ℃ using a water bath. Experiments were performed in triplicate for each sample, and results were presented as average ± S.D.

3.4 *In Vitro* Biological Assessment

An important issue in the application of nanocarriers in delivery of bioactive compounds is the degree of toxicity of the nanocarrier itself. As a result, *in vitro* biological assays could be performed in order to ensure the biocompatibility of the proposed systems. Moreover, the efficacy of the delivery systems should be investigated, by ensuring that the encapsulated agent successfully penetrates through cell membrane. As long as encapsulated agent has a potent anticancer action, it is important to cause similar effect upon encapsulation. Thus, clarifying the mechanism of cell death promoted by the bioactive compound is also a relevant issue. In this session, techniques that were performed to investigate *in vitro* biological effect both of nanocarriers and their cargo, are presented.

3.4.1 Cell Culture

The cells of selected cell lines are grown in monolayer cultures using DMEM as cell culture medium. The DMEM solution except from 4.5 g/L, L-glutamine and pyruvate, contained 10% v/v fetal bovine serum (FBS) and 1% v/v of penicillin/ streptomycin antibiotic mixture. For several cell lines, 1% v/v of non-essential amino acids were also added. The amount of nutrient used was proportional to the size of the culture surface, while the cells were incubated at a constant temperature of 37℃ and providing 5% CO_2 which is necessary for pH adjustment. Cells are detached from the

culture surface (T25/T75 flasks or 6-well culture plates) by the addition of trypsin. The cells are first rinsed twice with PBS 1X solution and then trypsin solution (0.25% wt. in PBS 1X) is added. Trypsin is able to hydrolyze the proteins involved in adhering of the cells to the surface, on lysine and arginine residues. The time of trypsinization depends on the cell line and usually lasts a few minutes. Detached cells in trypsin solution are collected and cell culture medium is added to prevent further trypsinization. Solution is centrifuged (1800 rpm, 5 minutes, 25℃) and the supernatant is removed. Cell pellet is dissolved in medium and a small quantity is transferred to a Neubauer plate (hemocytometer) to measure the cells.

Depending on the assay, cell pellet may be collected and in case of Western Blot, extraction of proteins is required. Preparation of whole protein extract from cell precipitate is performed using Radio-immunoprecipitation Assay buffer (RIPA buffer). Cell pellet is suspended in cold PBS 1X solution and centrifuged (1800 rpm, 10 minutes, 4℃). After centrifugation, the supernatant was removed and a certain amount of RIPA buffer, and a mixture of sodium orthovanadate (1 mM), PMSF (2 mM) and protease inhibitor cocktail is added. Mild resuspension is followed by incubation on ice for 60 minutes (performing gentle mixing every 10 minutes). By the time incubation is complete, the solution is centrifuged (10,400 rpm, 10 minutes, 4℃). The supernatant, which contains the total protein extract, can be stored at -20℃ until use.

3.4.2 Cell proliferation Assay

In the literature, cell viability assays are crucial as a first step in the process of evaluating the potent toxicity of the proposed nanodispersions. There are many protocols and assays proposed, depending on the materials used. The main idea in all protocols is to detect the cell proliferation rate using simple and quantitive methods, especially spectrometry. In this study, SRB and MTT assays were applied to determine the effect of nanodispersions' ingredients on cell lines, but also the effect of their cargo [167,168]. SRB (sulphorhodamine B) and MTT (3 - [4,5 - dimethylthiazol-2-yl] - 2,5 - diphenyl-tetrazolium bromide; thiazolylblue) are water-soluble dyes. SRB produces a pink solution and MTT produces a yellowish solution. SRB possesses two sulfonic groups that can bind to specific amino-acids in mild acidic conditions and disconnect in alkaline conditions. The binding of SRB is stoichiometric and can give information

about the relative cell mass. MTT is dissolved and converted to an insoluble violet formazan due to the cleavage of the tetrazole ring by specific enzymes, namely dehydrogenases (Figure 22).

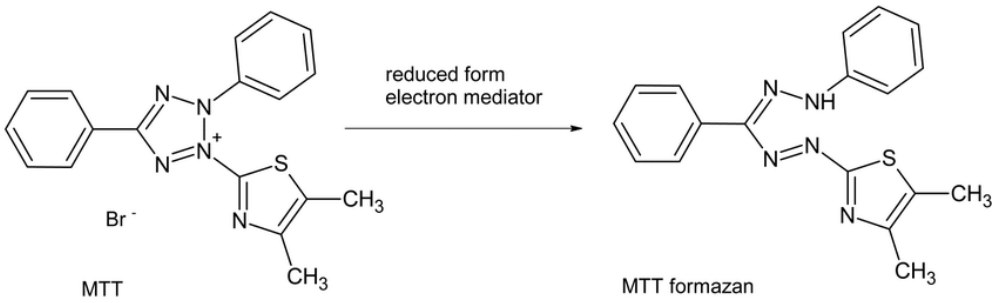

Figure 22. Reaction of MTT, catalyzed by dehydrogenases [169].

This water-insoluble formazan can be solubilized using isopropanol, dimethyl sulfoxide (DMSO) or other organic solvents, and the absorbance of the produced solution can be measured photometrically at 595nm. The absorbance measured, is proportional to the concentration of the pigment. The conversion of yellowish MTT into a formazan violet complex has been used to develop a method of determining cell viability. As shown in Fig. 23, the wells in violet indicate the formation of the formazan complex and thus, indicate the existence of alive cells. The wells in yellow showed that MTT was not converted into the formazan complex and thus, cells are not alive.

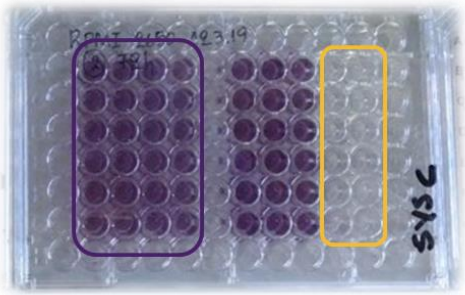

Figure 23. Picture of 96-well plate when performing MTT assay (photo of experiment of this thesis).

The principle of this method is that only alive cells have active mitochondrial dehydrogenases that can perform this enzymatic reaction, while dead cells do not. Thus, the effect of an agent on the viability and the rate of cell proliferation can be determined and therefore evaluate its cytotoxicity. The percentage of cell viability can be obtained by:

$$\% \text{ Cell Viability} = \frac{A}{A_0} * 100$$

where A represents the optical absorbance of cells in treatment, A_0 represents the optical absorbance of untreated cells (control sample) at 595nm.

3.4.3 Confocal Laser Microscopy (CLM)

Confocal microscopy was performed to observe the behavior of the microemulsion as an effective vesicle to deliver bioactives to cell populations. In general, this method provides images of good quality, but since the nanodroplets are, on most of the cases, transparent these images usually display low contrast. Laser light is directed and scanned from the rotating mirrors (Figure 24). The light then crosses the microscope and stimulates the fluorescent sample. The fluoresced light that is transmitted from the sample travels backwards across the microscope and is re-scanned by the rotating mirrors. The light crosses a dichroic mirror and then through a screen with a hole to erase all non-specific light signal until finally reaches the detector. The light that emerges from the pinhole is finally measured by a detector [170].

In this study, a specific number of cells (1.5x105 cells/well of 6-well plate) are coated on a microscopic coverclip and allowed to adhere to its surface for about 24 hours, incubated in culture medium. Subsequently, loaded microemulsion, in which Nile Red was encapsulated, is administered and cells were left for 24, 48 and 72 hours. Nile Red is a lipophilic red pigment that was used as a standard lipophilic compound to stain the oil phase of microemulsion. After the treatment onset, cell culture medium is removed, and each coverslip is rinsed with PBS 1X. The cells are then fixed using methanol for 10 minutes followed by labeling of the cytoskeleton with a green fluorescent secondary antibody against β-actin. The cells are then incubated for 10-15

minutes and the coverslip is washed twice with PBS 1X, placed on a microscopic observation plate, and mounted with a suitable Mowiol medium. Observation is made on a Leica 626 TCS SPE laser scanning confocal microscope (Leica Microsystems GmbH, Wetzlar, Germany) and several visual field images were obtained with LAS AF software (Leica Lasertechnik, Heidelberg, Germany).

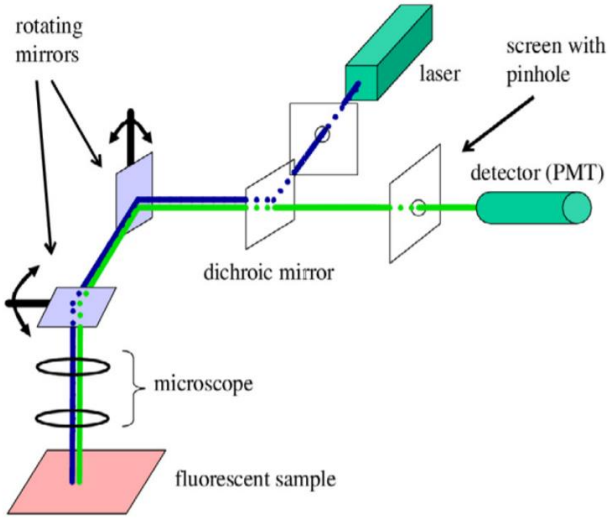

Figure 24. Schematic diagram of a conventional confocal microscope [170].

3.4.4 Cell Cycle - Fluorescence-activated Cell Sorting Analysis (FACS Analysis)

Flow cytometry is a useful tool that enables measuring specific characteristics of moieties (single cells, nuclei, microorganisms etc.), often related to fluorescence or other optical properties. These characteristics usually derive from selected antibodies or dyes. The principle function of flow cytometry is based on light scattering and fluorescence emission of a source of light, usually a laser, which hits the moving particles [171]. Light scattering gives information about the structure of the moiety, while fluorescence emission gives quantitative information about the proposed characteristic/property. This is feasible, as the fluorescence intensity is relative to the quantity of fluorescent probe bonded to the cell or cellular department [172].

Flow cytometry is divided into two different categories depending on the result obtained, namely non-sorting analysis and sorting analysis. Non-sorting analysis can measure light scattering and fluorescence emission and sorting type analysis is able to

sort moieties in groups with different characteristics. Fluorescent activated cell sorters (FACS) have the capacity to separate labeled cells from a mixed moiety population (Figure 25) [173]. Fluorescent activated cell sorting analysis (FACS) is a laser-based technology proposed for the study of particular moieties suspended in fluid, when passing by an electronic detection apparatus. Data are displayed as events on histograms or/and dot plots. By performing this technique, the researcher is able to analyze whole blood, cell cultures, separated tissues, isolated nuclei, bacteria, yeasts, parasites etc.

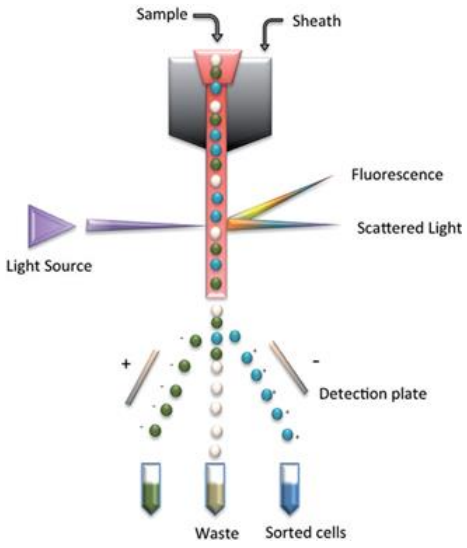

Figure 25. Cell sorting in the flow of cells suspension [172].

In this study, fluorescent activated cell sorting analysis was performed to investigate cell cycle of treated cells, in order to understand and clarify possible disruptions that nanodispersions may cause. For this reason, cells were labelled using propidium iodide (PI), a fluorescent agent, which interposes between the clones of DNA. It is important, when quantifying DNA, to remove any RNA, using RNase. Propidium iodide, in general, interferes with the bases in double-stranded nucleic acids. In a technical aspect, propidium iodide is excitated by blue light and emits fluorescence to red.

In a typical diagram of flow cytometric analysis based on quantitation of the nuclear DNA content, each peak corresponds to the sample nuclei in different phases of the cell cycle, including the G0/G1, S and G2/M phases (Figure 26). In diploid cells

the signal of their DNA content corresponds to a single narrow peak representing the G0/G1 phase of the cell cycle (1 fluorescence unit). During the G1 phase, a cell grows synthesizing nutrients and enzymes that are required for DNA replication and cell division on later stages of cell cycle. The S phase of a cell cycle occurs before mitosis or meiosis and is responsible for the replication of DNA. Subsequently, DNA of a cell is doubled before mitosis or meiosis and before splitting into daughter cells. G_2 phase is the third phase in the cell cycle, which is directly leading to mitosis, following the ending of S phase. Consequently, cells that are in S phase will contain more DNA than cells in G1 and thus, they will pick up more propidium iodide and will fluoresce more intensively. The fluorescence intensity of cells in G2, will be approximately doubled compared to the cells in G1. A subG1 peak may be visible on the left of G0/G1 peak, corresponding to DNA fragments that may emerge during apoptosis. Thus, this method can also detect and estimate the cumulative apoptotic death that applies for most cell types [173].

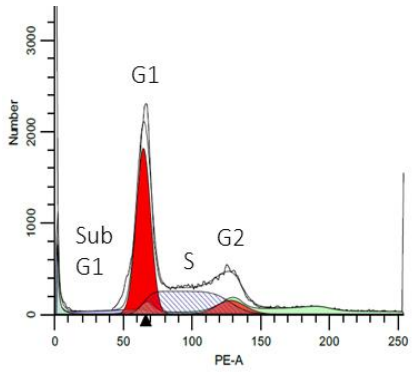

Figure 26. Diagram of flowcytometric analysis of non-treated cells harvested at 48,72h. Cells' sorting was based of DNA content (diagram obtained from experiment of this thesis).

3.4.5 Investigating protein profile – Western Blotting

Protein profile related to death/survival pathways was investigated and the study was focused on specific proteins involved in apoptosis and cell cycle check points. The main goal was to clarify the cell death mechanism, caused by loaded microemulsions and relate the effect of the encapsulated compound to

antiproliferative and potent anticancer activity. By performing sodium dodecyl sulfate (SDS)/polyacrylamide gel electrophoresis, the proteins of the total protein extract are separated due to their different molecular weight. SDS is a negatively charged ionic surfactant that interacts with the hydrophobic regions of the protein molecules and triggers their denaturation. As referred in literature, each SDS molecule binds at every second amino acid and this kind of binding is not dependent on the amino acid sequence. Thus, the protein molecules are detached from other proteins or lipids, become water soluble and are separated depending on their molecular weight [174].

Electrophoresis gel contains two parts; stacking gel and separating gel and each part plays a different role in the procedure. The stacking gel accumulates the protein sample into a sharp band before it enters the separating gel. This modification allows to incorporate to the gel large sample volumes. Separating gel is the gel where separation of proteins occurs. These two parts differentiate in concentration of SDS and polyacrylamide, but they also have different pH values. By the time proteins samples are loaded, a standard protein (marker) is used in order to identify the molecular weight of an unspecified protein (Figure 27).

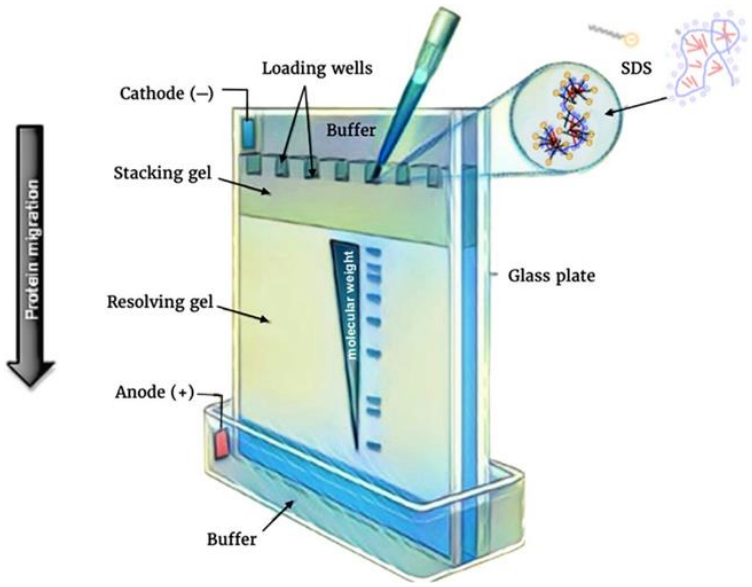

Figure 27. Western Blot set up device for SDS-PAGE electrophoresis [175].

Upon completion of electrophoresis, the proteins separated on the polyacrylamide gel are transferred to a nitrocellulose membrane (0.2 μm pore) by a

special transport apparatus. Nitrocellulose membrane is then incubated with the primary antibody (selected according to the unknown protein) under gentle stirring, either overnight at 4℃ or for one hour at 25℃. The membrane is then rinsed several times with TBS-Tween solution (TBS 1X, 0.1% Tween 20), while stirring. Then it is incubated with secondary antibody, which is selected according to the organism in which the immunization has been performed, to produce the primary antibody. Incubation is also performed under mild agitation and lasts 1 hour at room temperature (25℃) and dark conditions. Finally, the membrane is rinsed several times, while stirring.

The method used for the immunodetection of proteins, was performed using an Enhanced Chemilunescent Substrate (ECL) reagent, which is based on chemi-luminescence. More specifically, the secondary antibody is bound to the horseradish peroxidase (Horse Radish Peroxidase, HRP) enzyme which catalyzes the oxidation of luminol. Luminol is oxidized in the presence of HRP/Peroxide in the presence of chemical enhancers (phenols) in alkaline conditions. Returning to its initial state, luminol produces light at 428 nm and thus, can be visually detected. By performing this reaction, it is possible to detect the position of the antigen-antibody complex.

3.4.6 Genotoxicity – Comet Assay

The comet assay, that is also described in literature as the single cell gel electrophoresis assay (SCG or SCGE assay), is a technique by which DNA damage in eukaryotic cells can be quantified. Comet assay is based on quantification of the DNA fragments which migrate out of the nuclei when electrophoresis occurs. The main advantage of comet assay is its ability to evaluate cellular heterogeneity in response to agents that cause DNA damage. The head region represents the DNA that does not migrate out of the nucleus, and the fragments leaving the nucleus and the cell body in the tail. In the case of a large extent of damage, a "comet" of DNA fragments, that migrate out of cell nucleus (head) is observed (Figure 28). The amount of DNA released from the comet's head during electrophoresis is proportional to the intensity of the fluorescence and thus, to the degree of genotoxicity of the agent [176,177].

Firstly, cells of selected cell lines are placed in six-well culture plates for 24 hours and then incubated with the potent genotoxic agent. After the treatment, cell pellet is

collected and suspended in PBS 1X. Suspension is transferred into low-melting point agarose (0.85% in PBS) and is mixed gently by pipetting, in 37℃ waterbath. Immediately, 2 drops of the mixture are transferred to each of the two ends of the agarose pre-coated slide (1% low-melting-point agarose in PBS) of each sample. After covering the coverslips, above each drop, the plates of all samples are placed at 4℃ for 45 minutes approximately. Coverslips are removed gently, and the slides are engrossed in pH 10 lysis buffer (5 M NaCl, 0,5 M EDTA pH 8, 1 M Tris pH 8 και 1% Triton X-100) for 2 h at 4℃. Then, they are rinsed with ddH_2O, and positioned in electrophoresis buffer where they are allowed to unwind for 40 min. The electrophoresis is performed at 255 mA for 20 min. After the electrophoresis, the cells were rinsed first with neutralization buffer (0.4 M Tris, pH 7.5 with HCl) for 10 min at 4℃ and then with ddH_2O for 10 min at 4℃. Gels were left to dry overnight. Then, cells are stained with 1 ml of SYBR Gold solution (1 ml/10 ml Tris-EDTA buffer) and left in the dark for 30 min. Images are obtained at 400X magnification, using a fluorescence microscope. From each slide 100 cells were selected and photographed randomly using Comet assay 5.0 image analysis software.

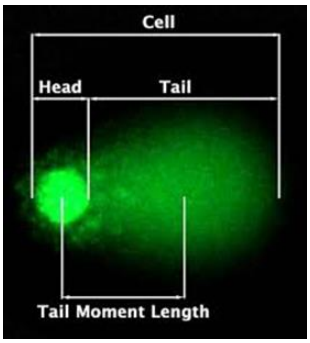

Figure 28. A comet of DNA fragments when released out of the nucleus during electrophoresis (Source: ADME/Tox, Cell Imaging, Cell-based Assays).

In order to connect the degree of DNA fragmentation with the genotoxicity of the agent used for treatment, several parameters are calculated, namely tail moment and olive tail moment. The tail moment is defined as the tail length multiplied by the fraction of total DNA in the tail:

$$\text{Tail moment} = \text{Tail length} * \% \text{ of DNA in the tail}$$

Olive tail moment represents the percentage of total DNA in the tail and the distance between the centers of the mass of head and tail regions:

$$\text{Olive moment} = (\text{Tail mean} - \text{Head mean}) * \%\ \text{of DNA in the tail}$$

In this study, the percentage of DNA in the tail, relative to the head, was calculated using ImageJ Open Comet software [178]. Statistical analysis was performed with nonparametric Mann–Whitney rank sum test.

3.5 *Ex vivo* Biological Assessment

Skin is considered as one of most important routes for nanodispersions, when proposed for topical administration. Skin is one of the major barriers to overcome in order to achieve dermal or transdermal drug delivery of bioactive agents. In the literature, only few compounds tend to pass through this barrier and penetrate into stratum corneum (SC) or deeper and finally either concentrate topically (dermal delivery) or get into systemic blood flow (transdermal delivery) [179]. In order to fully elucidate the efficiency of the proposed nanosystems, skin permeation studies are performed. Hence, the subject of this application is to evaluate the efficacy of nanosystems through an *ex vivo* approach that would result in better therapeutic response and demonstrate the feasibility of transdermal delivery of a lipophilic model and lead-compounds.

3.5.1 *Ex vivo* permeation studies

The assessment of transdermal delivery of bioactive molecules is an important issue in the preclinical evaluation of the proposed drug delivery nanosystems. In this context, *ex vivo* permeation protocols were applied using porcine ear skin in order to assess the retention of each bioactive compound (Ibuprofen, DPS-2) in skin. Permeation protocols were applied using modified Franz diffusion cells and porcine ear skin as a model membrane. In Franz cell device, each cell contains a donor compartment and a receptor compartment separated by the membrane (Figure 29).

The permeation trend of bioactive compounds from drug nanocarriers were determined by calculating the % percentage of drug that permeated in the receiver compartment of the cell, during time. The quantity of the drug was determined using LC MS-MS procedure [95]. To prepare porcine ear skin, hair was removed by shaving to obtain a clear surface without destroying hair follicles. The upper part of the skin, which contained the whole epidermis, was removed using scalper. Skin, which was removed, was kept in a paper immersed in PBS 1X solution to retain humidity until use. Concurrently, the trans-epidermal water loss (TEWL) (Tewameter® TM 210; Courage Khazaka, Koln, Germany) was measured before the experiment, to ensure compatibility of this part of skin.

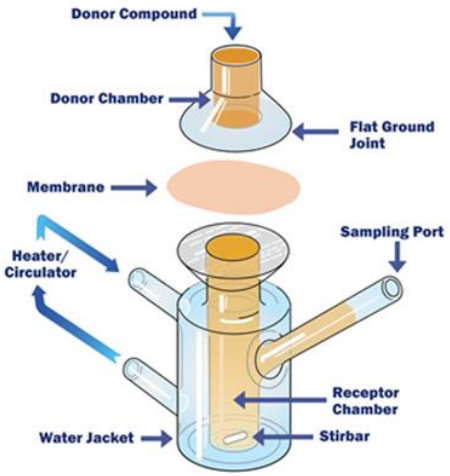

Figure 29. Franz cell diffusion device (Source: www.permeagear.gr)

The temperature in Franz cell waterbath water bath remained constant at 32°C, as this is the mean temperature of porcine ear skin surface. Receptor chamber of Franz cell device is was covered with a mixture of 80% PBS 1X solution – 20% ethanol, as we take into consideration that all compounds tested are slightly soluble or insoluble in water (chamber volume: 12 mL; effective diffusion area: 2.01 cm2). Skin is was placed between donor and receptor chamber and left to equilibrate for 30 minutes. Each of the investigated micro- and nanoemulsions were added on the surface of membrane on the donor compartments, which were then covered with Parafilm™ to prevent ingredients' evaporation. Permeation study was performed for 30 hours. Samples were taken from receptor chamber for analysis at 3h, 6h, 9h, 21h, 24h, 27h and 30h after

treatment. LC MS/MS technique is used to determine the compounds' content in all samples obtained from receptor chamber. Moreover, after the end of permeation study, skin content is extracted to evaluate the quantity of the compound that remained in epidermis and did not permeate skin barrier. For this reason, skin samples are cleaned using PBS 1X solution and are cut in small pieces to increase the surface of extraction. Extraction is performed using methanol (HPLC grade) and samples are left to shake for 24 hours. Then, samples were put in ultrasound bath for 15 minutes at room temperature and were centrifuged until transparence of supernatant was observed (3000 rpm, 15-30 minutes, 25℃). Supernatant was stored at 4 ℃ and skin is was discarded. LC MS/MS technique is was used to quantify the skin's content in all samples. The experiments were conducted at the Faculty of Pharmacy of the University of Belgrade in Serbia.

3.5.2 Differential tape stripping

Differential tape stripping is performed on the porcine ear skin to determine the quantity of drug retained in the stratum corneum (SC) and hair follicles. Even though there are specific differences between human and porcine hair follicles structure and anatomy, the *ex vivo* model of porcine ear is widely used [180]. Thus, differential tape stripping using porcine ear skin would contribute to the evaluation of the quantity of each bioactive compound that penetrates through the superficial skin layers. These experiments could also give information about the affinity of bioactive compound to hair follicles, forming a kind of depot for prolonged delivery [181].

To prepare porcine ear skin, hair was removed by shaving to obtain a clear surface without destroying hair follicles. The upper part of the skin, which contains the whole epidermis, was removed using scalper. Skin, which was removed, can be kept in a paper immersed in PBS 1X solution to retain humidity until use. At the same time, the trans-epidermal water loss (TEWL) (Tewameter® TM 210; Couragep Khazaka, Koln, Germany) was measured before stripping as a baseline value and also after the stripping of 4th, 8th, and 12th tape to standardize removed SC thickness. The investigated micro- and nanoemulsions were applied in skin at an infinite dose and left for 2 hours (sample volume: 1 mL; effective diffusion area: 4.02 cm^2). During this time, the mass of each adhesive tape is measured before use.

Adhesive tapes are pressed onto the skin. The procedure was repeated for 10 times. Afterwards, a drop of cyanoacrylate superglue was applied in the center the treated site and was covered with adhesive tape. The superglue was left for 10 minutes and then, the adhesive tape was removed, containing the follicular content of the drug. After removal of stratum corneum (SC) layers, each tape was placed into a centrifuge tube and drug was extracted by choosing suitable solvent (70% ethanol for tapes containing stratum corneum and acetonitrile for tapes containing hair follicles). Then, samples were put in ultrasound bath for 15 minutes at room temperature and were centrifuged until transparence of supernatant was observed (4000 rpm, 15 minutes, 25℃). Supernatant was kept at 4 ℃ and skin was discarded. LC MS-MS technique was used to quantify the compounds' content in all samples. The experiments were conducted at the Faculty of Pharmacy of the University of Belgrade in Serbia.

3.5.3 Liquid chromatography–mass spectrometry (LC MS/MS Method)

Liquid chromatography–mass spectrometry (LC MS-MS) is a non-invasive analytical method used for the isolation and quantification of compounds of interest. When mass spectrometry and high pressure liquid chromatography are combined the method is known as LC-MS. Liquid chromatography (LC) refers to an analytical method which is used to quantify ingredients of a mixture. The device contains a column that contains porous medium, such as polymers and silica. When a sample is inserted through injection, it is adsorbed on the medium, and then the suitable solvent travels through the column to separate the ingredients, based on their comparative affinity to the column materials and the solvent. The component which has the highest affinity to the medium is the last to elute. High affinity corresponds to compounds that need more time to reach the end of the column. Mass spectrometry (MS) ionizes atoms in order to achieve their separation and detection in relation to their molecular masses and charges (mass to charge ratio – m/z) (Figure 30) [182].

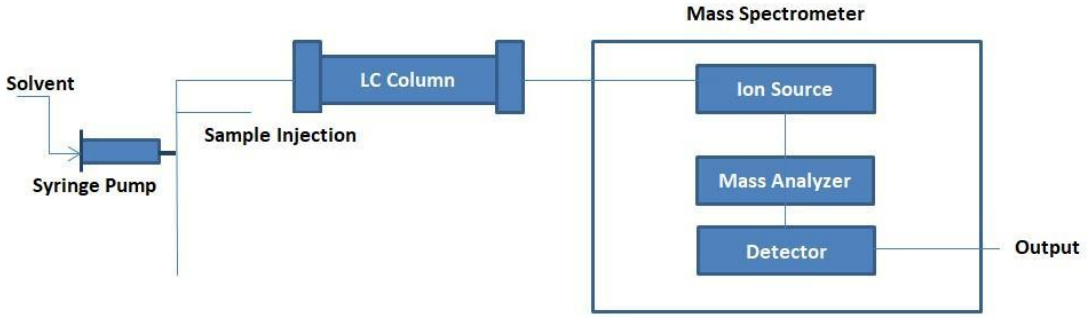

Figure 30. Schematic analysis of LC MS/MS device (source: www.chemyx.com).

In the present study, samples that contained DPS-2 were analyzed on Thermo Scientific Accela 1000 UPLC system coupled to Thermo Scientific TSQ Quantum Access MAX triple quadrupole mass spectrometer. The analysis was performed on UHPLC chromatograph ACELLA (Thermo Fisher Scientific Inc., Madison, WI, USA), coupled to a triple quadrupole mass spectrometer TSQ Quantum Access MAX (Thermo Fisher Scientific Inc., Madison, WI, USA) with heated electrospray ionization (HESI) interface. The column was Zorbax Eclipse XDB C18 (150 mm x 4.6 mm, 5 µm particle size). Mobile phase was acetonitrile/0.1% formic acid = 60:40 (v/v), flow rate was 0.5 mL min^{-1}, column temperature was set to 30 ºC and injection volume was 10 µL. DPS2 was detected and quantified in positive HESI mode (m/z = 504.4).

Concentration of ibuprofen was determined on the same instrument but under different conditions. The column was Zorbax Eclipse XDB C18 (150 mm x 4.6 mm, 5 µm particle size). Mobile phase was methanol/20 mM ammonium-acetate = 90:10 (v/v), flow rate was 0.6 mL min^{-1}, column temperature was set to 35 ºC and injection volume was 10 µL. Ibuprofen was detected and quantified in negative HESI mode (m/z = 205.1 - 161.1). The experiments were conducted at the Faculty of Pharmacy of the University of Belgrade in Serbia.

Chapter 4

Results and discussion

Chapter 4 – Results

4.1 Microemulsions as carriers of potent BRAF^{V600E} inhibitors

The subject of this study was the formulation and structural characterization of oil-in-water (o/w) microemulsions based on non-toxic materials as delivery systems of the lipophilic anticancer drug PLX 4720 (Figure 31) and of a potent BRAF^{V600E} inhibitor, DPS-2 (Figure 32). PLX 4720 is a commercially available pharmaceutical analog of Vemurafenib, which is a selective inhibitor of BRAF^{V600E} kinase, acting through MARK/ERK signaling pathway. MAPK/ERK pathway, monitors cell proliferation, differentiation and survival. Thus, BRAF blocks cell proliferation and causes tumor regressions. DPS-2, is a benzothiophene analogue, which was designed to inhibit the BRAF^{V600E} kinase, and demonstrated high cytotoxicity in selected cancer cell lines [183,184]. Even though DPS-2 was not shown to be a selective BRAF^{V600E} inhibitor, it displayed significant cytotoxic activity in human colon cancer cell lines. Furthermore, an important hypothesis was whether DPS-2, could act as a lead compound to design new chemotherapeutic agents.

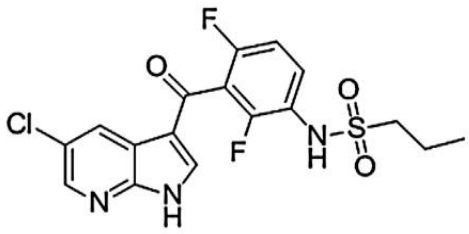

Figure 31. Chemical structure of PLX 4720 (https://www.medchemexpress.com/).

Triacetin, a triester of glycerol and acetic acid, was used as the oil phase, polysorbate 80 (Tween 80) was used as the non-ionic surfactant and phosphate buffered saline (PBS) was used as the aqueous phase. All the compounds are considered as non-toxic for food, cosmetics and medical applications. In particular, the use of both triacetin and Tween 80 in different colloidal nanodispersions, proposed as drug carriers, has been reported by numerous research groups [185,186]. More specifically, triacetin and Tween 80 were used in combination with other oils and

surfactants, respectively. The perspective of formulation of more simple systems, in terms of composition, such as o/w microemulsions have not been in the center of interest so far. The existence of the single-phase region was determined by constructing a ternary phase diagram from which a specific composition was chosen to study the structural characterization and biological evaluation. The structural characteristics of the selected system were determined by performing viscosity measurements, dynamic light scattering (DLS), electron paramagnetic resonance (EPR) spectroscopy and cryogenic-transmission electron microscopy (Cryo-TEM).

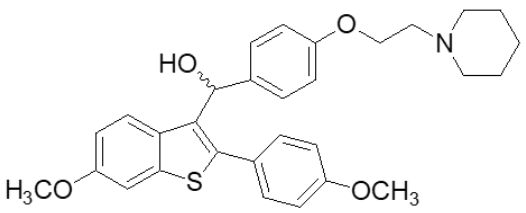

Figure 32. Chemical structure of DPS-2 [187].

4.1.1 Development of oil-in-water (o/w) microemulsions

Biocompatible o/w microemulsions composed of Tween 80 and triacetin were formulated to serve as carriers of the lipophilic drug PLX 4720. Initially, different ratios of aqueous phase and surfactant were mixed in a container and each mixture was stepwise titrated with oil phase at 25◦C until turbidity was visually observed. PLX 4720 was dissolved in the oil phase and through titration was encapsulated in the microemulsions. The highest equilibrium quantity of PLX 4720 that could be dissolved in triacetin at room temperature was 0.4 mg/mL (0.9 mM). The time needed for systems' equilibration between sequential additions of triacetin, variated from a few minutes to 24h. Phase alterations were observed by the presence of turbidity or phase separation. The single-phased region, that corresponded in microemulsions, was characterized as transparent and isotropic mixtures. Titration results were plotted on a triangular graph as ternary phase diagrams using the ProSim Ternary Diagram software 2.3.

The single-phase region that corresponded to clear and transparent o/w microemulsions was detected. As can be observed in Figure 33, as Tween 80

concentration increased, the quantity of dispersed oil phase was also increased, resulting in the expansion of single-phase area. In particular, even at low Tween 80 concentrations, the capacity of the microemulsion to encapsulate the dispersed oil phase was relatively high. More specifically, triacetin up to 10% w/w was entrapped in the microemulsions at surfactant concentration <50% w/w, while this ratio was furtherly increased for surfactant concentration >50% w/w. In order to assess the impact of encapsulation of PLX 4720 or DPS-2 to the boundaries of monophasic region, the same procedure was repeated in case of the drug dissolved in the oil phase of the microemulsions. The boundaries of the single-phase region of the phase diagrams were not altered in case of the drug-free (empty samples) and of the drug-loaded microemulsions (loaded samples).

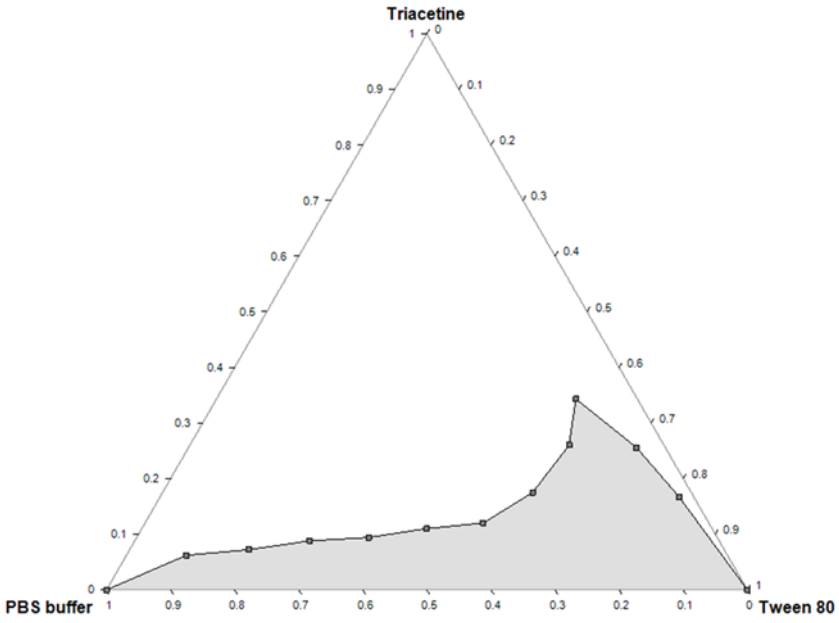

Figure 33. Ternary phase diagram for the proposed system at the temperature of 25 ◦C. The composition is expressed in weight ratios. Grey area represents the single phase region and clear area is the bi-phasic region. [188].

In the perspective of potential application of the o/w microemulsions in delivery of lipophilic drugs, surfactant concentration should be maintained relatively low. In parallel, the quantity of oil should be high enough to permit PLX 4720 or DPS-2 encapsulation, at an efficient dosage. Subsequently, the microemulsion's

composition that was selected for further study was 81.5% w/w PBS buffer, 10.6% w/w Tween 80 and 7.9% w/w triacetin. PLX 4720 concentration in the microemulsions was 31.5 μM. DPS-2 concentration in the microemulsion was 3.3mM.

4.1.2 Structural characterization of oil-in-water (o/w) microemulsions

4.1.2.1 Viscosity measurements

Viscosity of empty and drug-loaded microemulsions was evaluated, as it is a significant parameter, especially in different routes of administration. More specifically, for parenteral applications, the viscosity of the microemulsions should be kept in low levels enough to facilitate their fluidity and administration. Viscosity measurements of o/w empty and loaded microemulsions with PLX 4720, were performed and the data obtained were compared to the viscosity data of the aqueous phase (PBS buffer) and aqueous phase containing surfactant (PBS buffer/Tween 80 mixture). The viscosity of the aqueous phase (PBS buffer) was 0.89 ± 0.01 mPa*s. At a ratio of 9:1 between a PBS buffer and Tween 80, the viscosity was increased up to 2.29 ± 0.02 mPa*s. On the contrary, upon the incorporation of 7.9% w/w oil phase, the viscosity was slightly increased up to 2.49 ± 0.09 mPa*s. Finally, when PLX 4720 was encapsulated in o/w microemulsions the viscosity did not change at all (2.51 ± 0.09 mPa*). The obtained information revealed that the encapsulation of PLX 4720 did not significantly affect the viscosity of microemulsion.

The data obtained agree with various studies that refer to the viscosity of a microemulsion as a parameter that is affected by the concentrations of the surfactant, water and oil components. Subsequently, the viscosity is reduced as the quantity of water increases and it is increased when an amount of surfactant and/or cosurfactant is added [189]. It is significant to mention that viscosity measurements are of major importance in dermal/transdermal administration, as viscosity affects the retention of the formulation on the skin surface and it can also reduce the water evaporation rate on skin. Thus, microemulsion retains on the skin surface for a prolonged period, as compared to non-viscous formulations (e.g. aqueous solutions or solutions of drugs in organic solvents) and as a result, enhances skin penetration [190]. Additionally, in parenteral applications, the low viscosity of the proposed microemulsion is necessary

to facilitate sterile filtration and also the mixing with intravenous fluids [191]. To conclude, relatively low viscosity values, revealed that the proposed microemulsions are suitable as dermal or parenteral delivery vehicles of the lipophilic chemotherapeutic agent PLX 4720.

4.1.2.2 Dynamic Light Scattering (DLS)

Dynamic light scattering measurements of empty and loaded o/w microemulsions were performed to determine the size distribution and the degree of polydispersity of the dispersed oil nanodroplets. The polydispersity index (PdI) value is a parameter that measures particles' homogeneity and takes values within the range of 0 to 1; When PdI value is close to zero, the system is characterized as monodispersed. When empty o/w microemulsions were measured, an average diameter of 10.0 ± 0.1 nm was obtained. Upon the encapsulation of lipophilic drug PLX 4720, the average diameter of nanodroplets was also determined as 10.0 ± 0.1 nm. Subsequently, the encapsulation of PLX 4720 did not affect the size of nanodroplets. Moreover, the polydispersity index value of the system was slightly increased, from 0.17 ± 0.02 to 0.21 ± 0.03. Taking into consideration DLS results, we can presume that the encapsulation of PLX 4720 in the dispersed oil phase caused the formulation of homogenous carriers characterized by relatively small colloidal particle sizes (Figure 34).

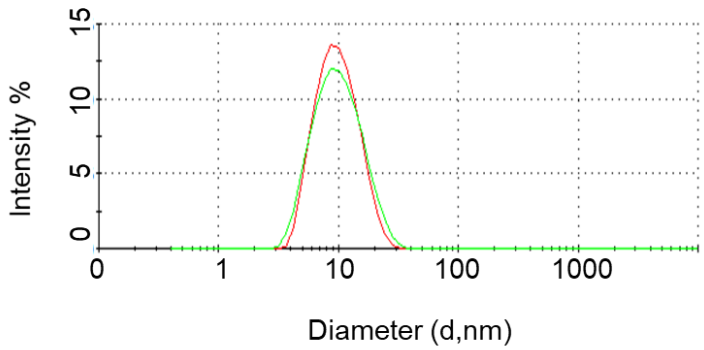

Figure 34. Size distribution of nanodroplet sizes. The red line refers to empty microemulsion and the green line refers to loaded o/w microemulsions. All experiments were performed in triplicate [188].

As observed, in the presence of DPS-2, the incorporation of the bioactive compound in the oil cores of the microemulsions did not significantly affect their size. More specifically, the average droplet diameter of dispersed oil droplets was 10 ± 0.1 nm for the empty and 10 ± 0.4 nm for the loaded microemulsions. Furthermore, the polydispersity index was slightly increased from 0.17 ± 0.02 to 0.27 ± 0.03 upon DPS-2 encapsulation. As DLS results are concerned, we can presume that encapsulation of DPS-2 resulted in the formulation of homogenous delivery systems that possess narrow size distribution of oil nanodroplets. Figure 35 represents distribution curves of the hydrodynamic radii of the empty and loaded microemulsions.

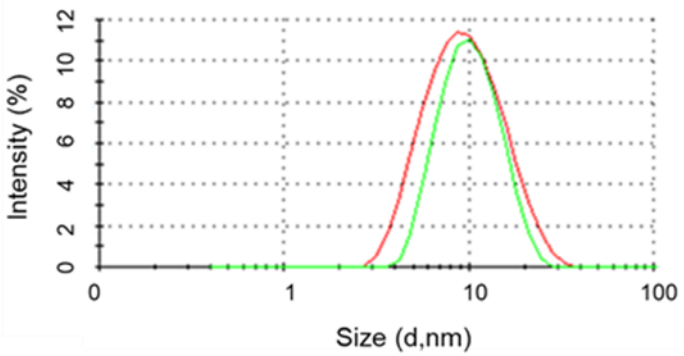

Figure 35. Size distribution of nanodroplet sizes. The red line refers to empty microemulsion and the green line refers to loaded o/w microemulsions. All experiments were performed in triplicate Intensity distribution of droplet sizes. DPS-2 concentration was 3.3 mM. Experiments were performed in triplicate [187].

These measurements indicated the formulation of homogenous microemulsions with relatively small colloidal particle sizes. Interestingly, particle size was not affected upon bioactive compounds' encapsulation, probably because of the location of the drug in the oil cores in all cases and additionally due to the low concentration, especially in the case of PLX 4720. Similar results have been reported for other lipophilic compounds such as testosterone enanthate, ibuprofen, ibuprofen eugenol ester, which were encapsulated in o/w microemulsions [192–194]. In such colloidal systems which are proposed for drug delivery, the size of droplets contributes to the bio-distribution of the encapsulated drug in the tissues. Due to the small size of dispersed phase, there is higher probability for interactions with skin lipids and

proteins, so microemulsions can significantly improve drug penetration and bioavailability [195]. Towards this approach, Izquierdo et al. indicated that droplet size of a nanodispersion affects the skin penetration of tetracaine, within 24h [196]. Subsequently, by decreasing the size of colloidal nanocarriers, it is likely to improve both the stability of these systems and also to achieve enhanced biodisposition [197,198].

4.1.2.3 Cryogenic-transition electron microscopy (Cryo-TEM) imaging

Cryogenic-transition electron microscopy (Cryo-TEM) imaging provides images at relatively high resolution, while captures any co-existent structures and micro-structural transitions. The following experiments were performed in collaboration with CryoEM Laboratory of Soft Matter, Technion, Haifa, Israel. O/w microemulsions were imaged by Cryo-TEM, to examine and describe the inner structure, morphology and shape of the oil nanodroplets. The micrographs that were obtained (Figure 36) indicated the existence of small structures (dark dots), that correspond to oil domains which are dispersed in the aqueous phase (grey areas).

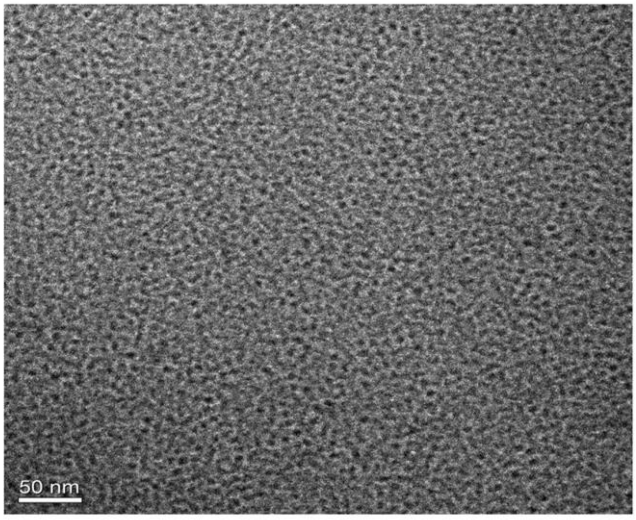

Figure 36. Cryo-TEM micrograph obtained for the o/w microemulsion [188].

The average diameter of nanodroplets was evaluated to be approximately 10 nm, which is in agreement with the results obtained by DLS. These data are coherent

with cryo-TEM images of o/w microemulsions, rich in phospholipids, containing 70-95% w/w aqueous phase, used as delivery systems of diclofenac [199]. Furthermore, Garti et al., focused on the formulation of fully water-dilutable microemulsions as delivery systems of riboflavin phosphate. The water content was 74 and 88% w/w, when small spheres were observed as dark spots, and the average diameter on nanodroplets was determined at 7 nm [200]. Moreover, Margulis-Goshen et al., studied the formulation of microemulsion for the encapsulation of celecoxib (2.5 % wt. celecoxib), 17.5 % wt. sec-butanol, 30 % wt. surfactant mixture composed of lecithin, glycyrrhizic acid and ammonium glycyrrhizinate, and 50 % wt. water. Cryo-TEM data, indicated the presence of discrete droplets of oil that had a mean diameter of a few nanometers [201]. Moreover, Chatzidaki et al., indicated the existence of 7.7nm nanodroplets when Cryo-TEM was performed in w/o microemulsions composed of Miglyol 810, IPM, lecithin, ethanol, propylene glycol and water [202].

4.1.2.4 Electron Paramagnetic Resonance Spectrometry (EPR)

EPR spectroscopy using the spin-probing technique can be applied to study the properties of the interface of the surfactants' monolayer in micro- and nanoemulsions. An amphiphilic compound, which possess unpaired electrons, is introduced into the sample and the obtained spectrum is affected by the compound's microenvironment. Thus, any change in the spectrum may be associated with structural changes in the system before and after encapsulation of the bioactive compound. In this study, 5-doxyl stearic acid (5-DSA) was used to determine the interfacial properties of the chosen o/w microemulsions. 5-DSA is a spin-labelled fatty acid that contains stearic acid and a doxyl group which is bonded to the C-5 position of the hydrocarbon chain. Information reflecting the rigidity/flexibility of the spin probe's microenvironment, close to the region where doxyl ring is located, can be obtained from EPR spectra analysis. In particular, in 5-DSA, the nitroxide is located closer to the polar head of the fatty acid and thus, closer to the surfactant polar heads. When 5-DSA is solubilized in microemulsions, it is localized at the interfaces interacting with the surfactant molecules.

EPR data obtained from the spectra, were analysed to get information regarding the motion of molecules and lipid order in the membranes. In particular,

order parameter (S) gives information about the flexibility of the surfactants' monolayer and rotational correlation time (τ_R) gives information about the mobility of the spin probe. Generally, EPR spectra of non-equal heights and widths are revealing the restrictive motion of the selected spin probe in the membrane. Subsequently, spin probe's spectra can provide useful data about the coherence of the surfactants layer, the flexibility of the membrane and the degree of compound's encapsulation [163].

In the present study, the experimental EPR spectra were simulated using an anisotropic rotational model based on the slow-motion theory developed by Schneider and Freed [203]. Figure 37 shows both experimental and simulated EPR spectrum of 5-DSA in loaded microemulsions with PLX 4720. Rotational correlation time (τ_R) values of 5-DSA were determined through the computational procedure and calculated as 5.3±0.3 ns for the empty microemulsion and 5.3±0.2 ns for the loaded microemulsion. Moreover, order parameter S values were determined as 0.56±0.03 for the empty microemulsion and 0.57±0.01 for the loaded microemulsions with PLX 4720 (Table 1). The samples were prepared and examined in two independent experiments and each experiment was performed in triplicates. The similarity that was observed in τ_R and S values clearly showed that PLX 4720 was located within the oily cores of the microemulsions and not interacting with the surfactants' monolayer.

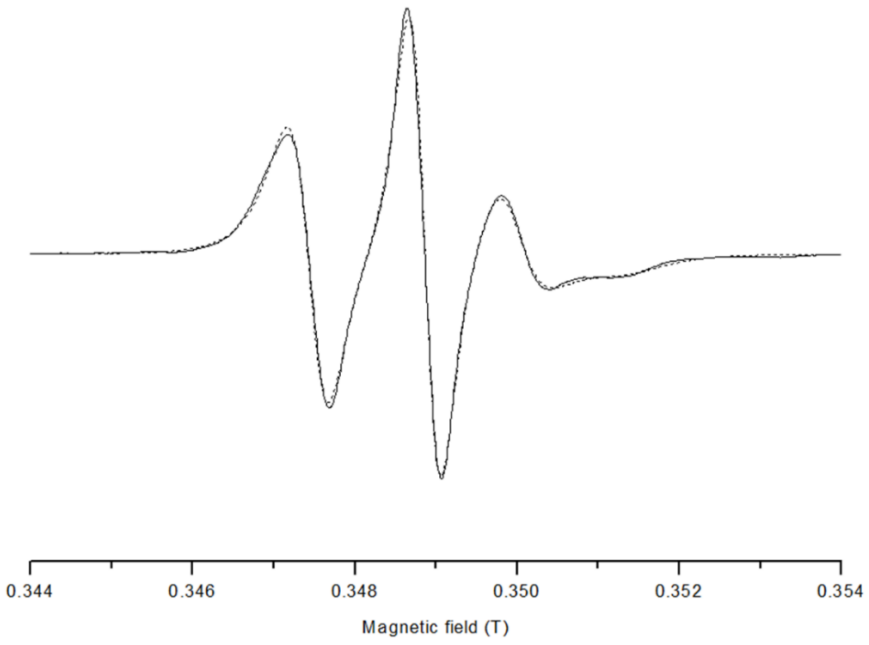

Figure 37. EPR spectra of 5-DSA in o/w microemulsions loaded with PLX 4720. The straight line represent experimental results and dotted line the results obtained through simulation [188].

Table 1. τ_R and S values calculated from EPR spectra of 5-DSA for empty and loaded o/w microemulsions. PLX 4720 concentration was 0.9mM. Experiments were performed in triplicate and the results are expressed as mean values ± standard deviation (SD).

Sample	**Rotational correlation time (τ_R) ns**	**Order Parameter S**
o/w empty microemulsion	5.3 ± 0.3	0.56 ± 0.03
o/w loaded microemulsion	5.3 ± 0.2	0.57 ± 0.01

EPR spectra of the spin-labelled fatty acid 5-DSA in empty and loaded microemulsions with DPS-2 were also recorded and evaluated. Figure 38 shows both experimental and simulated EPR spectra of 5-DSA in empty (Fig. 37a) and loaded microemulsions with DPS-2 (Fig. 37b). Furthermore, order parameter S and rotational correlation time τ_R values were determined for the empty and for the loaded microemulsion with DPS-2 (Table 2). The samples were formulated and examined in two independent experiments and each experiment was performed in triplicate.

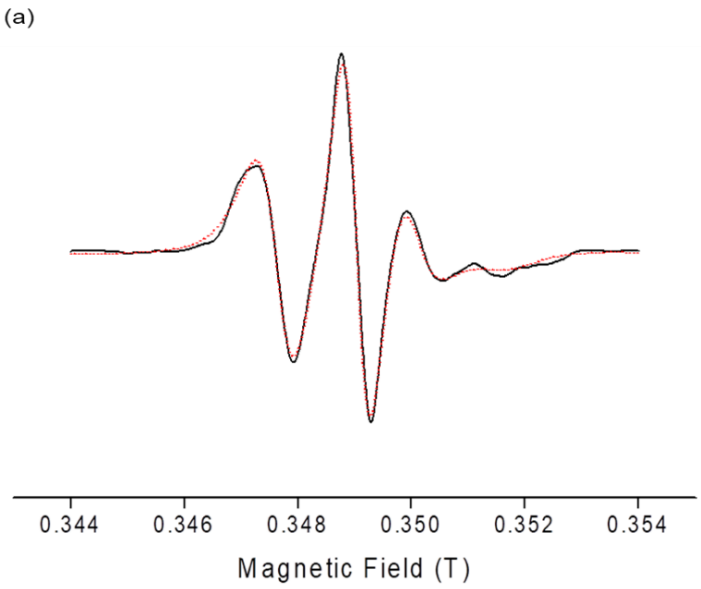

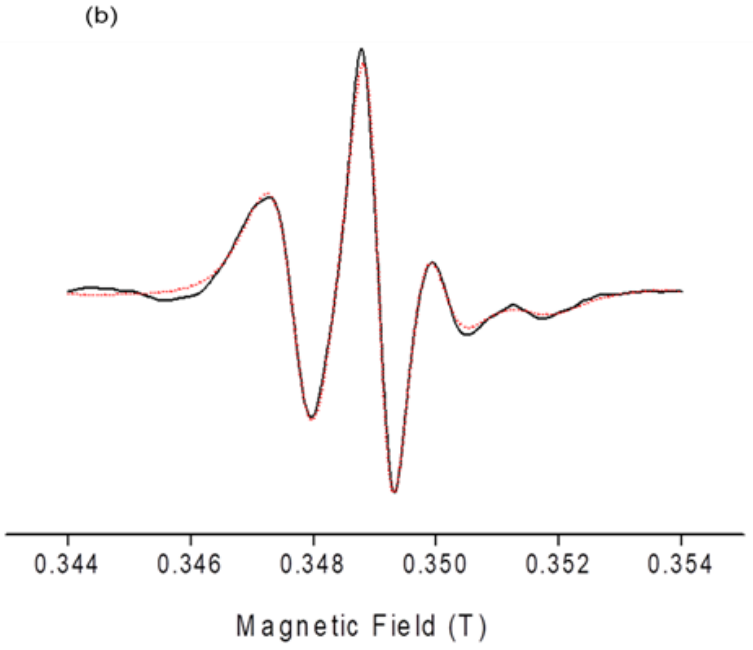

Figure 38. EPR spectra of 5-DSA in (a) empty and (b) loaded with DPS-2 o/w microemulsions. The experimental results are represented with black straight line and the simulate results with dotted line [187].

Table 2. τ_R and S values calculated from EPR spectra of 5-DSA for empty and loaded o/w microemulsions. DPS-2 concentration was 3.3 mM. Experiments were performed in triplicate and the results are expressed as mean values ± standard deviation (SD).

Sample	**Rotational correlation time (τ_R) ns**	**Order Parameter S**
o/w empty microemulsion	6.01 ± 0.20	0.45 ± 0.02
o/w loaded microemulsion	5.95 ± 0.19	0.48 ± 0.02

As it can be observed, the incorporation of DPS-2 in the oil cores of the microemulsions did not affect rotational correlation time (τ_R) value of 5-DSA since the observed slight decrease cannot be assessed as indicative of changes in system's structure. Table 2 also shows the order parameters S values for empty and loaded microemulsions with DPS-2 at specific oil and surfactant ratio. At oil phase weight fraction equal 7.9% w/w, both in the empty and loaded microemulsions with DPS-2,

the system was characterized by high order parameters S of 0.45 and 0.48, respectively, indicating a very restricted movement of 5-DSA in the interface. The observed slight increase of order parameter S, when DPS-2 was encapsulated, clearly eliminates DPS-2 participation in the surfactants' monolayer.

Overall, microemulsions composed of water, triacetin and Tween 80 were characterized by the presence of relatively rigid interfacial layers not allowing rapid wobbling of 5-DSA along its long molecular axis. Furthermore, in all cases, it was shown that DPS-2 did not participate with the interfacial film or interact with the surfactant molecules. The similarity that was observed in τ_R values was not considered important, indicating both PLX 4720 and DPS-2 were located within the oily cores of the microemulsions and not interacting with the surfactants' monolayer. It is important to note that the increased rigidity of the interface, as determined by the calculated values and the EPR spectra (Table 2 and Figure 38), did not prevent the release of the DPS-2.

Although enhanced drug solubility in such systems usually occurs from the solubilization at the interface [204], in this study, the bioactive compounds seem not to interact with surfactant molecules or participate to the formation of the interface. A possible explanation of this finding it is likely to be related to the increased solubility of the both PLX 4720 and DPS-2, in triacetin which was the dispersed oil phase, as compared to their solubility in the surfactants' monolayer at the temperature in which the experiments were performed. From another aspect, especially for PLX 4720, the concentration in the system was so small (nearly 30 times less than the spin probe) and thus, cannot cause measurable changes in the interface's structure. Overall, structural information obtained from EPR studies of nanodispersions could be of major importance in the perspective of using such delivery systems as drug carriers since rigidity of the surfactants monolayer has been strongly related to the permeability and bioavailability of the encapsulated bioactive compounds [205].

4.1.3 *In vitro* evaluation of oil-in-water (o/w) microemulsions

The cytotoxic effect of the empty and loaded microemulsions either with PLX 4720 or with DPS-2, was evaluated either through Sulforhodamine B (SRB) test or through thiazolyl blue tetrazolium bromide (MTT) cell proliferation assay, for PLX 4720 and DPS-2 respectively. The effective release of a model lipophilic dye namely Nile Red,

encapsulated in microemulsion, was evaluated through confocal microscopy. When encapsulated, both PLX 4720 and DPS-2 exhibited comparable cytotoxicity as when dissolved in dimethyl sulfoxide (DMSO) at the same concentration. Consequently, the oil cores of o/w microemulsions were proven effective biocompatible carriers of lipophilic bioactive molecules in *in vitro* biological assessment experiments. Further investigation of cell death induced by encapsulated DPS-2, was performed through fluorescence-activated cell sorting (FACS) analysis, Comet assay, and Western blotting. These experiments exhibited that DPS-2, although non-genotoxic directly, induced S phase delay in cell cycle progression accompanied by cdc25A degradation and a non-apoptotic cell death in both cell lines, which implied that DPS-2 was a deoxyribonucleic acid (DNA) replication inhibitor.

4.1.3.1 Cell Viability assays

PLX 4720 is generally administrated to cell cultures using dimethyl sulfoxide (DMSO) as a common solvent. However, DMSO is subjected to limitations in medical applications, as it has been reported to exhibit cytotoxic effects to cell cultures over a particular concentration [206]. In this context, o/w microemulsions are proposed as nanocarriers to replace DMSO when performing *in vitro* cell viability experiments. In the present study, human colon cell lines (Colo-205, HT-29, Caco-2) and MW 164 skin melanoma cells were tested, that both express $BRAF^{V600E}$ mutation and they are $p53^{null}$.

Sulforhodamine B (SRB) test was performed to evaluate the cell proliferation in two human colon cancer cell lines (Colo-205 and HT-29), bearing the $BRAF^{V600E}$ mutation. The lipophilic PLX 4720, either diluted in DMSO or encapsulated in o/w microemulsions was administrated in both cell lines. Before treatment, microemulsions were diluted in the cell culture medium (DMEM) at different ratios. In particular, microemulsions were diluted in the cell culture medium in a ratio ranging from 0.005% to 0.5% v/v in order to assess the cytotoxicity of the empty microemulsion. It was observed that microemulsions did not inhibit cell proliferation when diluted in ratios between 0.005% v/v and 0.2% v/v in the cell culture medium. When the concentration of empty microemulsions was raised up to 0.5% v/v, cell viability of Colo-205 cell line was slightly, though not significantly, decreased during the first 48h after the treatment onset, compared to the control samples.

Figures 39 and 40 show the percentage of cell viability in Colo-205 and HT-29 cell cultures after 48h after the treatment onset. DMEM and DMSO 0.1% were used as positive control samples. The effect of empty and loaded microemulsions with PLX 4720 was determined and were compared to the effect of PLX 4720 dissolved in DMSO at the same concentration. Microemulsions were administered to the cell culture after dilution in DMEM in a final ratio of 0.2% or 0.5% v/v in the medium. Cell viability results were very important as, the *in vitro* tests of different commercially used surfactants and surfactant mixtures in drug delivery systems are required for the investigation of potential irritation and cytotoxic effects [207,208]. Silva et al. also been reported that in high concentrations, both empty and loaded tween 80-based microemulsions may induce cytotoxicity probably due to high percentage of surfactant. However, in that study, the effect of microemulsions was significant low compared to drug solution [209].

As Figures 39 and 40 show, the treatment of both Colo-205 and HT 29 cell lines with empty microemulsions in a final ratio of 0.2% v/v in the medium, did not inhibit cell proliferation. Moreover, in the HT-29 cells no cytotoxicity was observed, even when the ratio of the microemulsions in the medium exceeded 0.5% v/v.

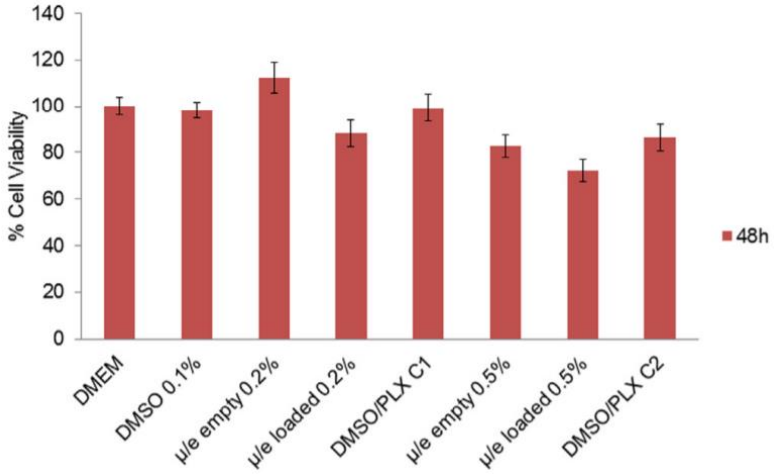

Figure 39. Results in cell proliferation assay using Colo-205 cell line 48h after the treatment onset. DMEM and DMSO 0.1% were used as positive control samples, μ/e empty refers to o/w microemulsions without the drug, μ/e loaded refers to o/w microemulsions loaded with PLX 4720, DMSO/PLX C1 refers to PLX 4720 dissolved in DMSO at a concentration of 0.063 M, DMSO/PLX C2 refers to PLX 4720 dissolved in

DMSO at a concentration of 0.12 M. Standard Deviation (S.D.) was used for error bar creation [188].

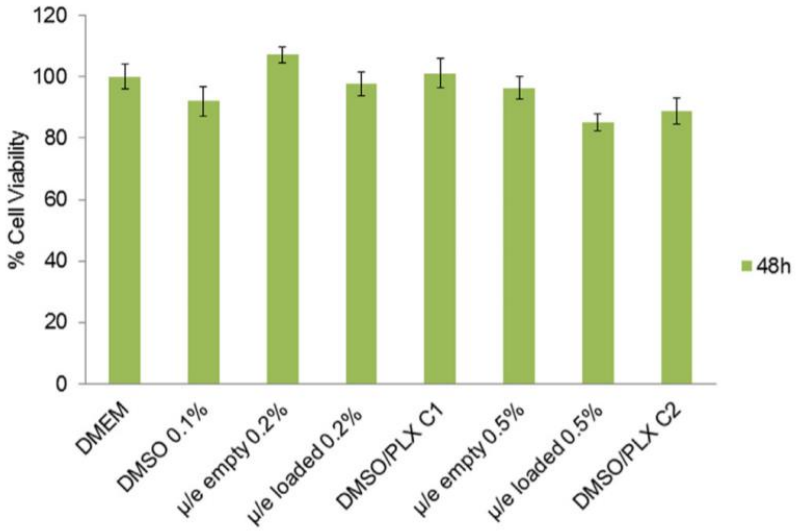

Figure 40. Results in cell proliferation assay using HT-29 cell line after 48h after the treatment onset. DMEM and DMSO 0.1% were used as positive control samples, μ/e empty refers to o/w microemulsions without the drug, μ/e loaded refers to o/w microemulsions loaded with PLX 4720, DMSO/PLX C1 refers to PLX 4720 dissolved in DMSO at a concentration of 0.063 M, DMSO/PLX C2 refers to PLX 4720 dissolved in DMSO at a concentration of 0.12 M. Standard Deviation (S.D.) was used for error bar creation [188].

Furthermore, all cell-based assays indicated a concentration-dependent relation with cell viability after 48h of treatment with PLX 4720 dissolved in DMSO. When the cells were treated with loaded microemulsions with PLX 4720, at two different concentrations (0.063 and 0.12 μM), the response observed, when it was compared to the response of PLX 4720 dissolved in DMSO at the same concentrations, was similar. It has been reposted that the combination of Tween 80 as surfactant and triacetin as the oil phase in delivery systems has been proven efficient. A microemulsion composed of triacetin, and Tween 80 and Transcutol-P was formulated to encapsulate celecoxib, a non-steroidal anti-inflammatory drug, proposed for dermal administration. I*n vivo* pharmacokinetic studies were performed, and results indicated enhanced bioavailability of drug, compared to drug solution [100].

Cell viability assay was performed using WM 164 and Caco-2 cell lines. The assessment was performed using the MTT assay, a method for sensitive quantification of viable cells. Both cell lines were bearing the $BRAF^{V600E}$ mutation and a non-functional p53 ($p53^{null}$) [210,211]. Cells were treated with the lipophilic compound DPS-2 either diluted in DMSO or encapsulated in o/w microemulsions, at the same concentration. The effect of empty and loaded microemulsions with DPS-2 was determined in comparison to its effect when dissolved in DMSO.

Microemulsions were administered into the cell culture upon dilution at a final ratio of 0.2% or 0.5% v/v in the culture medium, as it was previously observed that within this range the delivery systems do not exhibit any cytotoxicity, in the cell lines tested. The percentage of alive cells 48 and 72h after the treatment onset is shown in Figure 41 (DMEM and DMEM plus DMSO at 0.1% v/v were used as positive control. The mean (± standard deviation) of three independent experiments, each performed in 5 replicates, is presented.

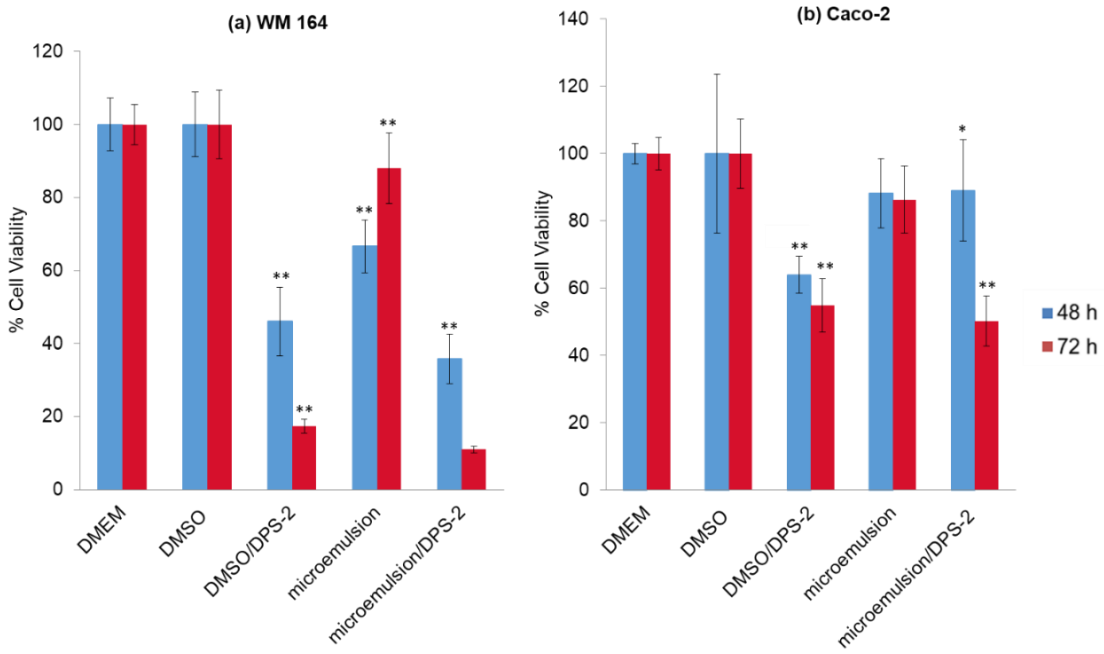

Figure 41. Results in cell proliferation assay using WM 164 (a) and Caco-2 (b) cell lines 48, 72h after the treatment onset. DMEM and DMSO 0.1% v/v were used as positive control samples, μ/e empty refers to o/w microemulsions without the drug, μ/e loaded

refers to o/w microemulsions loaded with at 5.6μM. DPS-2 was also solubilized in DMSO at 5.6 μM [187].

Statistically significant results are indicated by asterisks (*) when $p<0.05$ and (**) when $p<0.01$. The results were analyzed using Student's t-test. The concentration of DPS-2 solubilized in DMSO and of DPS-2 encapsulated in microemulsion was 5.6μM. As observed, empty o/w microemulsions, added at a final ratio of 0.2% v/v in the medium, did not inhibit cell proliferation, in all cell lines tested. In contrast, loaded o/w microemulsions with DPS-2 significantly affected cell viability, as the cytotoxic effect was significantly high at 72h, in all cell lines tested.

The effect was furtherly enhanced in Caco-2 cells when treatment was prolonged up to 96h (Figure 42). For reasons of comparison, cell proliferation assays were in parallel performed for the non-small cell lung carcinoma cell line A549 ($p53^{wt}$). A549 cells were treated under the same conditions and at the same time points (Figure 42); As observed, cell proliferation of A549 cells was not inhibit by DPS-2 and, despite their shorter doubling time (22h), a negligible (≈10%), non-statistically significant inhibition of cell proliferation was observed at 72h [212]. These findings revealed the compatibility of the proposed o/w microemulsions as delivery systems of the lipophilic compound DPS-2 for *in vitro* applications. It is important to mention that the encapsulation of DPS-2 in the oil cores of the microemulsions did not exhibit increased cytotoxicity as compared to DPS-2 dissolved in DMSO, at the same concentration.

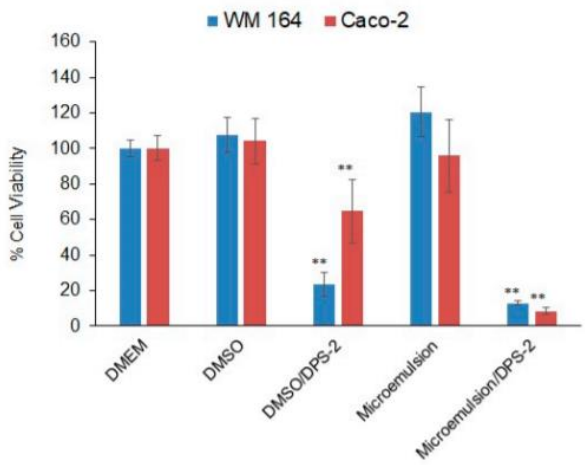

Figure 42. Results in cell proliferation assay using WM 164 and Caco−2 cell lines 96 h after the treatment onset. DMEM and DMSO 0.1% v/v were used as positive control

samples, μ/e empty refers to o/w microemulsions without the drug, μ/e loaded refers to o/w microemulsions loaded with at 5.6μM. DPS-2 was also solubilized in DMSO at 5.6 μM [187].

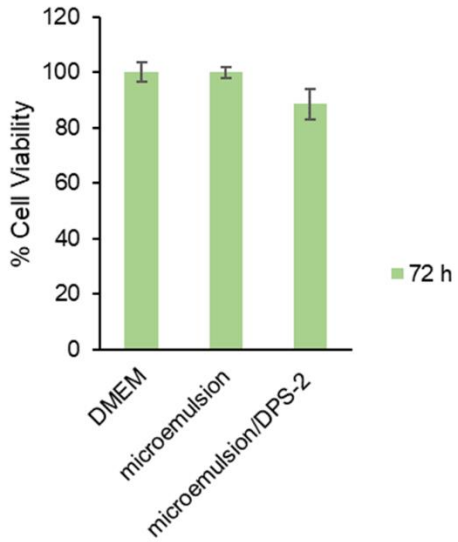

Figure 43. Results in cell proliferation assay using A549 cell line 72 h after the treatment onset. DMEM was used as positive control samples, μ/e empty refers to o/w microemulsions without the drug, μ/e loaded refers to o/w microemulsions loaded with at 5.6μM. DPS-2 was also solubilized in DMSO at 5.6 μM [187].

The selection of the cancer cell lines, used for *in vitro* assessment, is supported by the use of microemulsions for transdermal and oral drug delivery [213–215]. The oil cores of the formulated o/w microemulsions were proven efficient carriers of lipophilic compounds, such as PLX 4720 and DPS-2, in all cell lines tested. Moreover, when DPS-2 was encapsulated at a concentration of 5.6 μM, a significant decrease in the viability of the MW 164 skin melanoma and Caco-2 human epithelial colorectal adenocarcinoma cells was observed. Both cell lines were also treated in parallel with DPS-2 solubilized in DMSO at the same concentration. In MW 164 skin melanoma cells the cytotoxic effects of DPS-2, either dissolved in DMSO or encapsulated in o/w microemulsions, became prominent earlier (48 h), exhibiting the difference in each cell line's doubling time, which was 48 h in WM 164 vs. 62 h in Caco-2 [216,217]. The

cytotoxic effect was furtherly increased in Caco-2 cells when treatment was prolonged up to 96 h.

To sum up, the obtained information indicated the suitability of the formulated o/w microemulsions as delivery systems of the lipophilic compounds, PLX 4720 and DPS-2, to selected cell lines at given concentration in cell culture medium. Furthermore, the encapsulation of PLX 4720 and DPS-2 in the dispersed oil phase of the microemulsions, did not exhibit enhanced cytotoxicity as compared to the administration using DMSO as solvent.

4.1.3.2. Confocal Microscopy

The intracellular release of a model lipophilic compound, namely Nile Red, encapsulated in o/w microemulsions was examined by performing confocal microscopy. The oil phase was labelled with Nile Red, which is a red lipophilic dye, while the cytoskeleton of both cells lines was labeled with a green fluorescent secondary antibody against the anti-β-actin antibody. The transmembrane delivery of the oil phase was investigated for 3, 6, 24, 48, and 72h. The oil phase was colocalized with the cytoskeleton even at 6h after the treatment onset and remained as such as long as 72h.

Confocal microscopy has been used to evaluate the distribution of fluorescent compounds in cells or tissues, when encapsulated in microemulsions. Zhang et al., treated mouse skin cells with rhodamine B-loaded microemulsions to evaluate the dye's distribution within the cells. Fluorescence was observed in the cytoplasm of the cells, clearly showing that, rhodamine B was finely distributed in the cytoplasm in concentration and incubation time-dependent manner [218]. In another study, confocal microscopy was performed to evaluate the permeation rate of fluorescein isothiocyanate (FITC) through a microemulsion composed of lecithin, n-propanol, isopropyl myristate and water in stratum corneum, epidermis and dermis. Almost 30 min after the treatment onset, o/w lecithin-based microemulsions containing FITC, have exhibited increased fluorescence intensity in stratum corneum, hair follicles, epidermis and dermis layer in comparison to FITC dissolved in DMSO, at the same concentration [219].

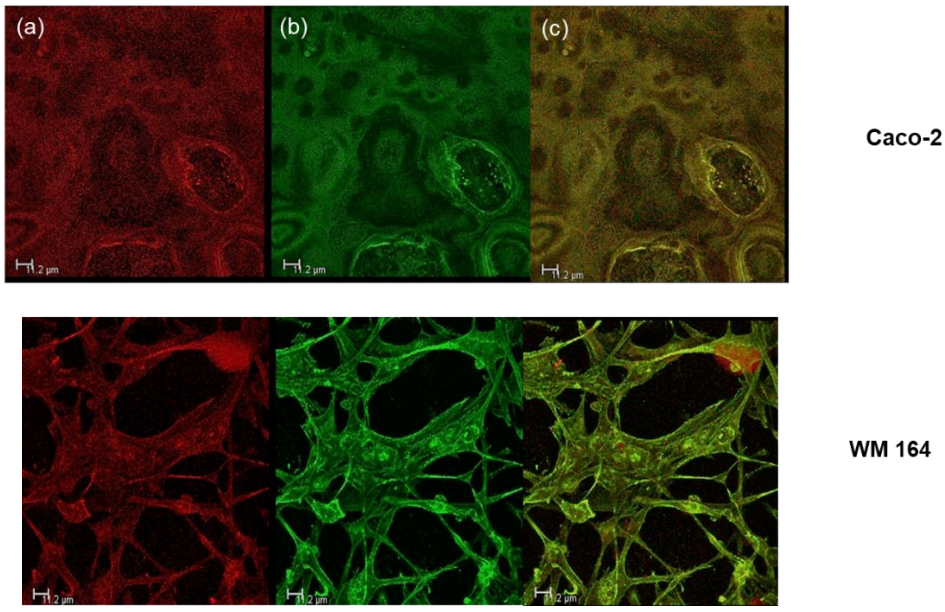

Figure 44. Confocal Microscopy revealed that the oil-phase was co-localized with the cytoskeleton in all cell lines tested within 72h. The red refers to staining with Nile Red used to label oil phase, the green refers staining with fluorescent antibody for β-actin used to label the cytoskeleton and yellow represents the merging of the two pictures [187].

4.1.3.3 Cell Cycle Analysis through Propidium Iodide Staining

Flowmetric analysis of DNA content was performed in parallel in WM 164 and Caco-2 cells DPS-2 was administered in both cell lines, either dissolved in DMSO or encapsulated in the o/w microemulsion (loaded sample) at the same concentration (5.6 μM) and samples were analyzed. Cells were cultured and analyzed at 24, 48, and 72h after the treatment onset. There was no significant increase in the sub-G1 phase, in all cases, indicating a non-apoptotic cell death induced. As shown in Figures 45a-d, in all cases DPS-2 treatment induced S phase delay in cell cycle progression. The S phase delay is generally associated with DNA Damage Response. In particular, cells respond to DNA damage by activating a complicated network of checkpoint signaling pathways to delay the progression of cell cycle, in order to repair the abnormalities [220].

More specifically, the DNA replication (or S phase checkpoint) controls the integrity of DNA synthesis and any abnormality in DNA synthesis can lead to replication fork stalling and activation of the relative checkpoint pathway [221]. In case

that the mechanism of checkpoint recovery fails, stalled forks can continue the procedure, expanding the possibility of DNA damage and replication fork collapse [222]. It has been reported that the inhibition of cell cycle progression, when induced by benzothiophene derivatives, could arise from cell cycle S phase arrest [223]. These findings, showing the inhibition of cell cycle progression of Caco-2 and WM 164 cells by DPS-2, enhance the hypothesis of cell cycle arrest mechanism.

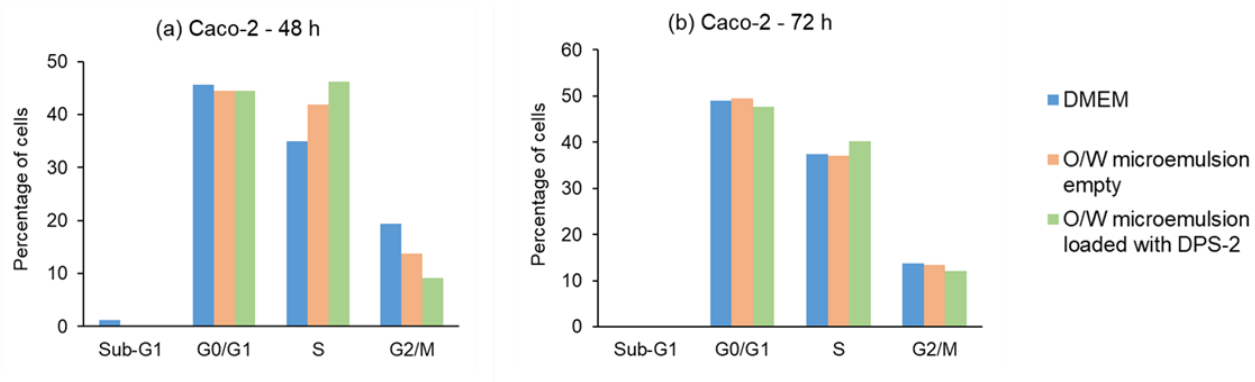

Figure 45a,b. Diagrams of cell cycle analysis of non-treated (DMEM) Caco-2 cells and treated Caco-2 cells with either o/w microemulsion empty 0.2% v/v or o/w microemulsion loaded with DPS-2 at 5.6μM. The nuclei were stained using propidium iodide A representative experiment out of triplicate is depicted [187].

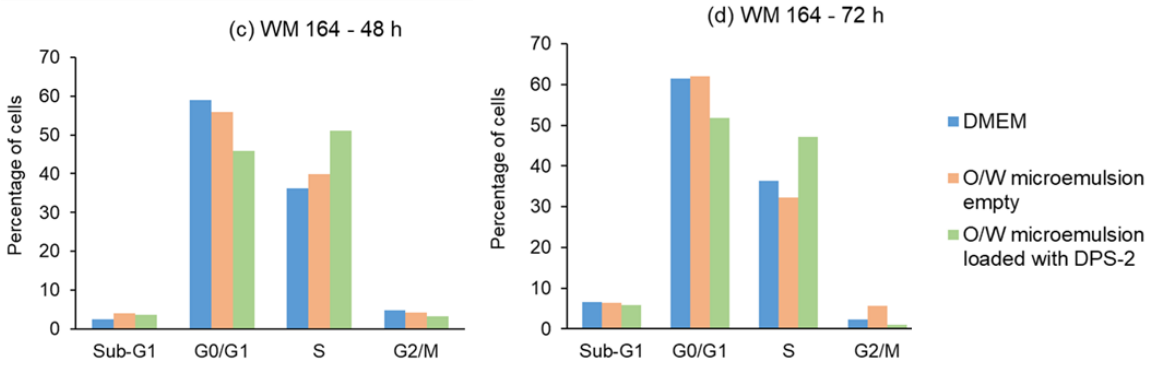

Figure 45c,d. Diagrams of cell cycle analysis of non-treated (DMEM) WM 164 cells and treated WM 164 cells with either o/w microemulsion empty 0.2% v/v or o/w microemulsion loaded with DPS-2 at 5.6μM. The nuclei were stained using propidium iodide A representative experiment out of triplicate is depicted [187].

As observed, empty o/w microemulsions slightly affect the progression of cell cycle. However, as these results were combined with cell viability assay, it seems that cells recover after few hours, as inhibition of cell proliferation was not observed in case of empty samples. On the contrary, when cells were treated with loaded microemulsions with DPS-2, an arrest in S-phase was observed. Teskac et al., reported that the incubation with solid-lipid nanoparticles loaded with resveratrol moved the selected keratinocytes from G1 phase to S phase of the cell cycle but S phase arrest was noticed. In case of empty solid lipid nanoparticles, no disturbance in cell cycle was observed [224].

As mentioned above, in all cell lines used in this study, p53 was inactive and thus, non-functional ($p53^{null}$). In order to investigate the role of functional p53 ($p53^{wt}$) in the cytotoxic effect of DPS-2, the A549 ($p53^{wt}$) non-small cell lung adenocarcinoma cell line was treated with DPS-2 in parallel. Both cell viability assay and cell cycle analysis were performed, for reasons of comparison. As observed, DPS-2 affected the G1 phase at 72h of treatment, however, only a negligible, not statistically important, increase of cytotoxicity was observed at the same time point as functional p53 seems to support DNA replication process, preserving DNA integrity before damage occurs (Figure 46). To conclude, these findings indicate that when p53 is inactive and non-functional, DPS-2 inhibited cell cycle progression and induced cell death through S phase arrest, which indicates damage at the DNA replication fork level [225].

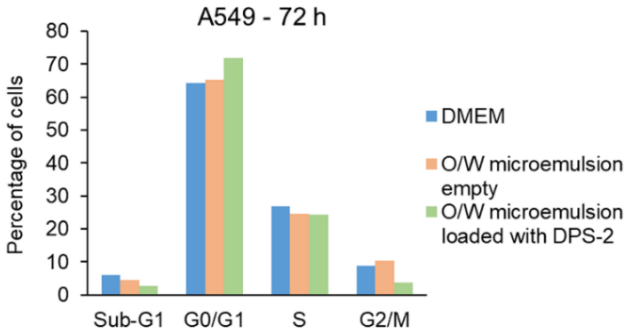

Figure 46. Diagrams of cell cycle analysis of non-treated (DMEM) A549 cells and treated A549 cells with either o/w microemulsion empty 0.2% v/v or o/w microemulsion loaded

with DPS-2 at 5.6μM. The nuclei were stained using propidium iodide A representative experiment out of triplicate is depicted [187].

4.1.3.4 Molecular Analysis by Western Blotting

The molecular mechanism of the induced cell death was examined through biochemical analysis of both DNA replication block and cell death markers, by performing Western blotting. The specific cleavage of poly(adenosine diphosphate-ribose) polymerase 1 (PARP-1), a nuclear protein implicated in DNA repair, to a 89 kDa fragment is related with activation of apoptosis and thus, is considered as a sensitive apoptotic marker. The fragmentation of PARP-1 often occurs through caspases-dependent proteolysis [226]. When DNA damage occurs, in the context of response, cells activate PARP-1 to enhance the approachability of DNA repair enzymes and transcription factors to chromatin. In the literature, a scientific debate has been reported concerning the role of PARP-1 in the monitoring of cell survival and/or cell death when DNA damage occurs [227]. Various research groups have indicated that PARP-1 contributes to the regulation of DNA repair and cell survival process. However, some other groups have shown that PARP-1 is involved in programmed cell death monitoring by different types of cell death such as apoptosis, autophagy or necrosis [228–230].

It is well-established that PARP-1 is cleaved into two fragments of 24 kDa and 89 kDa, indicating caspase-dependent apoptosis by caspases 3 and 7 [231]. As observed in Figure 47, PARP-1 cleavage was not detected in either cell line following DPS-2 treatment, in agreement with the lack of sub-G1 phase in cell cycle analysis [232]. The cell death induced by DPS-2 in WM 164 and Caco-2 cell lines was not apoptotic, as combined by the lack of sub-G1 phase in cell cycle analysis and confirmed by immunoblotting of PARP-1 cleavage. The obtained information revealed replication fork collapse due to DPS-2 treatment.

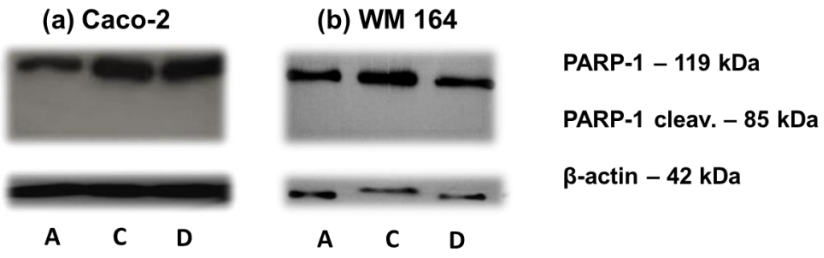

Figure 47. Cleavage of PARP as a biomarker for apoptosis. Immunoblot of Caco-2 (a) and WM 164 cell extracts (b) (40 μg) with a-PARP antibody detecting both the PARP fragment at 85KDa and the 119 kDa PARP form. β-actin was blotted on the same blot as control. DMEM (A); o/w microemulsion empty 0.2% v/v (C); o/w microemulsion loaded with DPS-2 at 5.6 μM (D) [187].

Moreover, the biochemical changes of cdc25A, which is a member of the cdc25 family of protein phosphatases were analyzed. In general, the cdc25 family act as positive regulators of the cell cycle. Cdc25A protein levels are firmly regulated and remain low throughout the S-phase. Then, they rise during mitosis. The protein itself is rapidly degraded when cells are exposed to agents that block DNA replication. Subsequently, cdc25A is required for progression from G1 to S phase and thus can be considered as a specific S phase arrest marker [233]. The DNA replication regulates the DNA synthesis and any abnormality in DNA synthesis can lead to replication fork stalling and activation of the relative checkpoint pathway [221]. If checkpoint recovery mechanisms fail, stalled forks can continue the procedure, increasing the possibility of DNA damage [222].

As clearly shown in Figure 48, a degradation of cdc25A, in agreement with the S phase arrest indicated in the cell cycle analysis, was observed in WM 164 and Caco-2 cells. The biochemical analysis confirmed the lack of apoptosis and induction of cell death through S phase arrest, indicating that DPS-2 inhibits DNA replication and thus cell proliferation, at the replication fork level. As stalled forks persist single-strand breaks (SSBs) and double-strand breaks (DSBs) were finally formed, the agent's cytotoxicity was furtherly increased in accordance with the results obtained from cell viability assay. The degradation of cdc25A as a response to genotoxic stress, is proteasome-dependent and independent of the p53-p21 [233]. The destruction of

cdc25A, that was observed at 72 h after the treatment with encapsulated DPS-2, was related to the S phase delay at 48 h, which along with cytotoxicity results enhances the hypothesis about secondary induction of DNA damage as a result of DNA replication fork stalling and collapse.

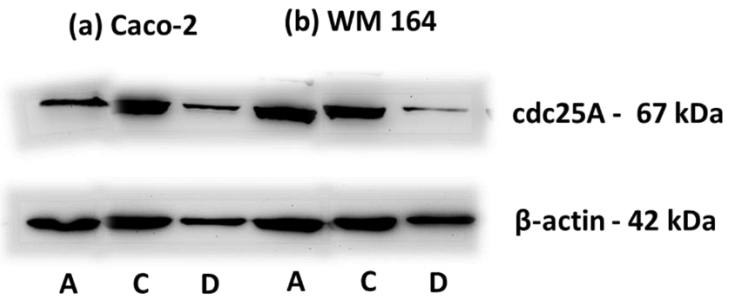

Figure 48. Detection of cdc25a in protein extracts of Caco-2 (a) and WM 164 (b) cells 72h after the treatment onset. All extracts (25 μg) were blotted with a-cdc25a antibody detecting the 67KDa form. β-actin was blotted on the same blot as control. DMEM (A); o/w microemulsion empty 0.2% v/v (C); o/w microemulsion loaded with DPS-2 at 5.6 μM (D) [187].

4.1.3.5 Comet Assay

Comet assay is defined as a sensitive tool to detect strand breaks in the DNA of cells [176]. Towards this approach, genotoxicity of DPS-2 was examined using Caco-2 cells 48 h after the treatment onset. As shown in Figure 49 by the tail DNA percentage diagram, no DNA damage was observed, suggesting that DPS-2 is not a direct genotoxic agent. When cell cycle analysis was performed, DPS-2 induced S phase arrest 48 h after the treatment onset, while cdc25A destruction was observed through Western blotting. It seems that DPS-2 is a potent cytotoxic agent, capable of stalling the DNA replication fork, directly activating the replication S phase checkpoint which is independent of p53 [220]. Even several peculiar values were observed, it seems that neither the microemulsion itself as a carrier nor the cytotoxic compound DPS-2 are direct genotoxic agents (Figure 49). As a result, DPS-2 inhibits cell proliferation, mainly by interacting and blocking sub-cellular pathways of cell cycle progression and not through DNA fragmentation.

Comet assay is still the most common method to evaluate the degree of genotoxicity of both bioactive compounds but also nanocarriers such as microemulsions. In most of the studies, the result of comet assay confirmed that the formulations components did not produce any noticeable DNA damage in cell lines tested. Natesan et al., with the aim of confirming the cellular safety of the developed Tween 80-based microemulsion, comet assay was carried out. In comparison to untreated cells, no significant increase in DNA damage was measured in the microemulsion-treated cells [234].

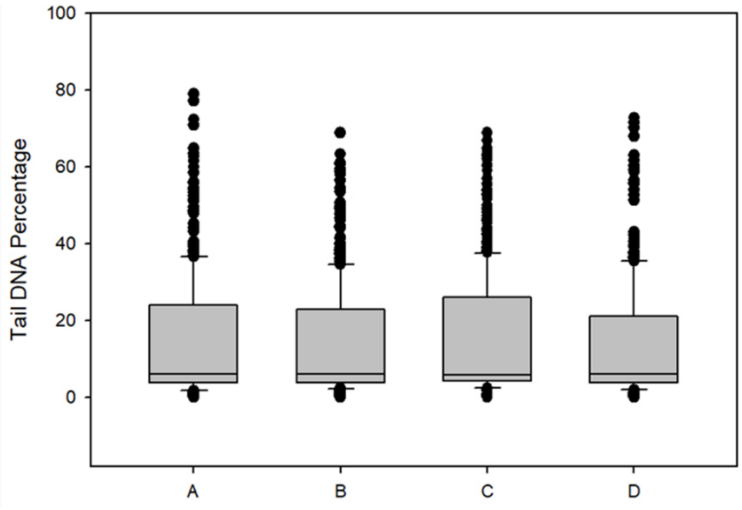

Figure 49. Box plots presenting the tail DNA percentage of Caco-2 cells after 48h after the treatment onset. DMEM (A); DPS-2 solubilized in DMSO at 5.6 μM (B); o/w microemulsion empty 0.2% v/v (C); o/w microemulsion loaded with DPS-2 at 5.6 μM (D) [187].

4.1.4 *Ex vivo* biological assessment of oil-in-water (o/w) microemulsions

The skin is considered as one of the most significant and challenging barriers to overcome in order to achieve dermal or transdermal delivery of bioactive compounds. In literature, only a few compounds tend to pass through this barrier and penetrate the stratum corneum layer or deeper and eventually they are either concentrated locally (dermal administration) or enter systemic blood flow (transdermal release). In order to evaluate the effectiveness of the formulated o/w nanodispersions, skin permeation studies were carried out.

4.1.4.1 Evaluation of skin penetration – Franz cell

Ex vivo permeation protocols, using porcine ear skin, were applied to assess the retention of DPS-2 on the skin. Permeability experiments were carried out using a modified Franz diffusion model and porcine ear was used as the selected biological membrane. In the Franz cell apparatus, cells consist of a donor chamber and a receptor chamber separated from the membrane. The permeability profile of DPS-2 was obtained by determining its percentage, passing through the cell acceptor compartment over time.

The permeated quantity of DPS-2 was detected using liquid chromatography coupled to mass spectrometry (LC-MS / MS) and the samples were taken at 3,6,9,21,24,27 and 30h after administration. In figure 50, the total quantity of DPS-2 that penetrated in full-thickness skin layers within 30h, is represented.

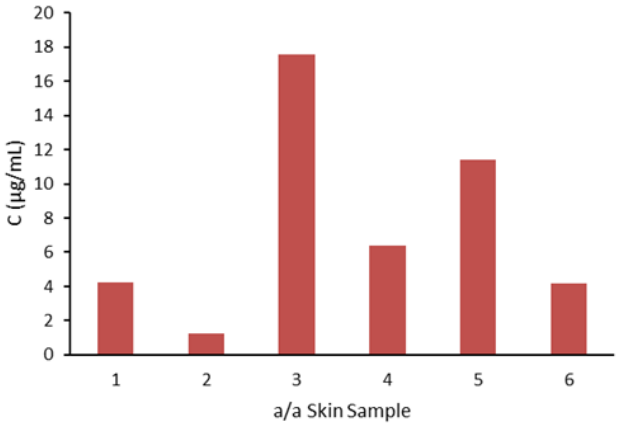

Figure 50. Diagram of quantification of DPS-2 in the skin layers after 30h. The amount is expressed in μg /mL.

The study was performed in three independent experiments, each in duplicate. In all cases DPS-2 was not detected in samples taken from receptor's department, indicating that it is not likely to pass through systemic circulation. Overall, the proposed o/w microemulsion is suitable to be used in dermal applications of bioactive compounds.

In the literature it has been shown that the layers of stratum corneum and epidermis are more lipophilic compared to dermis. Thus, the affinity of a strongly

lipophilic compound, such as DPS-2, with dermis is expected lower than the affinity of the same compound with epidermis. These data suggest that a more lipophilic compound has a high diffusion rate within the layers of stratum corneum and epidermis and the diffusion rate is decreased within dermis layers [235]. According to the results obtained, DPS-2 is more likely to be released in stratum corneum and epidermis than pass through dermis and reach blood circulation.

4.1.4.2 Differential Tape Stripping

Differential Tape Stripping was performed on porcine ear skin to quantify the amount of drug found in the stratum corneum layer (SC) and hair follicles. Although there are specific differences in anatomy among human and porcine hair follicles, several similarities are also identified. Thus, the *ex vivo* model of porcine ear is an applicable and reliable model to evaluate the penetration of bioactive compounds in SC. This method helps to evaluate the amount of DPS-2 that penetrates through the surface layers of the skin. Also, these experiments can reveal information on the affinity of DPS-2 to the hair follicles, forming a reservoir for their sustained release.

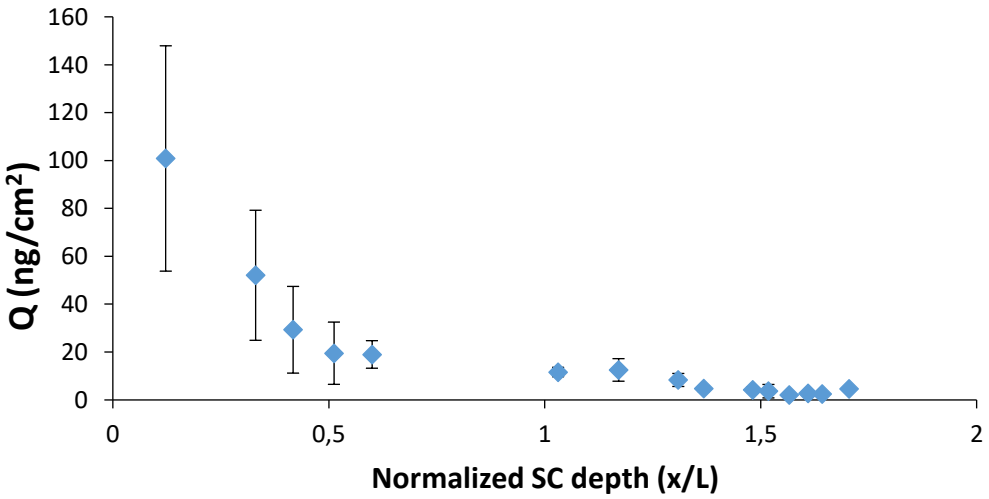

Figure 51. Representation of the quantity of DPS-2 (ng/cm^2) in relation to normalized stratum corneum depth.

The quantity of DPS-2 was detected using liquid chromatography coupled to mass spectrometry (LC-MS/MS) and samples were taken 2h after administration. The study was performed in five independent experiments. DPS-2 was detected in all samples taken from stratum corneum, in decreasing concentrations. As observed, DPS-2 presented relative high affinity with hair follicles as a quantity of almost 69.3 ng/mL passed in SC through hair, compared to the quantity of 599.2 ng/mL that was detected in full stratum corneum thickness. Moreover, fifteen (15) tapes were used to remove all layers of stratum corneum and as observed in Figure 51, the last tape contained almost 2ng/mL, which was the lower detection limit of LC MS/MS in this study. Thus, the encapsulated DPS-2 was distributed in stratum corneum within 2h of application and also the use of microemulsions facilitate the penetration of their cargo via hair follicles (Figure 51).

The mechanism by which micro- and nanoemulsions enhance cargo's permeation through hair follicles is possible to be enhanced due to a combination of different factors. Some of these include increased bioactive compound's solubility in the dispersed phase of the formulation, compatibility of the micro- and nanoemulsion with the lipophilic environment of the follicle and also due to the reduced barrier thickness in hair follicles [236]. In general, drug physicochemical properties contribute the most to the drug's preference for follicular penetration. More specifically, encapsulated drug's and hair follicles affinity is higher when the drug molecule is more lipophilic. As a result, the follicular route is described as an oil phase-loaded diffusion pathway. Despite all these, only a small quantity of the encapsulated drug is finally delivered through hair follicles, compared to other, alternative permeation mechanisms, which comes in agreement with the obtained results [235,237].

4.2 Nanoemulsions as carriers of a model lipophilic drug: the case of Ibuprofen

The subject of this study was the formulation and structural characterization of o/w nanoemulsions based on safe materials as delivery systems of the model lipophilic drug Ibuprofen ([(±)-2-(p-isobutyl phenyl)propionic acid]) (Figure 52). Ibuprofen is a commercially available non-steroid, anti-inflammatory drug (NSAID), used in different routes of administration, such as oral, topical, buccal etc. [238–240]. In the present study medium chain triglycerides (MCT), were used as the dispersed oil phase.

Polysorbate 80 (Tween 80), Labrasol® and soybean lecithin were used as surfactants. Distilled water was used as the aqueous phase. All the compounds are considered as non-toxic and suitable for use in food, cosmetic and medical applications.

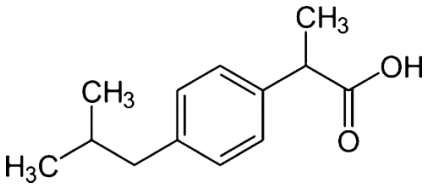

Figure 52. Chemical structure of Ibuprofen (https://www.sigmaaldrich.com/).

The structural study was performed by Dynamic Light Scattering (DLS) and Electron Paramagnetic Resonance (EPR) spectroscopy. DLS was used to determine the average diameter of the oil nanodroplets, to evaluate system's homogeneity by measuring the polydispersity index (PdI) but also to assess nanoemulsion's stability during storage. EPR spectroscopy was used to investigate the interfacial properties of the surfactants monolayer and to evaluate the impact of encapsulation of the chosen bioactive compounds, in nanoemulsion's structure. Moreover, *in vitro* assays for cell viability, of both empty and loaded nanoemulsions with Ibuprofen, in various cancer cell lines, among them the MW 164 skin melanoma cell line and the Caco-2 human epithelial colorectal adenocarcinoma cell line, were performed. Percentage of cell survival was measured to evaluate the effect of nanoemulsions' components and the effective release of the chosen lipophilic compound in cell cultures. In the context of a potential use of the proposed nanoemulsion for dermal applications, the effective release of Ibuprofen was examined by performing *ex vivo* studies.

4.2.1 Development of oil-in-water (o/w) nanoemulsions

Biocompatible o/w nanoemulsions composed of distilled water as the aqueous phase, medium chain triglycerides as the oil phase, and various surfactants such as soybean lecithin polysorbate 80 (suitable for use in cell culture) and Labrasol® (suitable for topical and oral administration) were developed. The formulation of the o/w nanoemulsions was performed, using high pressure homogenization and the

conditions (number of cycles, pressure, temperature) were defined. A pre-mix of the ingredients was prepared prior to homogenization using mechanical stirring. Following, the pre-mix was furtherly homogenized in the high pressure homogenizer until the desired size and size distribution of the oil nanodroplets was obtained. The developed systems were optically opaque.

Nanoemulsions composed of different ratios of aqueous to oil phase and also different combinations of surfactants were formulated. The nanoemulsion composed of 88% wt. distilled water, 2 wt% polysorbate 80, 3.75 wt%. Labrasol ALF®, 1.25% wt. soy lecithin and 5% wt. medium chain triglycerides was selected for further study. The conditions of homogenization were listed as follows: 10 homogenization cycles, pressure of 800 bar, temperature reached during homogenization was 42℃. The bioactive compound that was encapsulated in the proposed nanoemulsion was Ibuprofen, a standard lipophilic compound as a model drug to study the structure and efficacy of nanoemulsion. The encapsulation of Ibuprofen was performed at a concentration of 5mM, while a range of different concentrations in the cell culture medium were tested. Ibuprofen was directly dissolved in the oil phase in room temperature and then the nanoemulsion was formulated, as described above.

4.2.1 Structural characterization of oil-in-water (o/w) nanoemulsions

Techniques such as Dynamic Light Scattering (DLS) and electron Paramagnetic Resonance (EPR) spectroscopy were used for the structural characterization of both empty and loaded nanoemulsions with Ibuprofen. The techniques were used to evaluate the size and size distribution of the oil nanodroplets, the stability of the nanoemulsion during storage and to study the interfacial properties of the surfactants layer, before and upon encapsulation of Ibuprofen.

4.2.1.1 Dynamic Light Scattering (DLS)

Based on the experimental measurements of Dynamic Light Scattering, the encapsulation of Ibuprofen did not appear to affect neither the size distribution of the nanodroplets (Figure 53) nor the polydispersity index (PdI). The PdI values that were recorded, were less than 0.3 in case of empty sample and less than 0.2 in case of loaded

sample, ensuring nanoemulsion's homogeneity (Figure 54). At the same time, the nanoemulsion possessed a storage stability of approximately 40 days, before collapsing and phase separation.

It has been shown, that nanoemulsions containing medium chain triglycerides (MCT) as the oil phase were put in storage for up to 10 days, without observing any phase separation. However, nanoemulsions containing short chain triglycerides (SCT) presented phase separation only in a few hours, due to the Ostwald ripening mechanism [241]. It was found that the mean diameter of oil nanodroplets in empty and loaded nanoemulsions was slightly increasing during storage time. This comparatively slow process may be described by the Ostwald ripening in which bigger particles grow at the expense of smaller ones [62,63].

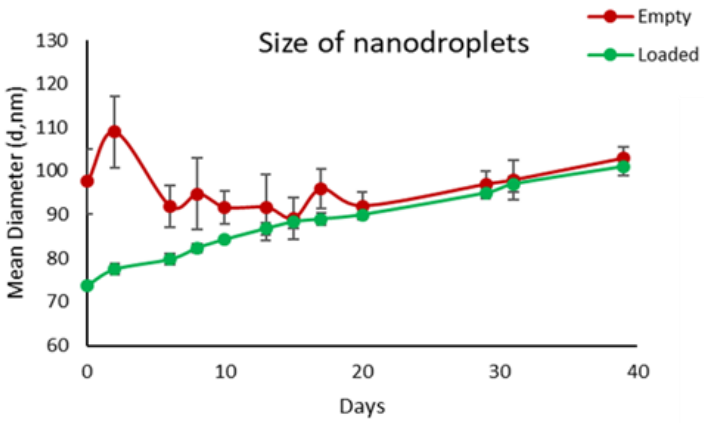

Figure 53. Mean diameter of nanodroplets in presence (green curve) and absence (red curve) of Ibuprofen.

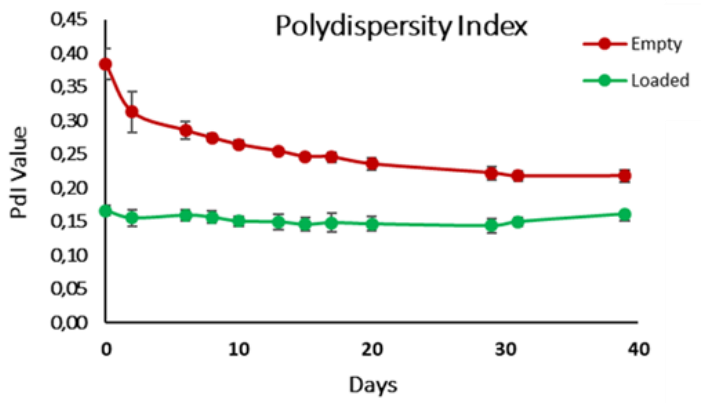

Figure 54. Diagram of Polydispersity index values (PdI) of the o/w nanoemulsion loaded with Ibuprofen (green curve) and o/w nanoemulsion empty (red curve).

As can be observed, incorporation of Ibuprofen in the oil cores of the nanoemulsions seemed to reduce the diameter of oil nanodroplets. Interestingly, after 10 days of storage, empty and loaded nanoemulsions presented similar size distribution. Taking into consideration DLS results, we can presume that encapsulation of Ibuprofen in the dispersed oil phase, caused the formulation of homogenous nanoemulsions with relatively small colloidal particle sizes.

4.2.1.2 Electron Paramagnetic Resonance Spectrometry (EPR)

Electron paramagnetic resonance spectroscopy (EPR) using the spin-probing technique was performed to study the interfacial characteristics of the surfactants' monolayer in both empty and loaded nanoemulsions with Ibuprofen. The spin-labelled fatty acid, 16-doxyl stearic acid (16-DSA), which was used as spin probe, is a spin label for membrane fluidity consisting of stearic acid and an N-oxyl radical (doxyl group) directly bonded to the C-16 of the hydrocarbon chain. When 16-DSA is solubilized in nanoemulsions, it is located and interact with the non-polar tails of surfactant molecules. Various Information considering the flexibility of the interface film, where the doxyl ring is localized, can be obtained.

In particular, in the case of 16-DSA, the nitroxide ring is closer to the non-polar region of the molecule and thus, closer to the surfactant non-polar tails. The EPR spectra from the spin-labelled fatty acid in empty and loaded nanoemulsions were obtained and analyzed. Figure 55 shows experimental EPR spectrum of 16-DSA in empty and loaded nanoemulsions. Furthermore, order parameter S and rotational correlation time τ_R values were determined for the empty and for the loaded nanoemulsions (Table 3). The samples were prepared and examined in tetraplicates for each sample.

Table 3. τ_R and S values obtained from EPR spectra of empty and loaded nanoemulsions. Ibuprofen concentration was 5 mM. Experiments were performed in triplicate and the results are expressed as mean values ± standard deviation (SD).

Sample	Rotational correlation time (τ_R) ns	Order Parameter S
o/w empty nanoemulsion	0.60 ± 0.03	0.04 ± 0.01
o/w loaded nanoemulsion	0.60 ± 0.04	0.04 ± 0.01

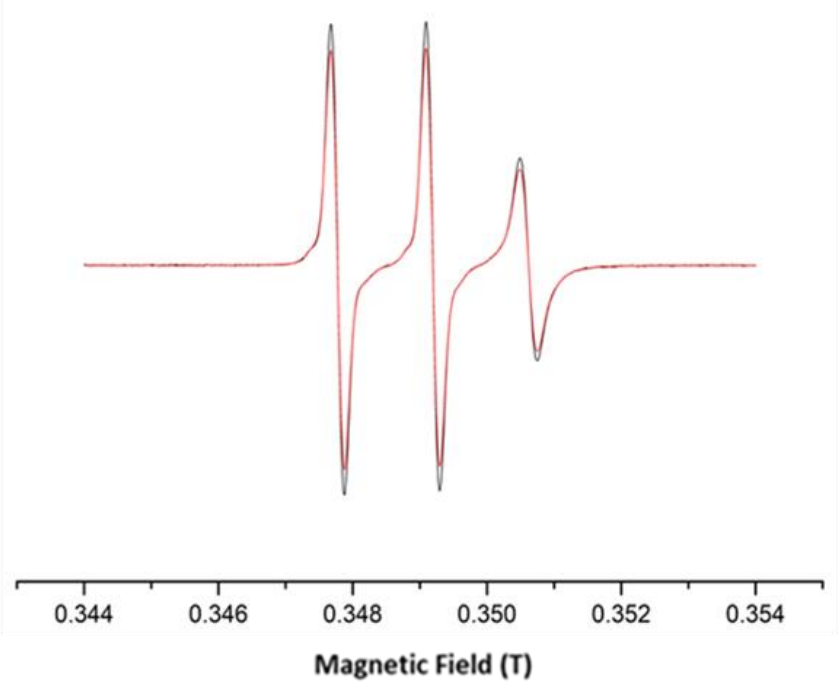

Figure 55. Electronic Paramagnetic Resonance (EPR) spectrum of the 16-DSA probe; (a) empty (black line) and (b) loaded with Ibuprofen (red line) nanoemulsion.

Based on these results, nanoemulsions composed of water, lecithin, Labrasol, Tween 80 and medium chain triglycerides were described by the presence of fluid interfacial layers possessing relatively low rigidity and allowing non-restricted movement of the spin probe along its long molecular axis. Moreover, in all cases, Ibuprofen did not interact with the surfactant molecules, as no significant difference between τ_R and S values was evidenced. The observed similarity in these values indicated the location of Ibuprofen within the oily cores of the nanoemulsions. Similar results were obtained when tacrolimus, a lipophilic drug, was encapsulated in lipid nanocarriers and τ_R and S values of 16-DSA spectra, did not represent any important alteration of the lipid dynamics [242].

4.2.2 *In vitro* biological assessment of o/w nanoemulsions

In order to assess the efficacy of o/w nanoemulsion as drug delivery systems and evaluate their cytotoxicity, the following *in vitro* approaches were carried out in the human MW 164 skin melanoma and Caco-2 epithelial colorectal adenocarcinoma cell lines.

4.2.2.1 Cell Proliferation Assay

Cell proliferation assays were carried out using the MTT assay. Cells were treated with Ibuprofen either dissolved in DMSO or encapsulated in o/w nanoemulsions, in a range of different concentrations. The impact of both empty and loaded nanoemulsions with Ibuprofen, was determined compared to its impact when dissolved in DMSO. The concentration of Ibuprofen dissolved in DMSO was exactly the same to the concentration of Ibuprofen encapsulated in the nanoemulsions. Nanoemulsions were administered into the cell culture following dilution at a ratio of 0.1% to 0.5% v/v to evaluate the potential cytotoxicity of the proposed delivery system. The percentage of cell viability 72h after treatment is shown in figures 56 and 57.

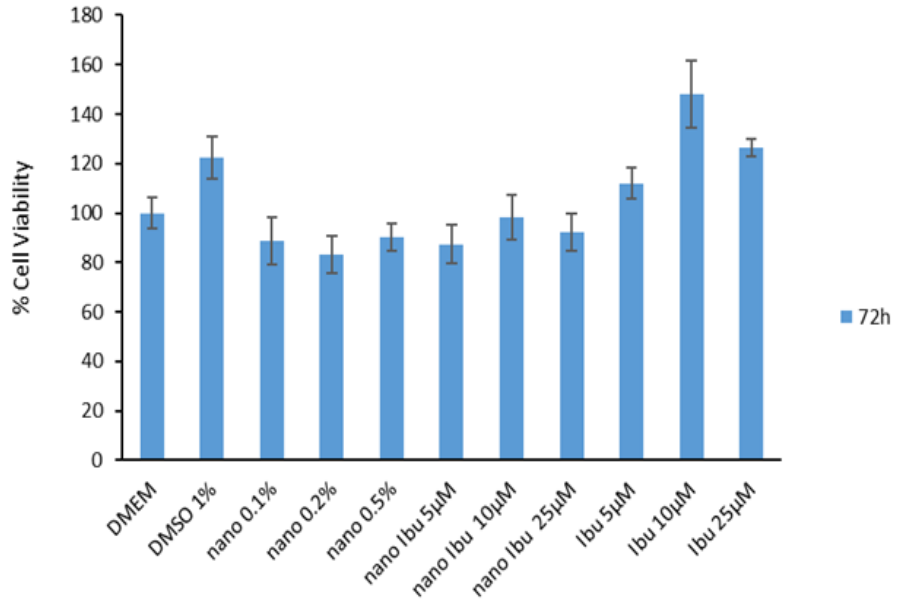

Figure 56. Results of cell proliferation assay in WM 164 cell line after 72h of treatment in WM 164 cell line after 72h of treatment.

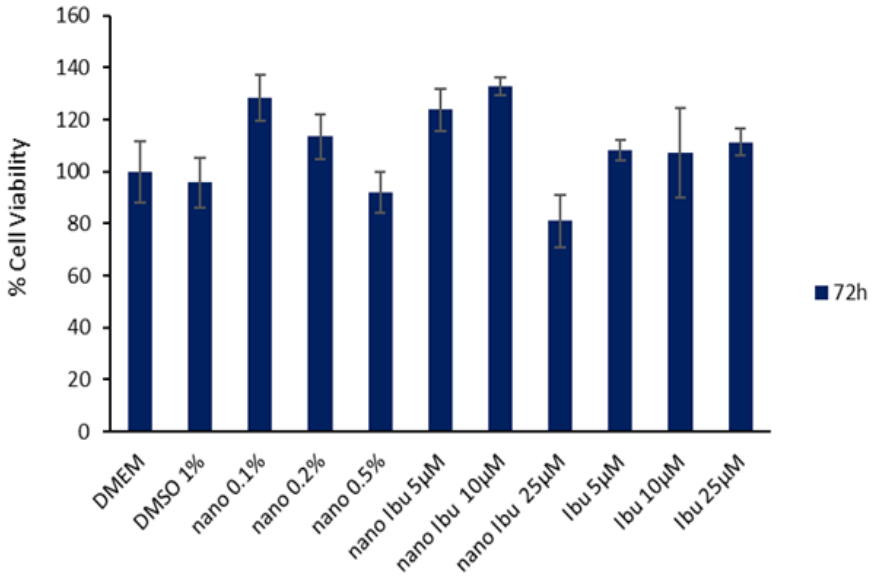

Figure 57. Results of cell proliferation assay in WM 164 cell line after 72h of treatment in Caco-2 cell line after 72h of treatment.

DMEM and DMEM plus DMSO at 0.1% v/v were used as positive control. The mean (± standard deviation) of three independent experiments, each performed in 5 replicates, is presented. The concentrations of both Ibuprofen solubilized in DMSO and Ibuprofen encapsulated in nanoemulsion, in cell culture medium, was within the range of 5μM to 25μM. As observed, o/w nanoemulsions (empty) at a final ratio of 0.5% v/v in the medium, did not affect cell viability in either cell line.

In case of non-ionic surfactants, the toxicity is expressed in a concentration-dependent manner. Toxicity levels were significantly different between non-ionic surfactants. The toxic effect is mainly explained by their amphiphilic structure which is similar to cell membrane structure, with which it interacts [39]. However, in various studies, especially in case of Tweens, no toxic effects have been reported. In particular, when Tween 80-based vehicles were used to deliver carotenoids to Caco-2 cells, the Tween-80 did not disrupt the cell membrane of the cells, as observed in the cell viability assay that was performed [243]. Moreover, it has been reported that the use of Labrasol in delivery vehicles, such as microemulsions, exhibited high tolerance and low toxicity *in vivo* [244]. Moreover, o/w nanoemulsions loaded with Ibuprofen did not significantly inhibited cell proliferation, as expected. In conclusion, the obtained information

indicate the suitability of the formulated o/w nanoemulsions as delivery systems of Ibuprofen into human cell lines.

4.2.3 *Ex vivo* biological assessment of oil-in-water (o/w) nanoemulsions

In the context of clarifying the efficacy of the developed nanoemulsions in dermal delivery, skin permeation studies were performed. Hence, the main subject was to evaluate the efficacy of nanoemulsions through an *ex vivo* approach. The following experiments were conducted at the Faculty of Pharmacy of the University of Belgrade in Serbia.

4.2.3.1 Evaluation of skin penetration – Franz cell

Ex vivo permeation protocols using porcine ear skin were applied to assess the retention of Ibuprofen in the skin. Permeability studies were carried out using a modified Franz diffusion model and porcine ear was chosen as the model biological membrane. In the Franz apparatus, each cell consists of a donor chamber and a receptor chamber separated from the membrane. The permeability profile of Ibuprofen released from nanoemulsion was obtained by determining the percentage of the bioactive compound passing through the cell acceptor compartment over time. The quantity of bioactive compounds was detected using liquid chromatography coupled to mass spectrometry (LC-MS/MS) and the samples were taken at 3,6,9,21,24,27 and 30h after administration.

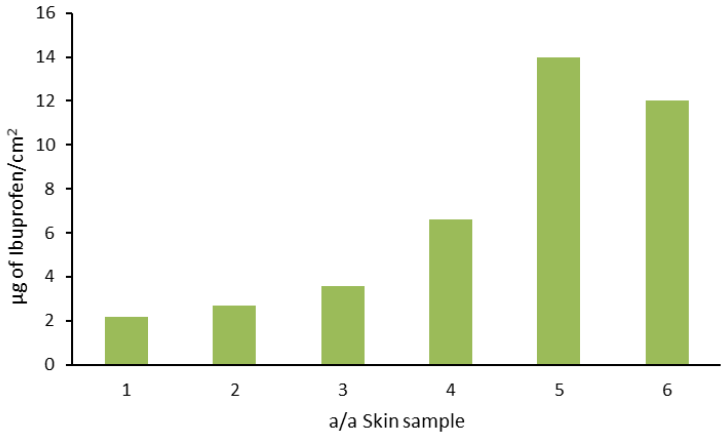

Figure 58. Diagram that represents the quantification of Ibuprofen in the receptor chamber after 30h. The amount is expressed in μg/cm^2.

In figure 58, the total amount of Ibuprofen that penetrated in full-thickness skin layers within 30h, is represented. The study was performed in three independent experiments, each in duplicate. Furthermore, Ibuprofen was detected in samples taken from receptor's department, indicating that even a small quantity of Ibuprofen is likely to pass through systemic circulation. In figure 59, the total quantity of Ibuprofen that remained in full-thickness skin layers within 30h, is represented. As observed, the quantity of Ibuprofen that was distributed topically is relatively high compared to the quantity of Ibuprofen detected in receptor medium.

In general, in various studies, Ibuprofen encapsulated in nanoemulsions seem to penetrate through full-thickness skin in a time-dependent manner, in accordance to the results obtained. In particular, when Tween 80-based nanoemulsions, loaded with ibuprofen, were applied in skin membrane, a constant increase of ibuprofen released in the receptor chamber was noticed up to 8 hours of administration. In that case, the permeation study was also performed using Franz cell device and skin as membrane [245]. Moreover, nanoemulsions facilitate the penetration of the encapsulated drug due to smaller droplet size, in comparison to aqueous/solvent solutions of drugs. In another study, the presence of medium chain triglycerides probably led to diffusion and blending of the oil phase with the stratum corneum lipids that facilitated the permeation of Ibuprofen [246].

Lecithin also played a major role in Ibuprofen's permeation as it has been characterized as a penetration enhancer agent. In this context, Zhou et al. reported an increase in bioactive compound's penetration that may resulted from an interference with the barrier properties of stratum corneum, probably because of the participation of lecithin in nanoemulsions used as topical delivery vehicles for lipophilic compounds [247].

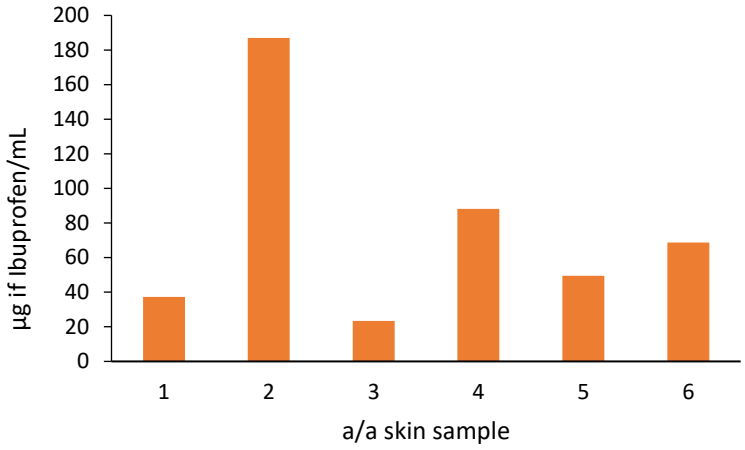

Figure 59. Diagram that represents the quantification of Ibuprofen in the full-thickness skin layers after 30h. The amount is expressed in µg/mL.

4.2.3.2 Differential Tape Stripping

Differential Tape Stripping was performed on porcine ear skin to quantify the amount of drug found in the stratum corneum layer (SC) and hair follicles. The quantity of Ibuprofen was detected using liquid chromatography coupled to mass spectrometry (LC-MS/MS) and samples were taken 2h after administration. The study was performed in five independent experiments. Ibuprofen was detected in all samples taken from stratum corneum, in decreasing concentrations (Figure 60).

In general, lipid-based nanocarriers enhance the skin permeation especially of lipophilic compounds through follicular or non-follicular way. More specifically, it has been reported that in case of Ibuprofen, the hair follicles played a minor role (<5%), in drug's permeation compared to other ways of permeation [248]. As observed, in accordance to previous studies, Ibuprofen did not present any affinity with hair follicles as it was not detected in hair follicles. Thus, the encapsulated Ibuprofen was distributed in stratum corneum within 2h of application. Nanoemulsions in this case did not facilitate the penetration of their cargo via hair follicles, as there was no detection of Ibuprofen in the extracts of hair follicles.

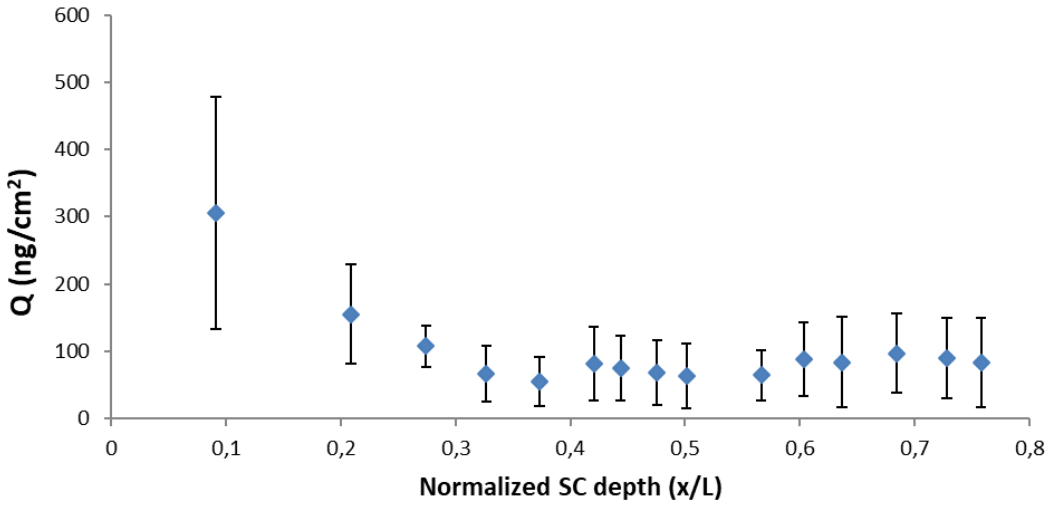

Figure 60. Representation of the quantity of Ibuprofen (ng/cm^2) in relation to normalized stratum corneum depth.

As previously mentioned, lecithin enhances permeation rate of encapsulated bioactive compounds. Thus, the presence of lecithin in a formulation increases the penetration of active substance [249]. On the contrary, the high content of water in o/w nanoemulsions increases dermal hydration and therefore contributes to the widening of intercellular junctions in stratum corneum by opening channels for delivery of drugs [250,251]. Therefore, it can be assumed that the combination of the presence of lecithin and the water-rich formulation is a potent explanation for the detection of Ibuprofen in receptor's chamber medium.

Chapter 5

Conclusions

Chapter 5 – Conclusions

5.1 Formulation and structural characterization of oil-in-water (o/w) microemulsions, as delivery systems of potent BRAF^{V600E} inhibitors

As the potential application of the proposed o/w microemulsions was the delivery of lipophilic drugs, the surfactant concentration was preferred to be low. Simultaneously, the oil content was high enough to permit the encapsulation of PLX 4720 at efficient levels. As a result, the composition of the microemulsions that was selected for further study was 81.5% w/w PBS buffer, 10.6% w/w Tween 80 and 7.9% w/w triacetin. Triacetin, (glyceryl triacetate), has been commonly reported in literature as safe and non-toxic food ingredient and thus, it was chosen as the oil phase of the microemulsions. It has been reported to be non-toxic against animals when they were exposure in oral and dermal administration and also in inhalation or parenteral administration [252]. Furthermore, Tween 80 that was used as the surfactant is a non-ionic amphiphile, which is extensively used in a variety of pharmaceutical formulations and products. To clarify the drug delivery efficacy of the proposed microemulsions, it is mandatory to determine their structural characteristics and also evaluate the impact of the drug on the system's micro-structure. Therefore, the microemulsions developed in this study were exposed in two different analytical techniques, DLS and EPR spectroscopy.

Dynamic Light Scattering was used to determine the size distribution of oil nanodroplets. When empty o/w microemulsions were analysed, an average diameter of 10.0 ± 0.1 nm was obtained. The encapsulation of PLX 4720 did not alter the size of nanodroplets. Furthermore, the polydispersity index value of the microemulsion was slightly increased, from 0.17 ± 0.02 to 0.21 ± 0.03. The nanodroplets size was not affected upon PLX 4720 encapsulation, most likely due to the location of the drug in the centre of the oil cores and also because the concentration of PLX 4720 was relatively low. Comparable results were obtained, when DPS-2 was encapsulated. The presence of a single population of oil nanodroplets of about 10 nm in diameter was observed. Upon encapsulation of DPS-2, comparable size distribution of nanodroplets was observed confirming the drug's location in the center of oil nanodroplets. In recent years, researchers have reported important results in developing o/w microemulsions

that are suitable as delivery systems of lipophilic drugs for oral or topical administration. Particularly, the selective or targeted transportation of anticancer agents to cancer cells, remains a major issue and still requires the formulation of efficient, biocompatible nanocarriers including microemulsions [253,254].

In the literature, in colloidal delivery systems such as emulsions, microemulsions and micelles, the size of the particles plays a significant role for the biodistribution of the drug after administration. The decrease of size of colloidal nanocarriers enhances their stability and also permits more favourable biodisposition [197,198]. Furthermore, the proposed o/w microemulsions were liquid formulations of relatively low viscosity, fact that confirms their appropriateness as delivery vehicles of the lipophilic chemotherapeutic compounds PLX 4720 and DPS-2.

The enhanced drug solubility in nanodispersions usually occurs due to the high solubilization capacity at the interface [204]. In contrast, in the present study, the selected bioactive compounds seemed to have no interaction with the surfactants' monolayer. This conclusion could be possibly connected to the increased solubility of PLX 4720 in triacetin (in case of PLX 4720) as compared to the solubility in the surfactants' monolayer. Furthermore, τ_R and S values were comparable in all cases and indicated that both PLX 4720 and DPS-2 were located inside the oily cores of the microemulsions and did not interact with the interface. Interestingly, the increased rigidity of the interfacial layer, as revealed by the order parameter values, did not prevent the release of the encapsulated bioactive molecules, as reflected by the *in vitro* and *ex vivo* assays.

Oil-in-water (o/w) microemulsions that composed of non-toxic ingredients were formulated as delivery vehicles of PLX 4720, a lipophilic drug against $BRAF^{V600E}$ kinase which is strongly related to melanomas and other cancer types. The analysis of structural characteristics of the empty and drug-loaded microemulsions indicated the formulation of delivery systems with low viscosity, narrow size distribution and relatively small colloidal particle sizes. The degree of drug encapsulation in the oil cores of the microemulsions was determined by different spectroscopic techniques.

5.2 In vitro & *ex vivo* evaluation of oil-in-water (o/w) microemulsions, as delivery systems of potent $BRAF^{V600E}$ inhibitors

Microemulsions, as nanocarriers, did not affect cell viability when administrated at colon cancer cell cultures in specific ratios. On the contrary, PLX 4720 and DPS-2, when encapsulated in microemulsions showed comparable response with the drug dissolved in DMSO which is the most common solvent for lipophilic drugs' administration. DMSO is considered to facilitate the transport of small molecules through cell membranes.

The clarification of the molecular mechanism that triggers the cytotoxic effect of an agent towards cancer cells, is of major importance for the formulation of effective therapeutics. Towards this approach, the elucidation of the molecular mechanism, that was triggered by the cytotoxic effect of the benzothiophene analogue DPS-2, is essential. To this point, due to the plethora of pharmaceutical and biological effects of the benzothiophene core structure, a large number of benzothiophene derivatives have been developed as lead compounds. These molecules are furtherly developed in the form of clinical drugs, with high therapeutic efficacy, against different diseases and pathologies [255].

The proposed microemulsions, empty and loaded with DPS-2, were subjected to *in vitro* biological assessment, using MW 164 skin melanoma and Caco-2 human epithelial colorectal adenocarcinoma cell lines. The choice of these cancer cell lines was supported by the use of microemulsions for transdermal and oral drug delivery by other research groups [213,215]. The formulated o/w microemulsions were proven efficient delivery systems of lipophilic compounds in all cell lines tested. Moreover, when DPS-2 was encapsulated at a concentration of 5.6 μM, significantly inhibited cell proliferation of the MW 164 skin melanoma and Caco-2 human epithelial colorectal adenocarcinoma cells. Both cell lines were also treated at the same time with DPS-2 solubilized in DMSO at same concentration. Although the empty o/w microemulsions seemed to slightly inhibited cell proliferation, the cells were totally recovered after 48h, indicating that DNA replication checkpoint recovery and replication fork restarted [220].

In cell cycle analysis, the data indicated that DPS-2 induced S phase delay 48h after the treatment onset while cdc25A degradation, that was detected through Western blotting at 72h in both cancer cell lines, confirmed this hypothesis. It seems that DPS-2 acts as a potent cytotoxic agent, capable of delaying the DNA replication fork and activating the replication S phase checkpoint which is independent of p53

[220]. In parallel, the cell cycle analysis of A549 cells ($p53^{wt}$) upon treatment under the same conditions and at the same time points was performed and, in that case, the DPS-2 administration induced G1 arrest at 72h, both encapsulated in microemulsion and dissolved in DMSO. On the contrary, as verified by the comet assay data, DPS-2 is not a direct genotoxic agent. This result, in accordance with cytotoxicity findings, supports the hypothesis that DNA damage is secondary induced as a result of DNA replication fork delaying and collapse. Interestingly, the same results were obtained when DPS-2, was administered via DMSO at the same concentration (5.6 μM), as samples were analyzed in parallel.

Through the *ex vivo* experiments, it was clarified that encapsulated DPS-2 was distributed within full-thickness of stratum corneum and performed high affinity to hair follicles. Moreover, DPS-2 was not found in the receptor buffer medium of Franz cell device, indicating that encapsulated DPS-2 when administrated dermally, it is not likely to enter blood circulation. Overall, the proposed o/w microemulsions are suitable carriers to deliver a potent chemotherapeutic agent through skin and enhance the maintance of the agent topically.

5.3 Nanoemulsions as carriers of a model lipophilic drug: the case of Ibuprofen – Formulation, structural study and in vitro/ex vivo evaluation

Biocompatible o/w nanoemulsions composed of Tween 80, soy lecithin, Labrasol, medium chain triglycerides and distilled water were formulated as delivery systems for the encapsulation of Ibuprofen, an anti-inflammatory, non-steroid drug. To deeply understand the potent application of the developed nanoemulsions in drug delivery, it is mandatory to specify their structural characteristics and also the effect of encapsulation on the microstructure. Subsequently, the nanoemulsions formulated in this study were subjected to Dynamic Light Scattering and Electron Paramagnetic Resonance Spectrometry. During this process, both empty and loaded nanoemulsions exhibited almost 40-days stability upon storage. Moreover, the results of spin-labelling technique indicated that Ibuprofen was located inside the oily cores of nanodroplets, without interacting with the interface layer.

The *in vitro* biological evaluation of the developed empty and loaded nanoemulsions in MW 164 skin melanoma and Caco-2 human epithelial colorectal

adenocarcinoma cell lines, followed structural characterization. As observed, the nanoemulsions did not affect cell viability when administrated at a ratio of 0.5% v/v in culture medium and thus, they were proven suitable and efficient delivery systems for drug delivery in the selected cell lines. Furthermore, Ibuprofen encapsulated and administrated at a concentration range of 5-25 μM, did not substantially affect cell viability of the MW 164 skin melanoma and Caco-2 human epithelial colorectal adenocarcinoma cells.

The *ex vivo* approach, indicated that encapsulated Ibuprofen was promptly distributed within full-thickness of stratum corneum, without performing high affinity to hair follicles. Contrary to the case of DPS-2, Ibuprofen was detected, even in small quantity, in the receptor buffer medium of Franz cell device. According to this result, the encapsulated Ibuprofen, when administrated dermally, it is likely to enter blood circulation. Overall, the proposed o/w nanoemulsions are suitable carriers to deliver a model lipophilic drug through skin but taking into consideration the possible effects of the small quantity of Ibuprofen that escapes from skin layers. In this case, nanoemulsions enhances the transdermal delivery of Ibuprofen.

5.4 General Conclusions

Oil-in-water (o/w) nanodispersions based on safe materials were formulated as efficient delivery systems of bioactive compounds with pharmacological interest. The selected compounds were PLX 4720, a lipophilic drug against $BRAF^{V600E}$ kinase which is strongly related to melanomas and other cancer types and DPS-2 which is a novel, potent cytotoxic agent in a variety of cancer cell lines. Furthermore, ibuprofen, was used as a model lipophilic drug for dermal administration. The structural characterization of the empty and loaded nanodispersions reflected the formulation of low viscous and homogenous delivery systems with the droplet sizes to range in the nanoscale. The degree of drug encapsulation within the oil cores of the nanodispersions was indirectly tested by applying different spectroscopic techniques. In all cases, the developed nanodispersions did not induce cell proliferation when administrated at selected cell cultures in specific ratios. However, PLX 4720 and DPS-2 when encapsulated in microemulsions showed comparable response with the drug dissolved in DMSO, commonly used as solvent in medical applications.

PLX 4720 and Ibuprofen are commercially available drugs and thus, their activity is well-studied. For this reason, they were used for proof-of-concept to evaluate the structure of the formulated nanodispersions, but also the suitability of such systems in dermal drug delivery. On the contrary, DPS-2, is an in-house synthesised benzothiophene analogue, designed as lead compound to inhibit $BRAF^{V600E}$ kinase. DPS-2 has emerged as a novel lead compound as it showed significant cytotoxic activity in selected human cancer cell lines. This point of view is furtherly verified by the results shown that DPS-2 applies its cytotoxic activity through delaying and finally collapse of the DNA replication fork.

There is a rising interest in research in drug delivery systems, especially in case of chemotherapeutic agents. At the same time, innovative strategies in this field are emerged compared to conventional therapies. Nanodispersions, due to their structure, allow the encapsulation and protection of bioactive compounds and overcome biological barriers, such as skin. In particular, in the field of pharmaceuticals, the effective administration of lipophilic substances is a major problem mainly due to the decrease their water solubility and limited bioavailability. The developed nanodispersions, that are proposed in this thesis, could contribute to overcome problems related to administration through skin barrier and low water solubility of the compounds, and also to enhance their penetration through skin layers. To conclude, the information obtained in this thesis could potentially contribute to the design and formulation of nanodispersions based on biocompatible materials to be used as carriers of lipophilic drugs, replacing DMSO which is actually used in most medical applications. The cytotoxic effects of DMSO on cell cultures and model organisms are currently investigated, and the proposal of such a replacement could be of foremost significance in the drug delivery field.

References

[1] P. Boisseau, B. Loubaton, Nanomedicine, nanotechnology in medicine, Comptes Rendus Phys. 12 (2011) 620–636. doi:10.1016/j.crhy.2011.06.001.

[2] M. Fanun, Microemulsions as delivery systems, Curr. Opin. Colloid Interface Sci. 17 (2012) 306–313. doi:10.1016/j.cocis.2012.06.001.

[3] T.P.U. Ravi, T. Padma, Nanoemulsions for drug delivery through different routes, Res. Biotechnol. 2 (2011) 1–13.

[4] M. Rawat, D. Singh, S. Saraf, S. Saraf, Nanocarriers: Promising Vehicle for Bioactive Drugs, Biol. Pharm. Bull. 29 (2006) 1790–1798. doi:10.1248/bpb.29.1790.

[5] B. Mishra, B.B. Patel, S. Tiwari, Colloidal nanocarriers: a review on formulation technology, types and applications toward targeted drug delivery, Nanomedicine Nanotechnology, Biol. Med. 6 (2010) 9–24. doi:10.1016/j.nano.2009.04.008.

[6] H.R. Dhanasekaran, P. Haridoss, Drug delivery nanosystems—An introduction, Elsevier Inc., 2018. doi:10.1016/B978-0-323-50922-0.00001-8.

[7] J.M. Rabanel, V. Aoun, I. Elkin, M. Mokhtar, P. Hildgen, Drug-Loaded Nanocarriers : Passive Targeting and Crossing of Biological Barriers, Curr. Med. Chem. 19 (2012) 3070–3102.

[8] J. Zink, N. Khashab, J. Fraser, M.E. Belowich, M. Liong, M.W. Ambrogio, Y.A. Lau, K.K. Cotı, H.A. Khatib, J.I. Zink, M. Khashab, J.F. Stoddart, Mechanised nanoparticles for drug delivery, Nanoscale. 1 (2009) 16–39. doi:10.1039/b9nr00162j.

[9] A. Sangtani, O.K. Nag, L.D. Field, J.C. Breger, J.B. Delehanty, Multifunctional nanoparticle composites: progress in the use of soft and hard nanoparticles for drug delivery and imaging, Wiley Interdiscip. Rev. Nanomedicine Nanobiotechnology. 9 (2017) 1–23. doi:10.1002/wnan.1466.

[10] X. Chen, Y. Tang, B. Cai, H. Fan, "One-pot" synthesis of multifunctional GSH-CdTe quantum dots for targeted drug delivery, Nanotechnology. 25 (2014). doi:10.1088/0957-4484/25/23/235101.

[11] I. Theochari, V. Papadimitriou, A. Xenakis, Nanocarriers for effective drug delivery, in: P. Nguyen Tri, T.-O. Do, T.A. Nguyen (Eds.), Smart Nanocontainers,

1st ed., Elsevier, 2019.

[12] M.M.A. Abdel-Mottaleb, D. Neumann, A. Lamprecht, Lipid nanocapsules for dermal application: A comparative study of lipid-based versus polymer-based nanocarriers, Eur. J. Pharm. Biopharm. 79 (2011) 36–42. doi:10.1016/j.ejpb.2011.04.009.

[13] I. Nikolic, D. Jasmin Lunter, D. Randjelovic, A. Zugic, V. Tadic, B. Markovic, N. Cekic, L. Zivkovic, D. Topalovic, B. Spremo-Potparevic, R. Daniels, S. Savic, Curcumin-loaded low-energy nanoemulsions as a prototype of multifunctional vehicles for different administration routes: Physicochemical and in vitro peculiarities important for dermal application, Int. J. Pharm. 550 (2018) 333–346. doi:10.1016/j.ijpharm.2018.08.060.

[14] J.K. Vasir, V. Labhasetwar, Biodegradable nanoparticles for cytosolic delivery of therapeutics, Adv. Drug Deliv. Rev. 59 (2007) 718–728. doi:10.1016/j.addr.2007.06.003.

[15] D.G. Schroeder, A., Heller, D.A., Winslow, M.M., Dahlman, J.E., Pratt, G.W., Langer, R., Jacks, T., Anderson, Treating metastatic cancer with nanotechnology, Nat. Rev. Cancer. 12 (2012) 39–50. doi:10.1038/nrc3180.

[16] I. Danielsson, B. Lindman, The definition of microemulsion, Colloids and Surfaces. 3 (1981) 391–392. doi:10.1016/0166-6622(81)80064-9.

[17] T.P. Hoar, J.H. Schulman, Transparent Water-in-Oil Dispersions: the Oleopathic Hydro-Micelle, Nature. 152 (1943) 102–103.

[18] S. Gibaud, D. Attivi, Microemulsions for oral administration and their therapeutic applications, Expert Opin. Drug Deliv. 9 (2012) 937–951. doi:10.1517/17425247.2012.694865.

[19] J.H. Schulman, J.B. Montagne, Formation of microemulsions by amino alkyl alcohols, Ann. New York Acad. Sci. 92 (1961) 366–371.

[20] W. Stoeckenius, J.H. Schulman, L.M. Prince, The structure of myelin figures and microemulsions as observed with the electron microscope, Kolloid-Zeitschrift. 1679 (1958) 170–180. doi:10.1007/BF01502567.

[21] S. Gupta, S.P. Moulik, Biocompatible microemulsions and their prospective uses in drug delivery, J. Pharm. Sci. 97 (2008) 22–45. doi:10.1002/jps.21177.

[22] M.J. Lawrence, G.D. Rees, Microemulsion-based media as novel drug delivery systems, Adv. Drug Deliv. Rev. 64 (2012) 175–193.

doi:10.1016/j.addr.2012.09.018.

[23] E. Karasulu, B. Karaca, Places of microemulsion and emulsion in cancer therapy: In vitro and in vivo evaluation, in: Taylor Fr. Gr., 2008.

[24] J. Flanagan, H. Singh, Microemulsions: A potential delivery system for bioactives in food, Crit. Rev. Food Sci. Nutr. 46 (2006) 221–237. doi:10.1080/10408690590956710.

[25] D.J. Mcclements, Edible nanoemulsions : fabrication , properties , and functional performance, Softmatter. 7 (2011) 2297–2316. doi:10.1039/c0sm00549e.

[26] Z.-J. Yu, R.D. Neuman, Reversed micellar solution-to-bicontinuous microemulsion transition in sodium bis (2-ethylhexyl) phosphate/n-heptane/water system, Langmuir. 11 (1995) 1081–1086. doi:10.1021/la00004a010.

[27] R.C. Santana, F.A. Perrechil, R.L. Cunha, High- and Low-Energy Emulsifications for Food Applications: A Focus on Process Parameters, Food Eng. Rev. 5 (2013) 107–122. doi:10.1007/s12393-013-9065-4.

[28] M. Fanun, Properties of microemulsions based on mixed nonionic surfactants and mixed oils, J. Mol. Liq. 150 (2009) 25–32. doi:10.1016/j.molliq.2009.09.008.

[29] D.J. McClements, Nanoemulsions versus microemulsions: Terminology, differences, and similarities, Soft Matter. 8 (2012) 1719–1729. doi:10.1039/c2sm06903b.

[30] C. Solans, P. Izquierdo, J. Nolla, N. Azemar, Nano-emulsions, Curr. Opin. Colloid Interface Sci. 10 (2005) 102–110. doi:10.1016/j.cocis.2005.06.004.

[31] D.J. McClements, Edible nanoemulsions: Fabrication, properties, and functional performance, Soft Matter. 7 (2011) 2297–2316. doi:10.1039/c0sm00549e.

[32] P. Calvo, J.L. Vila-Jato, M.J. Alonso, Comparative in vitro evaluation of several colloidal systems, nanoparticles, nanocapsules, and nanoemulsions, as ocular drug carriers, J. Pharm. Sci. 85 (1996) 530–536. doi:10.1021/js950474+.

[33] L. Wang, X. Li, G. Zhang, J. Dong, J. Eastoe, Oil-in-water nanoemulsions for pesticide formulations, J. Colloid Interface Sci. 314 (2007) 230–235. doi:10.1016/j.jcis.2007.04.079.

[34] Y. Singh, J.G. Meher, K. Raval, F.A. Khan, M. Chaurasia, N.K. Jain, M.K. Chourasia, Nanoemulsion: Concepts, development and applications in drug delivery, J. Control. Release. 252 (2017) 28–49. doi:10.1016/j.jconrel.2017.03.008.

[35] J.D. Hines, R.K. Thomas, P.R. Garrett, G.K. Rennie, J. Penfold, Investigation of Mixing in Binary Surfactant Solutions by Surface Tension and Neutron Reflection: Anionic/Nonionic and Zwitterionic/Nonionic Mixtures, J. Phys. Chem. 5647 (1997) 9215–9223. doi:10.1021/jp972099a.

[36] D. Ghosh, A.K. Pradhan, S. Mondal, N.A. Begum, D. Mandal, Proton transfer reactions of 4′-chloro substituted 3-hydroxyflavone in solvents and aqueous micelle solutions, Phys. Chem. Chem. Phys. 16 (2014) 8594–8607. doi:10.1039/c3cp52209a.

[37] N.A. Monteiro-Riviere, A.O. Inman, Y.Y. Wang, R.J. Nemanich, Surfactant effects on carbon nanotube interactions with human keratinocytes, Nanomedicine Nanotechnology, Biol. Med. 1 (2005) 293–299. doi:10.1016/j.nano.2005.10.007.

[38] E. Lémery, S. Briançon, Y. Chevalier, C. Bordes, T. Oddos, A. Gohier, M.A. Bolzinger, Skin toxicity of surfactants: Structure/toxicity relationships, Colloids Surfaces A Physicochem. Eng. Asp. 469 (2015) 166–179. doi:10.1016/j.colsurfa.2015.01.019.

[39] C. Maupas, B. Moulari, A. Béduneau, A. Lamprecht, Y. Pellequer, Surfactant dependent toxicity of lipid nanocapsules in HaCaT cells, Int. J. Pharm. 411 (2011) 136–141. doi:10.1016/j.ijpharm.2011.03.056.

[40] A. Bera, A. Mandal, Microemulsions: a novel approach to enhanced oil recovery: a review, J. Pet. Explor. Prod. Technol. 5 (2015) 255–268. doi:10.1007/s13202-014-0139-5.

[41] T.G. Mason, N. Wilking, K. Meleson, C.B. Chang, S.M. Graves, Nanoemulsions: formation, structure, and physical properties, J. Phys. Condens. Matter. 18 (2006) 636–666. doi:10.1088/0953-8984/18/41/R01.

[42] B.P. Binks, Particles as surfactants-similarities and differences, Colloid Interface Sci. 7 (2002) 21–41. doi:10.1016/S1359-0294(02)00008-0.

[43] M. Parkinson, Biosurfactants, Biotechnol. Adv. 3 (1985) 65–83. doi:10.1016/0734-9750(85)90006-0.

[44] E. Fuguet, C. Ràfols, M. Rosés, E. Bosch, Critical micelle concentration of surfactants in aqueous buffered and unbuffered systems, Anal. Chim. Acta. 548 (2005) 95–100. doi:10.1016/j.aca.2005.05.069.

[45] J. Rao, D.J. McClements, Lemon oil solubilization in mixed surfactant solutions: Rationalizing microemulsion & nanoemulsion formation, Food Hydrocoll. 26

(2012) 268–276. doi:10.1016/j.foodhyd.2011.06.002.

[46] T. Tadros, P. Izquierdo, J. Esquena, C. Solans, Formation and stability of nano-emulsions, Adv. Colloid Interface Sci. 108–109 (2004) 303–318. doi:10.1016/j.cis.2003.10.023.

[47] J.V.L. Henry, P.J. Fryer, W.J. Frith, I.T. Norton, Emulsification mechanism and storage instabilities of hydrocarbon-in-water sub-micron emulsions stabilised with Tweens (20 and 80), Brij 96v and sucrose monoesters, J. Colloid Interface Sci. 338 (2009) 201–206. doi:10.1016/j.jcis.2009.05.077.

[48] C. Qian, D.J. Mcclements, Formation of nanoemulsions stabilized by model food-grade emulsifiers using high-pressure homogenization: Factors affecting particle size, Food Hydrocoll. 25 (2011) 1000–1008. doi:10.1016/j.foodhyd.2010.09.017.

[49] T. Delmas, P. Poulin, M.E. Cates, How To Prepare and Stabilize Very Small Nanoemulsions, Langmuir. 27 (2011) 1683–1692. doi:10.1021/la104221q.

[50] D.J. McClements, J. Rao, Food-Grade nanoemulsions: Formulation, fabrication, properties, performance, Biological fate, and Potential Toxicity, Crit. Rev. Food Sci. Nutr. 51 (2011) 285–330. doi:10.1080/10408398.2011.559558.

[51] P. Sanguansri, M.A. Augustin, Nanoscale materials development-a food industry perspective, Food Sci. Technol. 17 (2006) 547–559. doi:10.1016/j.tifs.2006.04.010.

[52] L. Lee, I.T. Norton, Comparing droplet breakup for a high-pressure valve homogeniser and a Microfluidizer for the potential production of food-grade nanoemulsions, J. Food Eng. 114 (2013) 158–163. doi:10.1016/j.jfoodeng.2012.08.009.

[53] J.P. Canselier, H. Delmas, A.M. Wilhelm, B. Abismaïl, Ultrasound emulsification - An overview, J. Dispers. Sci. Technol. 23 (2002) 333–349. doi:10.1080/01932690208984209.

[54] S. Abbas, K. Hayat, E. Karangwa, M. Bashari, X. Zhang, An Overview of Ultrasound-Assisted Food-Grade Nanoemulsions, Food Eng. Rev. 5 (2013) 139–157. doi:10.1007/s12393-013-9066-3.

[55] D. Amadei, M.D. Chatzidaki, J. Devienne, J. Monteil, M. Cansell, A. Xenakis, F. Leal-Calderon, Low shear-rate process to obtain transparent W/O fine emulsions as functional foods, Food Res. Int. 62 (2014) 533–540. doi:10.1016/j.foodres.2014.03.069.

[56] P. Fernandez, J. Rieger, K. Angelika, Nano-emulsion formation by emulsion phase inversion, Colloids Surfaces A Physicochem. Eng. Asp. 251 (2004) 53–58. doi:10.1016/j.colsurfa.2004.09.029.

[57] C. Solans, I. Solé, Nano-emulsions: Formation by low-energy methods, Curr. Opin. Colloid Interface Sci. 17 (2012) 246–254. doi:10.1016/j.cocis.2012.07.003.

[58] C. Mabille, F. Leal-Calderon, J. Bibette, V. Schmitt, Monodisperse fragmentation in emulsions: Mechanisms and kinetics, Europhys. Lett. 61 (2003) 708–714. doi:10.1209/epl/i2003-00133-6.

[59] F. Ostertag, J. Weiss, D.J. McClements, Low-energy formation of edible nanoemulsions: Factors influencing droplet size produced by emulsion phase inversion, J. Colloid Interface Sci. 388 (2012) 95–102. doi:10.1016/j.jcis.2012.07.089.

[60] I.B. Ivanov, K.D. Danov, P.A. Kralchevsky, Flocculation and coalescence of micron-size emulsion droplets, Colloids Surfaces A Physicochem. Eng. Asp. 152 (1999) 161–182. doi:10.1016/S0927-7757(98)00620-7.

[61] A. Gupta, H.B. Eral, T.A. Hatton, P.S. Doyle, Nanoemulsions: Formation, properties and applications, Soft Matter. 12 (2016) 2826–2841. doi:10.1039/c5sm02958a.

[62] P. Taylor, Ostwald ripening in emulsions, Adv. Colloid Interface Sci. 75 (1998) 107–163. doi:10.1016/S0001-8686(98)00035-9.

[63] F. Leal-calderon, V. Schmitt, J. Bibette, Emulsion science: basic principles, 2nd ed., Springer Science & Business Media, New York, 2007. doi:10.1007/978-0-387-39683-5.

[64] I.M. Lifshitz, V. V. Slyozov, The kinetics of precipitation from supersaturated solid solutions, J. Phys. Chem. Solids. 19 (1961) 35–50. doi:10.1016/0022-3697(61)90054-3.

[65] Y. Li, S. Le Maux, H. Xiao, D.J. McClements, Emulsion-based delivery systems for tributyrin, a potential colon cancer preventative agent, J. Agric. Food Chem. 57 (2009) 9243–9249. doi:10.1021/jf901836f.

[66] K.P. Velikov, E. Pelan, Colloidal delivery systems for micronutrients and nutraceuticals, Soft Matter. 4 (2008) 1964–1980. doi:10.1039/b804863k.

[67] T. Frising, C. Noïk, C. Dalmazzone, The liquid/liquid sedimentation process: From droplet coalescence to technologically enhanced water/oil emulsion gravity separators: A review, J. Dispers. Sci. Technol. 27 (2006) 1035–1057.

doi:10.1080/01932690600767098.

[68] N. Anton, T.F. Vandamme, Nano-emulsions and micro-emulsions: Clarifications of the critical differences, Pharm. Res. 28 (2011) 978–985. doi:10.1007/s11095-010-0309-1.

[69] N. Anton, J.P. Benoit, P. Saulnier, Design and production of nanoparticles formulated from nano-emulsion templates-A review, J. Control. Release. 128 (2008) 185–199. doi:10.1016/j.jconrel.2008.02.007.

[70] P.N. Ezhilarasi, P. Karthik, N. Chhanwal, Nanoencapsulation Techniques for Food Bioactive Components: A Review, Food Bioprocess Technol. 6 (2013) 628–647. doi:10.1007/s11947-012-0944-0.

[71] M.R. Mozafari, J. Flanagan, L. Matia-merino, A. Awati, A. Omri, Z.E. Suntres, H. Singh, Recent trends in the lipid-based nanoencapsulation of antioxidants and their role in foods, J. Sci. OfFood Agric. 86 (2006) 2038–2045. doi:10.1002/jsfa.

[72] C. Pinto Reis, R.J. Neufeld, A.J. Ribeiro, F. Veiga, Nanoencapsulation I. Methods for preparation of drug-loaded polymeric nanoparticles, Nanomedicine Nanotechnology, Biol. Med. 2 (2006) 8–21. doi:10.1016/j.nano.2005.12.003.

[73] D.J. Mcclements, E.A. Decker, Y. Park, J. Weiss, Structural design principles for delivery of bioactive components in nutraceuticals and functional foods, 2009. doi:10.1080/10408390902841529.

[74] B.K. Kim, S.J. Hwang, J.B. Park, H.J. Park, Preparation and characterization of drug-loaded polymethacrylate microspheres by an emulsion solvent evaporation method, J. Microencapsul. 19 (2002) 811–822. doi:10.1080/0265204021000022770.

[75] H. Fessi, F. Puisieux, J.P. Devissaguet, N. Ammoury, S. Benita, Nanocapsule formation by interfacial polymer deposition following solvent displacement, Int. J. Pharm. 55 (1989) 1–4. doi:10.1016/0378-5173(89)90281-0.

[76] C. Janeth, M. Rivas, M. Tarhini, W. Badri, K. Miladi, H. Greige-gerges, Q.A. Nazari, S. Arturo, G. Rodríguez, R.Á. Román, H. Fessi, A. Elaissari, Nanoprecipitation process: From encapsulation to drug delivery, Int. J. Pharm. 532 (2017) 66–81. doi:10.1016/j.ijpharm.2017.08.064.

[77] K. Miladi, S. Sfar, H. Fessi, A. Elaissari, Nanoprecipitation Process: From Particle Preparation to In Vivo Applications, in: C. Vauthier, G. Ponchel (Eds.), Polym. Nanoparticles Nanomedicines, Springer International Publishing, Cham, 2016:

pp. 17–53. doi:10.1007/978-3-319-41421-8.

[78] C. Anandharamakrishnan, Liquid-Based Nanoencapsulation Techniques, 2014. doi:10.1007/978-1-4614-9387-7.

[79] L.B. Naves, C. Dhand, J.R. Venugopal, L. Rajamani, S. Ramakrishna, L. Almeida, Nanotechnology for the treatment of melanoma skin cancer, Prog. Biomater. 6 (2017) 13–26. doi:10.1007/s40204-017-0064-z.

[80] G.K. Menon, New insights into skin structure: Scratching the surface, Adv. Drug Deliv. Rev. 54 (2002) S3. doi:10.1016/S0169-409X(02)00121-7.

[81] M.A.F. Kendall, Y.F. Chong, A. Cock, The mechanical properties of the skin epidermis in relation to targeted gene and drug delivery, Biomaterials. 28 (2007) 4968–4977. doi:10.1016/j.biomaterials.2007.08.006.

[82] S.R. Slivka, L.K. Landeen, F. Zeigler, M.P. Zimber, R.L. Bartel, Characterization, barrier function, and drug metabolism of an in vitro skin model, J. Invest. Dermatol. 100 (1993) 40–46. doi:10.1111/1523-1747.ep12354098.

[83] T. Marjukka Suhonen, J. A. Bouwstra, A. Urtti, Chemical enhancement of percutaneous absorption in relation to stratum corneum structural alterations, J. Control. Release. 59 (1999) 149–161. doi:10.1016/S0168-3659(98)00187-4.

[84] V.M. Meidan, M.C. Bonner, B.B. Michniak, Transfollicular drug delivery - Is it a reality?, Int. J. Pharm. 306 (2005) 1–14. doi:10.1016/j.ijpharm.2005.09.025.

[85] F. Shakeel, S. Shafiq, N. Haq, F.K. Alanazi, I.A. Alsarra, Nanoemulsions as potential vehicles for transdermal and dermal delivery of hydrophobic compounds: An overview, Expert Opin. Drug Deliv. 9 (2012) 953–974. doi:10.1517/17425247.2012.696605.

[86] K. Raza, M. Kumar, P. Kumar, R. Malik, G. Sharma, M. Kaur, O.P. Katare, Topical Delivery of Aceclofenac : Challenges and Promises of Novel Drug Delivery Systems, Biomed Res. Int. 2014 (2014) 1–12.

[87] H. Trommer, R.H.H. Neubert, Overcoming the stratum corneum: The modulation of skin penetration. A review, Skin Pharmacol. Physiol. 19 (2006) 106–121. doi:10.1159/000091978.

[88] E. Larrucea, A. Arellano, S. Santoyo, P. Ygartua, Combined effect of oleic acid and propylene glycol on the percutaneous penetration of tenoxicam and its retention in the skin, Eur. J. Pharm. Biopharm. 52 (2001) 113–119. doi:10.1016/S0939-6411(01)00158-8.

[89] J. Cázares-Delgadillo, A. Naik, Y.N. Kalia, D. Quintanar-Guerrero, A. Ganem-Quintanar, Skin permeation enhancement by sucrose esters: A pH-dependent phenomenon, Int. J. Pharm. 297 (2005) 204–212. doi:10.1016/j.ijpharm.2005.03.020.

[90] D. Iliev, U. Hinnen, P. Elsner, Skin roughness is negatively correlated to irritation with DMSO, but not with NaOH and SLS, Exp. Dermatol. 6 (1997) 157–160. doi:10.1111/j.1600-0625.1997.tb00199.x.

[91] U.A. Shinde, S.H. Modani, K.H. Singh, Design and Development of Repaglinide Microemulsion Gel for Transdermal Delivery, AAPS PharmSciTech. 19 (2018) 315–325. doi:10.1208/s12249-017-0811-4.

[92] R. Shaimaa, A. Ali, E.A. Nabil, S.R. Aly, Microemulsion loaded hydrogel as a promising vehicle for dermal delivery of the antifungal sertaconazole: design, optimization and ex vivo evaluation, Drug Dev. Ind. Pharm. 43 (2017) 1351–1365. doi:10.1080/03639045.2017.1318899.

[93] V. Rastogi, P. Yadav, A. Verma, J.K. Pandit, Ex vivo and in vivo evaluation of microemulsion based transdermal delivery of E. coli specific T4 bacteriophage: A rationale approach to treat bacterial infection, Eur. J. Pharm. Sci. 107 (2017) 168–182. doi:10.1016/j.ejps.2017.07.014.

[94] V. Savić, M. Todosijević, T. Ilić, M. Lukić, E. Mitsou, V. Papadimitriou, S. Avramiotis, B. Marković, N. Cekić, S. Savić, Tacrolimus loaded biocompatible lecithin-based microemulsions with improved skin penetration: structure characterization and in vitro/in vivo performances, Int. J. Pharm. 529 (2017) 491–505. doi:10.1016/j.ijpharm.2017.07.036.

[95] Y. Zhang, Z. Li, K. Zhang, H. Zhang, Z. He, Q. Xia, J. Zhao, N. Feng, Co-delivery of evodiamine and rutaecarpine in a microemulsion-based hyaluronic acid hydrogel for enhanced analgesic effects on mouse pain models, Int. J. Pharm. 528 (2017) 100–106. doi:10.1016/j.ijpharm.2017.05.064.

[96] K. Kumari, B., Kesavan, Effect of chitosan coating on microemulsion for effective dermal clotrimazole delivery, Pharm. Dev. Technol. 22 (2016) 617–626. doi:10.1080/10837450.2016.1230629.

[97] J. Zhang, B.B. Michniak-kohn, Investigation of microemulsion and microemulsion gel formulations for dermal delivery of clotrimazole, Int. J. Pharm. 536 (2018) 345–352. doi:10.1016/j.ijpharm.2017.11.041.

[98] J. Sood, B. Sapra, A.K. Tiwary, Microemulsion Transdermal Formulation for Simultaneous Delivery of Valsartan and Nifedipine : Formulation by Design, AAPS PharmSciTech. 18 (2017) 1901–1916. doi:10.1208/s12249-016-0658-0.

[99] N.D. Yehia, R., Hathout, R. M., Attia, D. A., Elmazar, M. M., Mortada, Anti-tumor efficacy of an integrated Methyl Dihydrojasmonate transdermal microemulsion system targeting breast cancer cells: In-vitro and In-vivo studies, Colloids Surfaces B Biointerfaces. 155 (2017) 512–521. doi:10.1016/j.colsurfb.2017.04.031.

[100] M. Cao, L. Ren, G. Chen, Formulation Optimization and Ex Vivo and In Vivo Evaluation of Celecoxib Microemulsion-Based Gel for Transdermal Delivery, AAPS PharmSciTech. 18 (2017) 1960–1971. doi:10.1208/s12249-016-0667-z.

[101] A.L. Paudel, K. S., Milewski, M., Swadley, C. L., Brogden, N. K., Ghosh, P., Stinchcomb, Challenges and opportunities in dermal / transdermal delivery, Futur. Sci. 1 (2010) 109–131.

[102] M.H.F. Sakeena, M.F. Yam, S.M. Elrashid, A.S. Munavvar, M.N. Azmin, Anti-infl ammatory and Analgesic Effects of Ketoprofen in Palm Oil Esters Nanoemulsion, J. Oleo Sci. 671 (2010) 667–671. doi:10.1016/j.mehy.2013.08.007.

[103] S. Khurana, N.K. Jain, P.M.S. Bedi, Nanoemulsion based gel for transdermal delivery of meloxicam : Physico-chemical , mechanistic investigation, Life Sci. 92 (2013) 383–392. doi:10.1016/j.lfs.2013.01.005.

[104] V.P. de Almeida Borges, V.R., Simon, A., Sena, A.R.C., Cabral, L.M. de Sousa, Nanoemulsion containing dapsone for topical administration : a study of in vitro release and epidermal permeation, Int. J. Nanomedicine. 8 (2013) 535–544. doi:10.2147/IJN.S39383.

[105] M.P. Alves, A.L. Scarrone, M. Santos, A.R. Pohlmann, S. Guterres, Human skin penetration and distribution of nimesulide from hydrophilic gels containing nanocarriers, Int. J. Pharm. 341 (2007) 215–220. doi:10.1016/j.ijpharm.2007.03.031.

[106] E. Abd, H.A.E. Benson, M.S. Roberts, J.E. Grice, Minoxidil Skin Delivery from Nanoemulsion Formulations Containing Eucalyptol or Oleic Acid : Enhanced Diffusivity and Follicular Targeting, Pharmaceutics. 10 (2018) 1–12. doi:10.3390/pharmaceutics10010019.

[107] M.C. Fontana, J.F.P. Rezer, K. Coradini, D.B.R. Leal, R.C.R. Beck, Improved efficacy

in the treatment of contact dermatitis in rats by a dermatological nanomedicine containing clobetasol propionate, Eur. J. Pharm. Biopharm. 79 (2011) 241–249. doi:10.1016/j.ejpb.2011.05.002.

[108] F. Shakeel, S. Shafiq, N. Haq, F.K. Alanazi, I.A. Alsarra, Nanoemulsions as potential vehicles for transdermal and dermal delivery of hydrophobic compounds: an overview, Expert Opin. Drug Deliv. 9 (2012) 953–974. doi:10.1517/17425247.2012.696605.

[109] F. Shakeel, N. Haq, A. Al-dhfyan, F.K. Alanazi, I.A. Alsarra, Chemoprevention of skin cancer using low HLB surfactant nanoemulsion of 5-fluorouracil : a preliminary study, Drug Deliv. 22 (2013) 573–580. doi:10.3109/10717544.2013.868557.

[110] G.H. Kim, J.H., Ko, J.A., Kim, J.T., Cha, D.S., Cho, J.H., Park, H.J., Shin, Preparation of a Capsaicin-Loaded Nanoemulsion for Improving Skin Penetration, J. Agric. Food Chem. 62 (2014) 725–732.

[111] A.C. Fernández-Campos, F., Clares Naveros, B., López Serrano, O., Alonso Merino, C., & Calpena Campmany, Evaluation of novel nystatin nanoemulsion for skin candidosis infections, Mycoses. 56 (2012) 70–81. doi:10.1111/j.1439-0507.2012.02202.x.

[112] S. Khandavilli, R. Panchagnula, Nanoemulsions as Versatile Formulations for Paclitaxel Delivery : Peroral and Dermal Delivery Studies in Rats, J. Invest. Dermatol. 127 (2007) 154–162. doi:10.1038/sj.jid.5700485.

[113] S. Alam, S. Ali, N. Alam, M. Raza, M.M. Safhi, In vivo study of clobetasol propionate loaded nanoemulsion for topical application in psoriasis and atopic dermatitis, Drug Invent. Today. 5 (2013) 8–12. doi:10.1016/j.dit.2013.02.001.

[114] F. Kuo, B. Subramanian, T. Kotyla, T.A. Wilson, S. Yoganathan, R.J. Nicolosi, Nanoemulsions of an anti-oxidant synergy formulation containing gamma tocopherol have enhanced bioavailability and anti-inflammatory properties, Int. J. Pharm. 363 (2008) 206–213. doi:10.1016/j.ijpharm.2008.07.022.

[115] J. Tagne, S. Kakumanu, R.J. Nicolosi, Preparations of the Anticancer Drug Dacarbazine Significantly Increase Its Efficacy in a Xenograft Mouse Melanoma Model, Mol. Pharm. 54 (2008) 61–66.

[116] S. Kakumanu, J.B. Tagne, T.A. Wilson, R.J. Nicolosi, A nanoemulsion formulation of dacarbazine reduces tumor size in a xenograft mouse epidermoid carcinoma

model compared to dacarbazine suspension, Nanomedicine Nanotechnology, Biol. Med. 7 (2011) 277–283. doi:10.1016/j.nano.2010.12.002.

[117] A. Hussain, S. Singh, T.J. Webster, F.J. Ahmad, New Perspectives in the Topical Delivery of Optimized Amphotericin B Loaded Nanoemulsions Using Excipients with Innate Anti-fungal Activities: A Mechanistic and Histopathological Investigation, Nanomedicine Nanotechnology, Biol. Med. 13 (2016) 1117–1126. doi:10.1016/j.nano.2016.12.002.

[118] F.L. Primo, L. Michieleto, M.A.M. Rodrigues, P. Macaroff, L.B. Bentley, A.C. Tedesco, P.C. Morais, Z.G.M. Lacava, M. Vito, Magnetic nanoemulsions as drug delivery system for Foscan s : Skin permeation and retention in vitro assays for topical application in photodynamic therapy (PDT) of skin cancer, J. Magn. Magn. Mater. 311 (2007) 354–357. doi:10.1016/j.jmmm.2006.10.1183.

[119] F. Shakeel, W. Ramadan, Transdermal delivery of anticancer drug caffeine from water-in-oil nanoemulsions, Colloids Surfaces B Biointerfaces. 75 (2010) 356–362. doi:10.1016/j.colsurfb.2009.09.010.

[120] S. Avramiotis, V. Papadimitriou, E. Hatzara, V. Bekiari, P. Lianos, A. Xenakis, Lecithin organogels used as bioactive compounds carriers. A microdomain properties investigation, Langmuir. 23 (2007) 4438–4447. doi:10.1021/la0634995.

[121] H. Wu, C. Ramachandran, N.D. Weiner, B.J. Roessler, Topical transport of hydrophilic compounds using water-in-oil nanoemulsions, Int. J. Pharm. 220 (2001) 63–75.

[122] X. Zhu, X. Zeng, X. Zhang, W. Cao, Y. Wang, H. Chen, T. Wang, H.I. Tsai, R. Zhang, D. Chang, S. He, L. Mei, X. Shi, The effects of quercetin-loaded PLGA-TPGS nanoparticles on ultraviolet B-induced skin damages in vivo, Nanomedicine Nanotechnology, Biol. Med. 12 (2016) 623–632. doi:10.1016/j.nano.2015.10.016.

[123] H. Ikehata, T. Ono, The Mechanisms of UV Mutagenesis, J. Radiat. Res. 52 (2011) 115–125. doi:10.1269/jrr.10175.

[124] A.J. Thomas, C.A. Erickson, The making of a melanocyte: The specification of melanoblasts from the neural crest, Pigment Cell Melanoma Res. 21 (2008) 598–610. doi:10.1111/j.1755-148X.2008.00506.x.

[125] J. Liu, M. Fukunaga-Kalabis, L. Li, M. Herlyn, Developmental pathways activated in melanocytes and melanoma, Arch. Biochem. Biophys. 563 (2014) 13–21.

doi:10.1016/j.abb.2014.07.023.

[126] H. Mochizuki, M. Breen, Comparative aspects of BRAF mutations in canine cancers, Vet. Sci. 2 (2015) 231–245. doi:10.3390/vetsci2030231.

[127] H. Davies, G.R. Bignell, C. Cox, P. Stephens, S. Edkins, S. Clegg, J. Teague, H. Woffendin, M.J. Garnett, W. Bottomley, N. Davis, E. Dicks, R. Ewing, Y. Floyd, K. Gray, S. Hall, R. Hawes, J. Hughes, V. Kosmidou, A. Menzies, C. Mould, A. Parker, C. Stevens, S. Watt, S. Hooper, H. Jayatilake, B.A. Gusterson, C. Cooper, J. Shipley, D. Hargrave, K. Pritchard-Jones, N. Maitland, G. Chenevix-Trench, G.J. Riggins, D.D. Bigner, G. Palmieri, A. Cossu, A. Flanagan, A. Nicholson, J.W.C. Ho, S.Y. Leung, S.T. Yuen, B.L. Weber, H.F. Seigler, T.L. Darrow, H. Paterson, R. Wooster, R. Wooster, M.R. Stratton, P.A. Futreal, Mutations of the BRAF gene in human cancer, Nature. 417 (2002) 949–954. doi:10.1038/nature00766.

[128] A.S. Dhillon, S. Hagan, O. Rath, W. Kolch, MAP kinase signalling pathways in cancer, Oncogene. 26 (2007) 3279–3290. doi:10.1038/sj.onc.1210421.

[129] J. Paluncic, Z. Kovacevic, P.J. Jansson, D. Kalinowski, A.M. Merlot, M.L.H. Huang, H.C. Lok, S. Sahni, D.J.R. Lane, D.R. Richardson, Roads to melanoma: Key pathways and emerging players in melanoma progression and oncogenic signaling, Biochim. Biophys. Acta - Mol. Cell Res. 1863 (2016) 770–784. doi:10.1016/j.bbamcr.2016.01.025.

[130] P.T.C. Wan, M.J. Garnett, S.M. Roe, S. Lee, D. Niculescu-Duvaz, V.M. Good, C.G. Project, C.M. Jones, C.J. Marshall, C.J. Springer, D. Barford, R. Marais, Mechanism of activation of the RAF-ERK signaling pathway by oncogenic mutations of B-RAF, Cell. 116 (2004) 855–867. doi:10.1016/S0092-8674(04)00215-6.

[131] M.A. Rahman, A. Salajegheh, R.A. Smith, A.K.Y. Lam, BRAF inhibitors: From the laboratory to clinical trials, Crit. Rev. Oncol. Hematol. 90 (2014) 220–232. doi:10.1016/j.critrevonc.2013.12.008.

[132] A.M. Menzies, G. V Long, Dabrafenib and Trametinib , Alone and in Combination for BRAF -Mutant Metastatic Melanoma, Clin. Cancer Res. 2012 (2014) 2035–2044. doi:10.1158/1078-0432.CCR-13-2054.

[133] E.W. Joseph, C.A. Pratilas, P.I. Poulikakos, M. Tadi, W. Wang, B.S. Taylor, E. Halilovic, Y. Persaud, F. Xing, A. Viale, J. Tsai, P.B. Chapman, G. Bollag, D.B. Solit, N. Rosen, The RAF inhibitor PLX4032 inhibits ERK signaling and tumor cell proliferation in a V600E BRAF-selective manner, Proc. Natl. Acad. Sci. U. S. A. 107

(2010) 14903–14908. doi:10.1073/pnas.1008990107.

[134] S.M. Wilhelm, J. Dumas, L. Adnane, M. Lynch, C.A. Carter, G. Schütz, K.H. Thierauch, D. Zopf, Regorafenib (BAY 73-4506): A new oral multikinase inhibitor of angiogenic, stromal and oncogenic receptor tyrosine kinases with potent preclinical antitumor activity, Int. J. Cancer. 129 (2011) 245–255. doi:10.1002/ijc.25864.

[135] D. Strumberg, J.W. Clark, A. Awada, M.J. Moore, H. Richly, A. Hendlisz, H.W. Hirte, J.P. Eder, H.-J. Lenz, B. Schwartz, Safety, Pharmacokinetics, and Preliminary Antitumor Activity of Sorafenib: A Review of Four Phase I Trials in Patients with Advanced Refractory Solid Tumors, Oncologist. 12 (2007) 426–437. doi:10.1634/theoncologist.12-4-426.

[136] H. Mishra, P.K. Mishra, A. Ekielski, M. Jaggi, Z. Iqbal, S. Talegaonkar, Melanoma treatment: from conventional to nanotechnology, J. Cancer Res. Clin. Oncol. 144 (2018) 2283–2302. doi:10.1007/s00432-018-2726-1.

[137] E.S. Hickman, M.C. Moroni, K. Helin, The role of p53 and pRB in apoptosis and cancer, Curr. Opin. Genet. Dev. 12 (2002) 60–66. doi:10.1016/S0959-437X(01)00265-9.

[138] R.J.C. Steele, A.M. Thompson, P.A. Hall, D.P. Lane, The p53 tumor suppressor gene, Br. J. Surg. 85 (1998) 1460–1467. doi:10.1046/j.1365-2168.1998.00910.x.

[139] U.M. Moll, O. Petrenko, The MDM2-p53 Interaction, Mol. Cancer Res. 1 (2003) 1001–1008.

[140] S. Shangary, S. Wang, Targeting the MDM2-p53 interaction for cancer therapy, Clin. Cancer Res. 14 (2008) 5318–5324. doi:10.1158/1078-0432.CCR-07-5136.

[141] M.F. Lavin, N. Gueven, The complexity of p53 stabilization and activation, Cell Death Differ. 13 (2006) 941–950. doi:10.1038/sj.cdd.4401925.

[142] J.H. Houtgraaf, J. Versmissen, W.J. van der Giessen, A concise review of DNA damage checkpoints and repair in mammalian cells, Cardiovasc. Revascularization Med. 7 (2006) 165–172. doi:10.1016/j.carrev.2006.02.002.

[143] D. Branzei, M. Foiani, Regulation of DNA repair throughout the cell cycle, Nat. Rev. Mol. Cell Biol. 9 (2008) 297–308. doi:10.1038/nrm2351.

[144] M.B. Kastan, J. Bartek, Cell-cycle checkpoints and cancer, Nature. 432 (2004) 316–323. doi:10.1038/nature03097.

[145] M.L. Tan, J.P. Ooi, N. Ismail, A.I.H. Moad, T.S.T. Muhammad, Programmed cell

death pathways and current antitumor targets, Pharm. Res. 26 (2009) 1547–1560. doi:10.1007/s11095-009-9895-1.

[146] J.F.R. Kerr, A.H. Wyllie, A.R. Currie, Apoptosis: a Basic Biological Phenomenon With Wide-, Br. J. Cancer. 26 (1972) 239–257.

[147] L. Ouyang, Z. Shi, S. Zhao, F.T. Wang, T.T. Zhou, B. Liu, J.K. Bao, Programmed cell death pathways in cancer: A review of apoptosis, autophagy and programmed necrosis, Cell Prolif. 45 (2012) 487–498. doi:10.1111/j.1365-2184.2012.00845.x.

[148] Y.Y. Zhou, Y. Li, W.Q. Jiang, L.F. Zhou, MAPK/JNK signalling: A potential autophagy regulation pathway, Biosci. Rep. 35 (2015) 1–10. doi:10.1042/BSR20140141.

[149] K. Moriwaki, J. Bertin, P.J. Gough, G.M. Orlowski, F.K.M. Chan, Differential roles of RIPK1 and RIPK3 in TNF-induced necroptosis and chemotherapeutic agent-induced cell death, Cell Death Dis. 6 (2015) e1636-11. doi:10.1038/cddis.2015.16.

[150] T. Vanden Berghe, A. Linkermann, S. Jouan-Lanhouet, H. Walczak, P. Vandenabeele, Regulated necrosis: The expanding network of non-apoptotic cell death pathways, Nat. Rev. Mol. Cell Biol. 15 (2014) 135–147. doi:10.1038/nrm3737.

[151] M. Goulielmaki, N. Assimomytis, J. Rozanc, E. Taki, I. Christodoulou, L.G. Alexopoulos, V. Zoumpourlis, A. Pintzas, D. Papahatjis, DPS-2: A Novel Dual MEK/ERK and PI3K/AKT Pathway Inhibitor with Powerful Ex Vivo and In Vivo Anticancer Properties, Transl. Oncol. 12 (2019) 932–950. doi:10.1016/j.tranon.2019.04.005.

[152] M.J. Lawrence, G.D. Rees, Microemulsion-based media as novel drug delivery systems, Adv. Drug Deliv. Rev. 45 (2000) 89–121.

[153] V. Papadimitriou, S. Pispas, S. Syriou, A. Pournara, M. Zoumpanioti, T.G. Sotiroudis, A. Xenakis, Biocompatible Microemulsions Based on Limonene Formulation, Structure, and Applications.pdf, Langmuir. 24 (2008) 3380–3386. doi:10.1021/la703682c.

[154] N. Garti, M. Avrahami, A. Aserin, Improved solubilization of Celecoxib in U-type nonionic microemulsions and their structural transitions with progressive aqueous dilution, Colloid Interface Sci. 299 (2006) 352–365. doi:10.1016/j.jcis.2006.01.060.

[155] P.A. Hassan, S. Rana, G. Verma, Making sense of Brownian motion: Colloid

characterization by dynamic light scattering, Langmuir. 31 (2015) 3–12. doi:10.1021/la501789z.

[156] X. Fan, W. Zheng, D.J. Singh, Light scattering and surface plasmons on small spherical particles, Light Sci. Appl. 3 (2014) 1–14. doi:10.1038/lsa.2014.60.

[157] S. Bhattacharjee, DLS and zeta potential - What they are and what they are not?, J. Control. Release. 235 (2016) 337–351. doi:10.1016/j.jconrel.2016.06.017.

[158] G. Yang, Y. Wang, Dynamic light scattering of DNA-ligand complexes, Methods Mol. Biol. 1837 (2018) 161–176. doi:10.1007/978-1-4939-8675-0_10.

[159] M. Danaei, M. Dehghankhold, S. Ataei, F.H. Davarani, R. Javanmard, A. Dokhani, S. Khorasani, M.R.M. Id, Impact of Particle Size and Polydispersity Index on the Clinical Applications of Lipidic Nanocarrier Systems, Pharmaceutics. 10 (2018) 1–17. doi:10.3390/pharmaceutics10020057.

[160] C.J. Pickard, F. Mauri, First-Principles Theory of the EPR g Tensor in Solids: Defects in Quartz, Phys. Rev. Lett. 88 (2002) 4. doi:10.1103/PhysRevLett.88.086403.

[161] S. Kempe, H. Metz, K. Mäder, Application of Electron Paramagnetic Resonance (EPR) spectroscopy and imaging in drug delivery research - Chances and challenges, Eur. J. Pharm. Biopharm. 74 (2010) 55–66. doi:10.1016/j.ejpb.2009.08.007.

[162] H.O. Griffith, P.C. Jost, Lipid Spin Labels in Biological Membranes, in: L.J. Berliner (Ed.), Spin Labeling - Theory Appl., Academic Press, 1976: pp. 454–484.

[163] I. Golfomitsou, E. Mitsou, A. Xenakis, V. Papadimitriou, Development of food grade o/w nanoemulsions as carriers of vitamin D for the fortification of emulsion based food matrices: A structural and activity study, J. Mol. Liq. 268 (2018) 734–742. doi:10.1016/j.molliq.2018.07.109.

[164] V. Papadimitriou, T.G. Sotiroudis, A. Xenakis, Olive oil microemulsions: Enzymatic activities and structural characteristics, Langmuir. 23 (2007) 2071–2077. doi:10.1021/la062608c.

[165] S. Stoll, A. Schweiger, EasySpin, a comprehensive software package for spectral simulation and analysis in EPR, J. Magn. Reson. 178 (2006) 42–55. doi:10.1016/j.jmr.2005.08.013.

[166] D. Danino, Cryo-TEM of soft molecular assemblies, Curr. Opin. Colloid Interface Sci. 17 (2012) 316–329. doi:10.1016/j.cocis.2012.10.003.

[167] J. Van Meerloo, G.J.L. Kaspers, J. Cloos, Cell Sensitivity Assays : The MTT Assay, in: S.P. Langdon (Ed.), Cancer Cell Cult. Methods Mol. Med., 2004: pp. 165–169. doi:10.1007/978-1-61779-080-5.

[168] V. Vichai, K. Kirtikara, Sulforhodamine B colorimetric assay for cytotoxicity screening, Nat. Protoc. 1 (2006) 1112–1116. doi:10.1038/nprot.2006.179.

[169] M. Twarużek, E. Zastempowska, E. Soszczyńska, I. Ałtyn, The use of in vitro assays for the assessment of cytotoxicity on the example of MTT test, Folia Biol. Oecologica. 14 (2019) 23–32. doi:10.1515/fobio-2017-0006.

[170] V. Prasad, D. Semwogerere, E.R. Weeks, Confocal microscopy of colloids, J. Phys. Condens. Matter. 19 (2007) 1–25. doi:10.1088/0953-8984/19/11/113102.

[171] F. Traganos, Flow Cytometry: Principles and Applications. I, Cancer Invest. 2 (1984) 149–163. doi:10.3109/07357908409020296.

[172] A. Adan, G. Alizada, Y. Kiraz, Y. Baran, A. Nalbant, Y. Baran, A. Nalbant, Flow cytometry : basic principles and applications, Crit. Rev. Biotechnol. 8551 (2016) 1–14. doi:10.3109/07388551.2015.1128876.

[173] M.J. Wilkerson, Principles and Applications of Flow Cytometry and Cell Sorting in Companion Animal Medicine, Vetinary Clin. North Am. Small Anim. Pract. 42 (2012) 53–71. doi:10.1016/j.cvsm.2011.09.012.

[174] J.M. Walker, SDS Polyacrylamide Gel Electrophoresis of Proteins, in: J.M. Walker (Ed.), Protein Electroforesis Handb., 2002: pp. 61–67.

[175] T. Gwozdz, K. Dorey, Western Blot, in: Basic Sci. Methods Clin. Res., Elsevier Inc., 2017: pp. 99–117. doi:10.1016/B978-0-12-803077-6.00006-0.

[176] A.R. Collins, The Comet Assay for DNA Damage and Repair, Mol. Biotechnol. 26 (2004) 249–261.

[177] W. Liao, M.A. Mcnutt, W. Zhu, The comet assay: A sensitive method for detecting DNA damage in individual cells, Methods. 48 (2009) 46–53. doi:10.1016/j.ymeth.2009.02.016.

[178] C.A. Schneider, W.S. Rasband, K.W. Eliceiri, NIH Image to ImageJ: 25 years of image analysis, Nat. Methods. 9 (2012) 671–675. doi:10.1038/nmeth.2089.

[179] J.J. Escobar-chávez, R. Díaz-torres, I.M. Rodríguez-, C.L. Domínguez-, R.S. Morales, E. Ángeles-anguiano, L.M. Melgoza-, Nanocarriers for transdermal drug delivery, Res. Reports Transdermal Drug Deliv. 1 (2012) 3–17. doi:10.2147/RRTD.S32621.

[180] A.S. Raber, A. Mittal, J. Schäfer, U. Bakowsky, J. Reichrath, T. Vogt, U.F. Schaefer, S. Hansen, C.M. Lehr, Quantification of nanoparticle uptake into hair follicles in pig ear and human forearm, J. Control. Release. 179 (2014) 25–32. doi:10.1016/j.jconrel.2014.01.018.

[181] T. Ilić, S. Savić, B. Batinić, B. Marković, M. Schmidberger, D. Lunter, M. Savić, S. Savić, Combined use of biocompatible nanoemulsions and solid microneedles to improve transport of a model NSAID across the skin: In vitro and in vivo studies, Eur. J. Pharm. Sci. 125 (2018) 110–119. doi:10.1016/j.ejps.2018.09.023.

[182] W.A. Korfmacher, Principles and applications of LC-MS in new drug discovery, Drug Discov. Today. 10 (2005) 1357–1367. doi:10.1016/S1359-6446(05)03620-2.

[183] J. Tsai, J.T. Lee, W. Wang, J. Zhang, H. Cho, S. Mamo, R. Bremer, S. Gillette, J. Kong, N.K. Haass, K. Sproesser, L. Li, K.S.M. Smalley, D. Fong, Y.L. Zhu, A. Marimuthu, H. Nguyen, B. Lam, J. Liu, I. Cheung, J. Rice, Y. Suzuki, C. Luu, C. Settachatgul, R. Shellooe, J. Cantwell, S.H. Kim, J. Schlessinger, K.Y.J. Zhang, B.L. West, B. Powell, G. Habets, C. Zhang, P.N. Ibrahim, P. Hirth, D.R. Artis, M. Herlyn, G. Bollag, Discovery of a selective inhibitor of oncogenic B-Raf kinase with potent antimelanoma activity, Proc. Natl. Acad. Sci. U. S. A. 105 (2008) 3041–3046. doi:10.1073/pnas.0711741105.

[184] G. Bollag, J. Tsai, J. Zhang, C. Zhang, P. Ibrahim, K. Nolop, P. Hirth, Vemurafenib: The first drug approved for BRAF-mutant cancer, Nat. Rev. Drug Discov. 11 (2012) 873–886. doi:10.1038/nrd3847.

[185] S.J. Choi, E.A. Decker, L. Henson, L.M. Popplewell, D.J. McClements, Stability of citral in oil-in-water emulsions prepared with medium-chain triacylglycerols and triacetin, J. Agric. Food Chem. 57 (2009) 11349–11353. doi:10.1021/jf902761h.

[186] S. Dasgupta, S. Dey, S. Choudhury, B. Mazumder, Topical delivery of aceclofenac as nanoemulsion comprising excipients having optimum emulsification capabilities: Preparation, characterization and in vivo evaluation, Expert Opin. Drug Deliv. 10 (2013) 411–420. doi:10.1517/17425247.2013.749234.

[187] I. Theochari, V. Papadimitriou, D. Papahatjis, N. Assimomytis, E. Pappou, H. Pratsinis, A. Xenakis, V. Pletsa, Oil-In-Water Microemulsions as Hosts for Benzothiophene-Based Cytotoxic Compounds: An Effective Combination, Biomimetics. 3 (2018) 13. doi:10.3390/biomimetics3020013.

[188] I. Theochari, M. Goulielmaki, D. Danino, V. Papadimitriou, A. Pintzas, A. Xenakis,

Drug nanocarriers for cancer chemotherapy based on microemulsions: The case of Vemurafenib analog PLX4720, Colloids Surfaces B Biointerfaces. 154 (2017) 350–356. doi:10.1016/j.colsurfb.2017.03.032.

[189] J.S. Yuan, M. Ansari, M. Samaan, E.J. Acosta, Linker-based lecithin microemulsions for transdermal delivery of lidocaine, Int. J. Pharm. 349 (2008) 130–143. doi:10.1016/j.ijpharm.2007.07.047.

[190] M. Benigni, S. Pescina, M.A. Grimaudo, C. Padula, P. Santi, S. Nicoli, Development of microemulsions of suitable viscosity for cyclosporine skin delivery, Int. J. Pharm. 545 (2018) 197–205. doi:10.1016/j.ijpharm.2018.04.049.

[191] Y. Yuan, X. Che, M. Zhao, Y. Wang, Y. Liu, A. Schwendeman, S. Li, Development of cyclosporine A microemulsion for parenteral delivery, J. Microencapsul. 32 (2015) 273–280. doi:10.3109/02652048.2015.1010461.

[192] L. Hu, J. Yang, W. Liu, L. Li, Preparation and evaluation of ibuprofen-loaded microemulsion for improvement of oral bioavailability, Drug Deliv. 18 (2011) 90–95. doi:10.3109/10717544.2010.522613.

[193] C. Malcolmson, D.J. Barlow, M.J. Lawrence, Light-scattering studies of testosterone enanthate containing soybean oil/C18:1E10/water oil-in-water microemulsions, J. Pharm. Sci. 91 (2002) 2317–2331. doi:10.1002/jps.10221.

[194] X. Zhao, D. Chen, P. Gao, P. Ding, K. Li, Synthesis of ibuprofen eugenol ester and its microemulsion formulation for parenteral delivery, Chem. Pharm. Bull. 53 (2005) 1246–1250. doi:10.1248/cpb.53.1246.

[195] I. Nikolic, E. Mitsou, I. Pantelic, D. Randjelovic, B. Markovic, V. Papadimitriou, A. Xenakis, D.J. Lunter, A. Zugic, S. Savic, Microstructure and biopharmaceutical performances of curcumin-loaded low-energy nanoemulsions containing eucalyptol and pinene: Terpenes' role overcome penetration enhancement effect?, Eur. J. Pharm. Sci. 142 (2020). doi:10.1016/j.ejps.2019.105135.

[196] P. Izquierdo, J.W. Wiechers, E. Escribano, M.J. García-Celma, T.F. Tadros, J. Esquena, J.C. Dederen, C. Solans, A study on the influence of emulsion droplet size on the skin penetration of tetracaine, Skin Pharmacol. Physiol. 20 (2007) 263–270. doi:10.1159/000106076.

[197] B.E. Rabinow, Nanosuspensions in drug delivery, Nat. Rev. Drug Discov. 3 (2004) 785–796. doi:10.1038/nrd1494.

[198] S. Heuschkel, A. Goebel, R.H.H. Neubert, Microemulsions - Modern Colloidal

Carrier for Dermal and Transdermal Drug Delivery, J. Pharm. Sci. 97 (2008) 603–631. doi:10.1002/jps.20995.

[199] A. Spernath, A. Aserin, L. Ziserman, D. Danino, N. Garti, Phosphatidylcholine embedded microemulsions: Physical properties and improved Caco-2 cell permeability, J. Control. Release. 119 (2007) 279–290. doi:10.1016/j.jconrel.2007.02.014.

[200] N. Lidich, E.J. Wachtel, A. Aserin, N. Garti, Water-dilutable microemulsions for transepithelial ocular delivery of riboflavin phosphate, J. Colloid Interface Sci. 463 (2016) 342–348. doi:10.1016/j.jcis.2015.02.011.

[201] K. Margulis-goshen, E. Kesselman, D. Danino, S. Magdassi, Formation of celecoxib nanoparticles from volatile microemulsions, Int. J. Pharm. 393 (2010) 230–237. doi:10.1016/j.ijpharm.2010.04.012.

[202] M.D. Chatzidaki, E. Mitsou, A. Yaghmur, A. Xenakis, V. Papadimitriou, Formulation and characterization of food-grade microemulsions as carriers of natural phenolic antioxidants, Colloids Surfaces A Physicochem. Eng. Asp. (2015). doi:10.1016/j.colsurfa.2015.03.060.

[203] D.J. Schneider, J.H. Freed, Calculating slow motional magnetic resonance spectra, in: Spin Labeling - Theory Appl., Springer, Boston, USA, 1989: pp. 1–79.

[204] A.S. Narang, D. Delmarre, D. Gao, Stable drug encapsulation in micelles and microemulsions, Int. J. Pharm. 345 (2007) 9–25. doi:10.1016/j.ijpharm.2007.08.057.

[205] J. Qi, J. Zhuang, W. Wu, Y. Lu, Y. Song, Z. Zhang, J. Jia, Q. Ping, Enhanced effect and mechanism of water-in-oil microemulsion as an oral delivery system of hydroxysafflor yellow A, Int. J. Nanomedicine. (2011) 985–991. doi:10.2147/IJN.S18821.

[206] M.D. Hall, K.A. Telma, K.E. Chang, T.D. Lee, J.P. Madigan, J.R. Lloyd, I.S. Goldlust, J.D. Hoeschele, M.M. Gottesman, Say no to DMSO: Dimethylsulfoxide inactivates cisplatin, carboplatin, and other platinum complexes, Cancer Res. 74 (2014) 3913–3922. doi:10.1158/0008-5472.CAN-14-0247.

[207] N. Vlachy, D. Touraud, J. Heilmann, W. Kunz, Determining the cytotoxicity of catanionic surfactant mixtures on HeLa cells, Colloids Surfaces B Biointerfaces. 70 (2009) 278–280. doi:10.1016/j.colsurfb.2008.12.038.

[208] Z. Ujhelyi, F. Fenyvesi, J. Váradi, P. Fehér, T. Kiss, S. Veszelka, M. Deli, M.

Vecsernyés, I. Bácskay, Evaluation of cytotoxicity of surfactants used in self-micro emulsifying drug delivery systems and their effects on paracellular transport in Caco-2 cell monolayer, Eur. J. Pharm. Sci. 47 (2012) 564–573. doi:10.1016/j.ejps.2012.07.005.

[209] A. Eduardo, G. Barratt, M. Chéron, E.S.T. Egito, Development of oil-in-water microemulsions for the oral delivery of amphotericin B, Int. J. Pharm. 454 (2013) 641–648. doi:10.1016/j.ijpharm.2013.05.044.

[210] Y. Liu, W.F. Bodmer, Analysis of P53 mutations and their expression in 56 colorectal cancer cell lines, Proc. Natl. Acad. Sci. U. S. A. 103 (2006) 976–981. doi:10.1073/pnas.0510146103.

[211] M. Rieber, M.S. Rieber, Signalling responses linked to betulinic acid-induced apoptosis are antagonized by MEK inhibitor U0126 in adherent or 3D spheroid melanoma irrespective of p53 status, Int. J. Cancer. 118 (2006) 1135–1143. doi:10.1002/ijc.21478.

[212] K.C. Bible, S.H. Kaufmann, Flavopiridol: A Cytotoxic Flavone That Induces Cell Death in Noncycling A549 Human Lung Carcinoma Cells, Cancer Res. 56 (1996) 4856–4861.

[213] A. Kogan, N. Garti, Microemulsions as transdermal drug delivery vehicles, Adv. Colloid Interface Sci. 123–126 (2006) 369–385. doi:10.1016/j.cis.2006.05.014.

[214] M.S. Erdal, G. Ozhan, M.C. Mat, Y. Ozsoy, S. Gungor, Colloidal nanocarriers for the enhanced cutaneous delivery of naftifine: Characterization studies and in vitro and in vivo evaluations, Int. J. Nanomedicine. 11 (2016) 1027–1037. doi:10.2147/IJN.S96243.

[215] X.Q. Chen, T. Ziemba, C. Huang, M. Chang, C. Xu, J.X. Qiao, T.C. Wang, H.J. Finlay, M.E. Salvati, L.P. Adam, O. Gudmundsson, M.J. Hageman, Oral Delivery of Highly Lipophilic, Poorly Water-Soluble Drugs: Self-Emulsifying Drug Delivery Systems to Improve Oral Absorption and Enable High-Dose Toxicology Studies of a Cholesteryl Ester Transfer Protein Inhibitor in Preclinical Species, J. Pharm. Sci. 107 (2018) 1352–1360. doi:10.1016/j.xphs.2018.01.003.

[216] M.-Y. Hsu, D.E. Elder, M. Herlyn, Melanoma: The Wistar Melanoma (WM) Cell Lines, in: Hum. Cell Cult., 2005: pp. 259–274. doi:10.1007/0-306-46872-7_14.

[217] J.C. Byrd, R. Dahiya, J. Huang, Y.S. Kim, Inhibition of mucin synthesis by benzyl-α-GalNAc in KATO III gastric cancer and Caco-2 colon cancer cells, Eur. J. Cancer.

31 (1995) 1498–1505. doi:10.1016/0959-8049(95)00248-H.

[218] Y.T. Zhang, Z. Bin Huang, S.J. Zhang, J.H. Zhao, Z. Wang, Y. Liu, N.P. Feng, In vitro cellular uptake of evodiamine and rutaecarpine using a microemulsion, Int. J. Nanomedicine. 7 (2012) 2465–2472. doi:10.2147/IJN.S30616.

[219] M. Changez, J. Chander, A.K. Dinda, Transdermal permeation of tetracaine hydrochloride by lecithin microemulsion: In vivo, Colloids Surfaces B Biointerfaces. 48 (2006) 58–66. doi:10.1016/j.colsurfb.2006.01.007.

[220] J. Bartek, C. Lukas, J. Lukas, Checking on DNA damage in S phase, Nat. Rev. Mol. Cell Biol. 5 (2004) 792–804. doi:10.1038/nrm1493.

[221] D.R. Iyer, N. Rhind, The intra-S checkpoint responses to DNA damage, Genes (Basel). 8 (2017). doi:10.3390/genes8020074.

[222] I. Chaudhury, D.M. Koepp, Recovery from the DNA replication checkpoint, Genes (Basel). 7 (2016). doi:10.3390/genes7110094.

[223] J.T. Anderson, A.E. Ting, S. Boozer, K.R. Brunden, J. Danzig, T. Dent, J.J. Harrington, S.M. Murphy, R. Perry, A. Raber, S.E. Rundlett, J. Wang, N. Wang, Y.L. Bennani, Discovery of S-phase arresting agents derived from noscapine, J. Med. Chem. 48 (2005) 2756–2758. doi:10.1021/jm0494220.

[224] K. Teskač, J. Kristl, The evidence for solid lipid nanoparticles mediated cell uptake of resveratrol, Int. J. Pharm. 390 (2010) 61–69. doi:10.1016/j.ijpharm.2009.10.011.

[225] I. Klusmann, S. Rodewald, L. Müller, M. Friedrich, M. Wienken, Y. Li, R. Schulz-Heddergott, M. Dobbelstein, p53 Activity Results in DNA Replication Fork Processivity, Cell Rep. 17 (2016) 1845–1857. doi:10.1016/j.celrep.2016.10.036.

[226] A. Koryllou, M. Patrinou-Georgoula, C. Troungos, V. Pletsa, Cell death induced by N-methyl-N-nitrosourea, a model SN1 methylating agent, in two lung cancer cell lines of human origin, Apoptosis. 14 (2009) 1121–1133. doi:10.1007/s10495-009-0379-x.

[227] J.A. Muñoz-Gámez, J.M. Rodríguez-Vargas, R. Quiles-Pérez, R. Aguilar-Quesada, D. Martín-Oliva, G. De Murcia, J.M. De Murcia, A. Almendros, M. Ruiz De Almodóvar, F.J. Oliver, PARP-1 is involved in autophagy induced by DNA damage, Autophagy. 5 (2009) 61–74. doi:10.4161/auto.5.1.7272.

[228] Hyo Chol Ha, S.H. Snyder, Poly(ADP-ribose) polymerase is a mediator of necrotic cell death by ATP depletion, Proc. Natl. Acad. Sci. U. S. A. 96 (1999) 13978–13982. doi:10.1073/pnas.96.24.13978.

[229] Z.Q. Wang, L. Stingl, C. Morrison, M. Jantsch, M. Los, K. Schulze-Osthoff, E.F. Wagner, PARP is important for genomic stability but dispensable in apoptosis, Genes Dev. 11 (1997) 2347–2358. doi:10.1101/gad.11.18.2347.

[230] S.W. Yu, H. Wang, M.F. Poitras, C. Coombs, W.J. Bowers, H.J. Federoff, G.G. Poirier, T.M. Dawson, V.L. Dawson, Mediation of poty(ADP-ribose) polymerase-1 - Dependent cell death by apoptosis-inducing factor, Science (80-.). 297 (2002) 259–263. doi:10.1126/science.1072221.

[231] V.J. Bouchard, M. Rouleau, G.G. Poirier, PARP-1, a determinant of cell survival in response to DNA damage, Exp. Hematol. 31 (2003) 446–454. doi:10.1016/S0301-472X(03)00083-3.

[232] M.G. Ormerod, Investigating the relationship between the cell cycle and apoptosis using flow cytometry, J. Immunol. Methods. 265 (2002) 73–80. doi:10.1016/S0022-1759(02)00071-6.

[233] N. Mailand, J. Falck, C. Lukas, R.G. Syljuåsen, M. Welcker, J. Bartek, J. Lukas, Rapid destruction of human Cdc25A in response to DNA damage, Science (80-.). 288 (2000) 1425–1429. doi:10.1126/science.288.5470.1425.

[234] S. Natesan, A. Sugumaran, C. Ponnusamy, V. Jeevanesan, G. Girija, R. Palanichamy, Development and evaluation of magnetic microemulsion: Tool for targeted delivery of camptothecin to BALB/c mice-bearing breast cancer, J. Drug Target. 22 (2014) 913–926. doi:10.3109/1061186X.2014.948878.

[235] Y.Y. Grams, S. Alaruikka, L. Lashley, J. Caussin, L. Whitehead, J.A. Bouwstra, Permeant lipophilicity and vehicle composition influence accumulation of dyes in hair follicles of human skin, Eur. J. Pharm. Sci. 18 (2003) 329–336. doi:10.1016/S0928-0987(03)00035-6.

[236] E. Abd, H.A.E. Benson, M.S. Roberts, J.E. Grice, Follicular Penetration of Caffeine from Topically Applied Nanoemulsion Formulations Containing Penetration Enhancers: In vitro Human Skin Studies, Skin Pharmacol. Physiol. 31 (2018) 252–260. doi:10.1159/000489857.

[237] V.M. Meidan, Methods for quantifying intrafollicular drug delivery: A critical appraisal, Expert Opin. Drug Deliv. 7 (2010) 1095–1108. doi:10.1517/17425247.2010.503954.

[238] L. Perioli, V. Ambrogi, F. Angelici, M. Ricci, S. Giovagnoli, M. Capuccella, C. Rossi, Development of mucoadhesive patches for buccal administration of ibuprofen,

J. Control. Release. 99 (2004) 73–82. doi:10.1016/j.jconrel.2004.06.005.

[239] J. Chen, Q.D. Jiang, Y.M. Wu, P. Liu, J.H. Yao, Q. Lu, H. Zhang, J.A. Duan, Potential of essential oils as penetration enhancers for transdermal administration of ibuprofen to treat dysmenorrhoea, Molecules. 20 (2015) 18219–18236. doi:10.3390/molecules201018219.

[240] M.A.C. Manoukian, C.W. Migdal, A.R. Tembhekar, J.A. Harris, C. DeMesa, Topical Administration of Ibuprofen for Injured Athletes: Considerations, Formulations, and Comparison to Oral Delivery, Sport. Med. - Open. 3 (2017). doi:10.1186/s40798-017-0103-2.

[241] T.J. Wooster, M. Golding, P. Sanguansri, Impact of Oil Type on Nanoemulsion Formation and Ostwald Ripening Stability, Langmuir. 24 (2008) 12758–12765. doi:10.1021/la801685v.

[242] L.M. Andrade, L.A.D. Silva, A.P. Krawczyk-Santos, I.C. de S.M. Amorim, P.B.R. da Rocha, E.M. Lima, J.L. V. Anjos, A. Alonso, R.N. Marreto, S.F. Taveira, Improved tacrolimus skin permeation by co-encapsulation with clobetasol in lipid nanoparticles: Study of drug effects in lipid matrix by electron paramagnetic resonance, Eur. J. Pharm. Biopharm. 119 (2017) 142–149. doi:10.1016/j.ejpb.2017.06.014.

[243] S.M. O'Sullivan, J.A. Woods, N.M. O'Brien, Use of Tween 40 and Tween 80 to deliver a mixture of phytochemicals to human colonic adenocarcinoma cell (CaCo-2) monolayers, Br. J. Nutr. 91 (2004) 757–764. doi:10.1079/bjn20041094.

[244] Z. Hu, R. Tawa, T. Konishi, A novel emulsifier , Labrasol , enhances gastrointestinal absorption of gentamicin, Life Sci. 69 (2001) 2899–2910.

[245] N. Salim, M. Basri, M.B.A. Rahman, D.K. Abdullah, H. Basri, Modification of palm kernel oil esters nanoemulsions with hydrocolloid gum for enhanced topical delivery of ibuprofen, Int. J. Nanomedicine. 7 (2012) 4739–4747. doi:10.2147/IJN.S34700.

[246] S.S. Salunkhe, N.M. Bhatia, J.D. Thorat, P.B. Choudhari, M.S. Bhatia, Formulation, development and evaluation of ibuprofen loaded nanoemulsion prepared by nanoprecipitation technique: Use of factorial design approach as a tool of optimization methodology, J. Pharm. Investig. 44 (2014) 273–290. doi:10.1007/s40005-014-0125-4.

[247] H. Zhou, Y. Yue, G. Liu, Y. Li, J. Zhang, Q. Gong, Z. Yan, M. Duan, Preparation and

Characterization of a Lecithin Nanoemulsion as a Topical Delivery System, Nanoscale Res. Lett. 5 (2010) 224–230. doi:10.1007/s11671-009-9469-5.

[248] C.-L. Fang, I. Aljuffali, Y.-C. Li, J.-Y. Fang, Delivery and targeting of nanoparticles into hair follicles, Ther. Deliv. Solut. 5 (2014) 991–1006. doi:10.4155/TDE.14.61.

[249] J.C. Schwarz, V. Klang, M. Hoppel, D. Mahrhauser, C. Valenta, Natural microemulsions: Formulation design and skin interaction, Eur. J. Pharm. Biopharm. 81 (2012) 557–562. doi:10.1016/j.ejpb.2012.04.003.

[250] M. Hoppel, H. Ettl, E. Holper, C. Valenta, Influence of the composition of monoacyl phosphatidylcholine based microemulsions on the dermal delivery of flufenamic acid, Int. J. Pharm. 475 (2014) 156–162. doi:10.1016/j.ijpharm.2014.08.058.

[251] M. Changez, M. Varshney, J. Chander, A.K. Dinda, Effect of the composition of lecithin/n-propanol/isopropyl myristate/water microemulsions on barrier properties of mice skin for transdermal permeation of tetracaine hydrochloride: In vitro, Colloids Surfaces B Biointerfaces. 50 (2006) 18–25. doi:10.1016/j.colsurfb.2006.03.018.

[252] M.Z. Fiume, Final report on the safety assessment of triacetin, Int. J. Toxicol. 22 (2003) 1–10.

[253] S.P. Callender, J.A. Mathews, K. Kobernyk, S.D. Wettig, Microemulsion utility in pharmaceuticals: Implications for multi-drug delivery, Int. J. Pharm. 526 (2017) 425–442. doi:10.1016/j.ijpharm.2017.05.005.

[254] J. Qi, J. Zhuang, W. Wu, Y. Lu, Y. Song, Z. Zhang, J. Jia, Q. Ping, Enhanced effect and mechanism of water-in-oil microemulsion as an oral delivery system of hydroxysafflor yellow A, Int. J. Nanomedicine. (2011) 985–991. doi:10.2147/IJN.S18821.

[255] R.S. Keri, K. Chand, S. Budagumpi, S. Balappa Somappa, S.A. Patil, B.M. Nagaraja, An overview of benzo[b]thiophene-based medicinal chemistry, Eur. J. Med. Chem. 138 (2017) 1002–1033. doi:10.1016/j.ejmech.2017.07.038.